3.2.1 Definition of extreme waves exposure indexes for the HR test site

Final Version

Deliverable Number 3.2.1

Project Acronym	PMO-GATE
Project ID Number	10046122
Project Title	Preventing, Managing and Overcoming natural-hazards risk to mitiGATE economic and social impact
Priority Axis	2: Safety and Resilience
Specific objective	2.2: Increase the safety of the Programme area from natural and man-made disaster
Work Package Number	3
Work Package Title	Assessment of single-Hazard exposure in coastal and urban areas
Activity Number	2
Activity Title	Assessment of meteo-tsunami exposure in coastal areas
Partner in Charge	UNIVERSITY OF SPLIT, FACULTY OF CIVIL ENGINEERING, ARCHITECTURE AND GEODESY
Partners involved	UNIVERSITY OF SPLIT, FACULTY OF CIVIL ENGINEERING, ARCHITECTURE AND GEODESY PUBLIC INSTITUTION RERA SD FOR COORDINATION AND DEVELOPMENT OF SPLIT DALMATIA COUNTY UNIVERSITY OF FERRARA, DEPARTMENT OF ENGINEERING
Status	Final
Distribution	Public

Summary

1 Introduction

1.1 Brief presentation of Activity 3.2

Activity 3.2 within Work Package 3 of PMO-GATE project relates to the assessment of flooding in coastal urban areas due to extreme waves exposure. Significant number of objects along the coastline are potentially exposed to flooding due to the impact of extreme waves on the sea surface generated by severe winds. Within this activity, an extreme waves flooding exposure analysis is performed for the particular test site of Kaštel Kambelovac. Furthermore, this activity addresses the main weak points potentially exposed to extreme waves flooding, which in combination with extreme waves exposure maps are used for flood risk assessment on the particular test site. In addition, existing flood risk management plans are evaluated along with the relevant EU legislation. Finally, a set of actions is defined in order to harmonize local flood risk management plans with EU requirements.

1.2 Description of the test site – Kaštel Kambelovac

Along the Croatian coast, flooding endangers many low-lying coastal areas potentially exposing significant number of objects to flood hazard. Many historical buildings and/or areas are located along the coastline, which are potentially endangered by coastal flooding as well and subject to significant consequences and damage. The City of Kaštela area is endangered by sea flooding due to its low-lying topography and significant number of cultural and household objects located near the coastline. The particular test site in PMO-GATE project is Kaštel Kambelovac, one of the seven settlements that form the City of Kaštela. This area covers around 45000 square meters and includes more than 400 objects.

The benefit of the chosen area reflects through diversity of objects considering construction, architecture and material, built from the 15th century until today. According to Marasović [1] the oldest objects in the area date back to 1467. These buildings were made of stone with a wooden floor construction, and they remained preserved until today with minor modifications over the years. Historical

part of the Kaštel Kambelovac is founded in the 16th century around the Tower of Cambi, as well as the church of St. Mihovil and Martin from the 19th century with a bell tower from 1860. This particular area is a mixture of private and public facilities, mostly built as masonry and concrete buildings. Plan view of the selected area is shown in Figure 1, where the green line defines the border of the test site, purple one defines the border of historical part, while the red line shows position of the natural coastline.

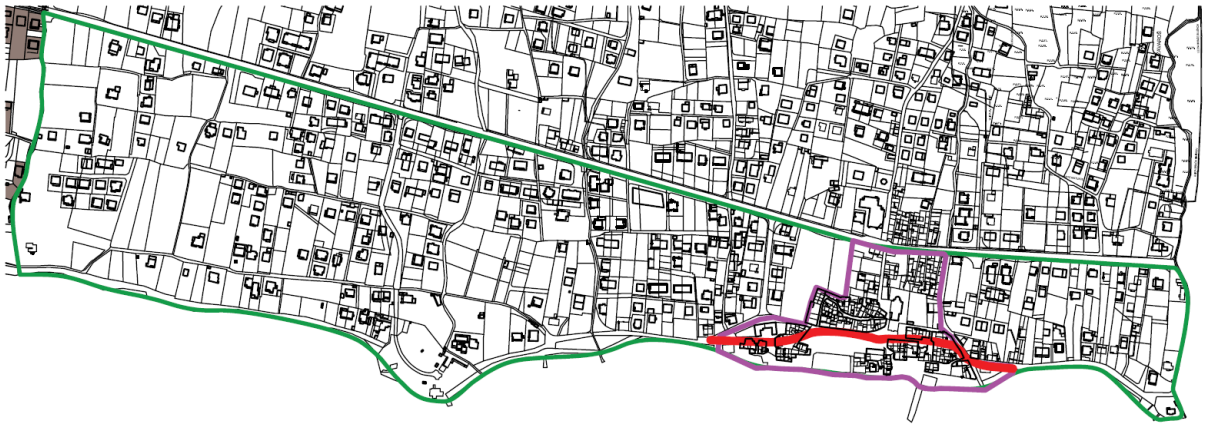

Figure 1. Plan view of the selected area (green line) with the mark of the natural coastline (red line) and the historical part (purple line)

Coastal flooding is considered one of the major threats for coastal urban areas. This is especially related to low-lying coastal areas such as City of Kaštela, where significant part of the city is located near the coastline. High population density in the coastal area of City of Kaštela, together with a large number of buildings and other assets makes this area highly vulnerable. Coastal flooding in the City of Kaštela is becoming more frequent and recent events caused damage to different assets, exposing the weak points within buildings and existing infrastructure.

2 Tidal characteristics at Kaštela bay

The nearest tide gauge near Kaštela Bay is located within the Institute of Oceanography and Fisheries (IOR) in Split, at the western border of peninsula Marjan. Time series of measured sea surface elevations with a total duration of five years have been obtained from the Marjan tide gauge, respectively for the period from 01.01.2010. to 31.12.2014.. The sampling frequency of the tide gauge has been set up to 1 hour for the entire time series. The measured water level elevation is referred to the HVRS71 vertical datum.

Due to maintenance and malfunction of the tide gauge IOR Marjan, the observed time series are characterised by periods without recorded values of the sea level. For the purpose of this work, a continuous time series is required so the longest continuous time series has been found from 25.01.2010. at 12:00 h to 27.06.2011. at 23:00 h with a total of 12444 data.

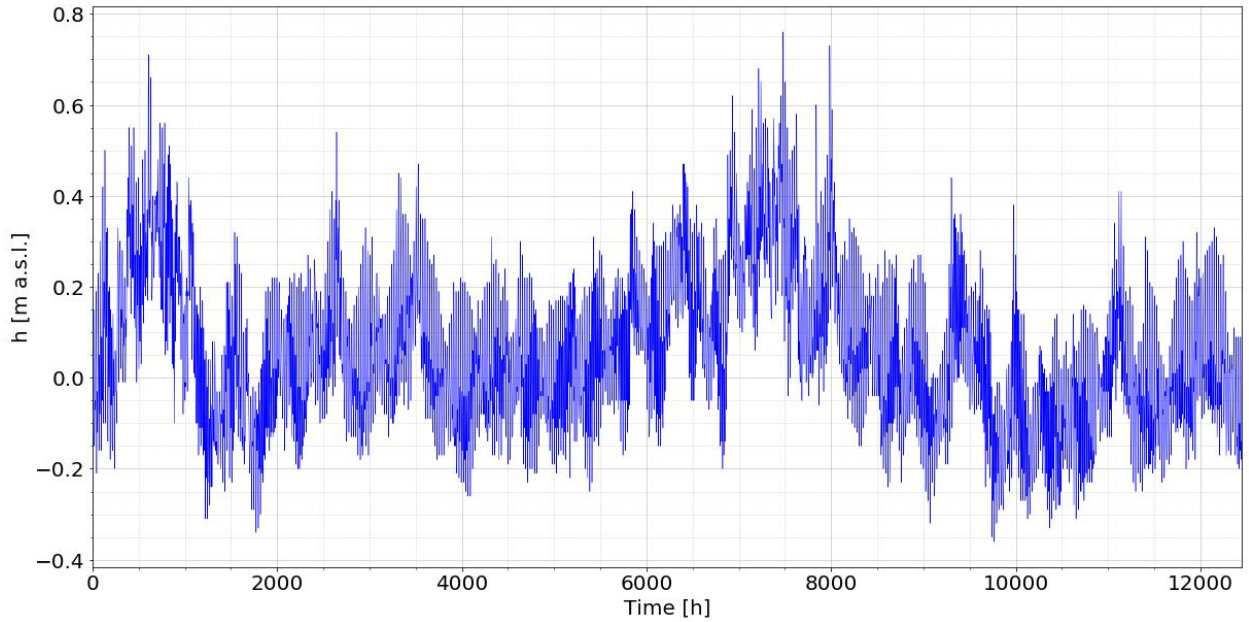

Figure 2. Measured sea level for period of 25.01.2010. at 12:00 to 27.06.2011. at 23:00

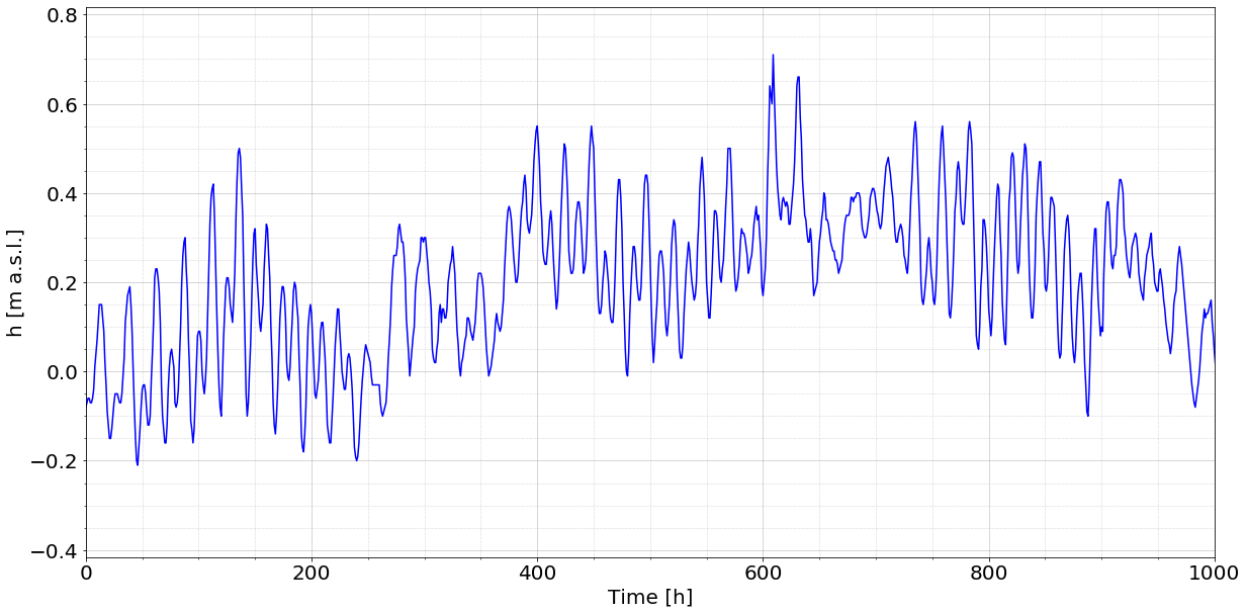

Figure 3. First 1000 data of sea level from Figure 2.

The tides at Adriatic Sea are of the mixed type with regular alternations of spring and neap tides. Selected time series are long enough to capture for all effects caused by tidal variations, and selected time series of 12444 data are used for further analysis.

3 Frequency domain analysis

In the research of Janeković and Kuzmić 2005. it was shown that tides in Adriatic Sea consist of in total 7 dominant constituents, of which three diurnal constituents, respectively O1, P1 i K1, and four semidiurnal constituents, respectively N2, M2, S2 i K2. Each constituent represents a sinusoidal function with associated amplitude, period, and phase. To determine the unknown values of the amplitudes, periods and phases, the signal is initially transferred from the time domain to the frequency domain.

Transformation from time domain to frequency domain is done with Discrete Fourier Transformation (DFT).

For observed sea level values $x_0, x_1, \dots, x_{n-1}$, series $X_0, X_1, \dots, X_{n-1}$ is defined with formula

$$X_k = \frac{1}{n}\sum_{j=0}^{n-1} x_j e^{\left(-\frac{2kj\pi i}{n}\right)}, \qquad k = 0, 1, \dots, n-1 \qquad (1)$$

where Eq.(1) represents Discrete Fourier Transformation of series $x_0, x_1, \dots, x_{n-1}$, where X_k represents value of k^{th} frequency, x_j is measured sea level in j step, k is the number of frequency and n is the total sample dimension.

Using Euler's formula Eq. (1) can be rewritten as

$$X_k = \sum_{j=0}^{n-1} \left[cos\left(\frac{2kj\pi}{n}\right) - i \times sin\left(\frac{2kj\pi}{n}\right)\right], \qquad k = 0, 1, \dots, n-1 \qquad (2)$$

or

$$X_k = A_k + iB_k, \qquad k = 0, 1, \dots, n-1 \qquad (3)$$

where A_k and B_k are complex numbers of k^{th} frequency. Frequency value X with index k corresponds to real frequency of

$$k\frac{f_s}{n}\ Hz \ (4)$$

where f_s represents sampling frequency.

Ba plotting the complex numbers A_k and B_k in complex domain, magnitude and phase of each frequency can be calculated as follows

$$M_k = \sqrt{A_k + B_k} \; ; \quad \varphi_k = \; tan^{-1} \frac{B_k}{A_k}, \quad (5)$$

where M_k represents magnitude of given frequency and ϕ_k phase of given frequency.

DFT results are often plotted as Amplitude Spectral Density (ASD). By normalizing magnitudes with number of samples, amplitude of each frequency can be calculated.

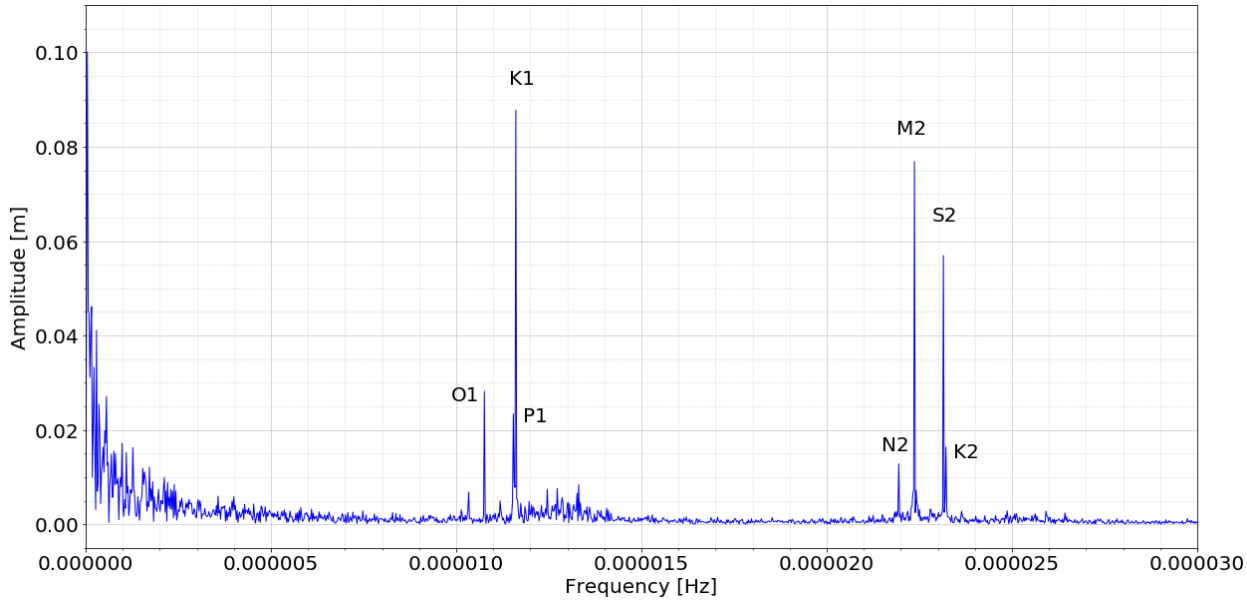

Figure 4. ASD for measured sea level reduced for the mean value

From Figure 4, 7 dominant tidal constituent can be easily recognised. In addition to the tidal constituents, an increase in amplitudes can be seen at frequencies closer to the zero frequency (the zero frequency corresponds to the mean). These frequencies are responsible for the emergence of a trend in the time series as a result of changes in barometric pressure, wind and other less significant effects [Wunsch 1972, Tsimplis and Vlahakis 1994]. From Figure 4 and using Eqs. (4) and (5), the amplitude, period and phase values of the tidal constituents are calculated and shown in Table 1.

Table 1. Tidal constituents with corresponding values of Amplitude, period and phase.

	Amplitude [m]	Period [h]	Phase [°]
O1	0,02821644	25,81743	-160,6065
K1	0,02339150	24,06963	105,3624
P1	0,08773618	23,93077	153,1416
N2	0,01279412	12,65921	65,3833
M2	0,07688095	12,41916	-31,55806
S2	0,05696792	12,00000	-126,8397
K2	0,01636003	11,96538	116,0807

4 Forecasting tidal oscillations

Based on determined tidal parameters, sea level can be simulated using linear superposition of sine functions with corresponding values of amplitudes, periods and phases as shown in Table 1:

$$h_t = \sum_{i=1}^{7} A_i \times \sin\left(\frac{2\pi t}{t_{pi}} + \frac{2\pi\varphi_i}{360}\right), \mathrm{t} = 0, 1, \ldots, 12443 \qquad (6)$$

Where h_t is simulated sea level [m], A_i is amplitude [m], t_{pi} is period [h] and φ_i phase [°] of i-th constituent, and t is time [h].

Simulated sea level (h_{sea}) in Figures 5-8. is calculated as a sum of tidal frequencies from Eq.(6), by takin constituent values from Table 1 and finally, reducing for mean sea level value.

$$h_{more} = h_t + \bar{h} \qquad (7)$$

where $\bar{h}$ represents mean sea level value calculated from measured sea level signal from Figure 2.

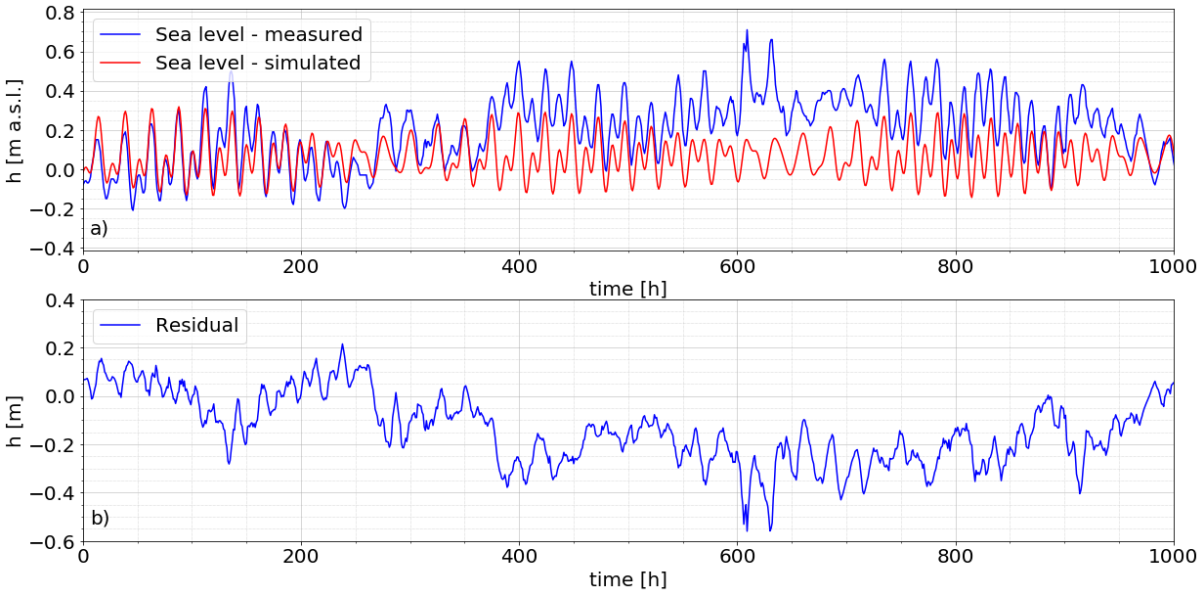

Figure 5. a) Measured and simulated sea level with 7fr for the first 1000 hours of observed sea level signal from Figure 2, b) Residual between simulated and measured sea level signal

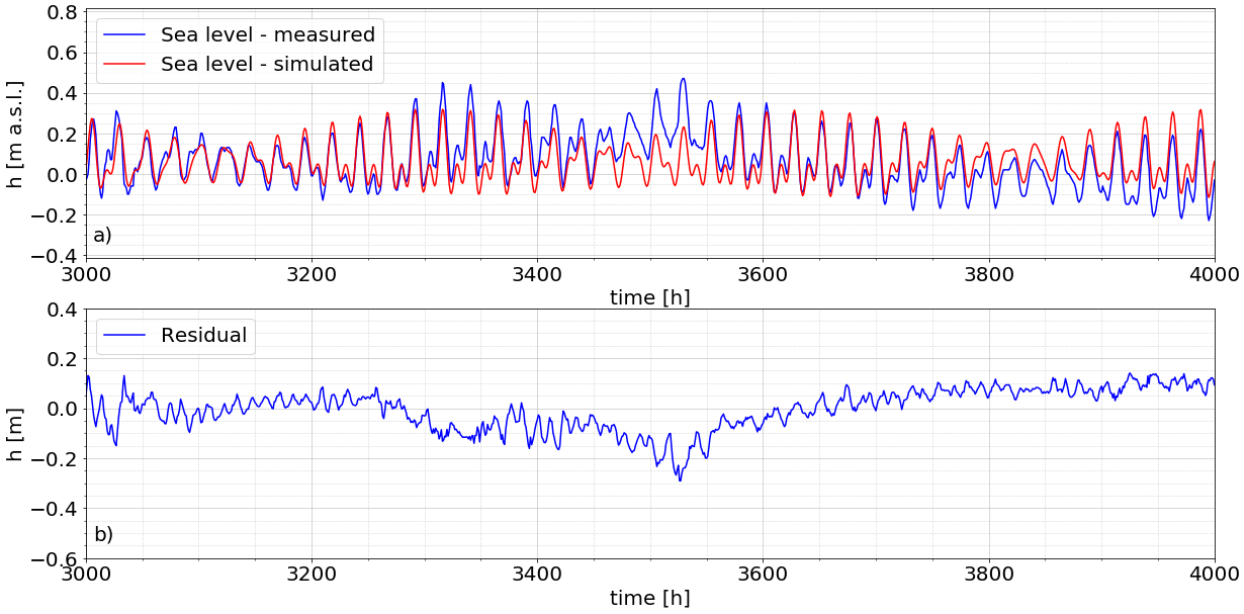

Figure 6. a) Measured and simulated sea level with 7fr between 3000 and 4000 hours of observed sea level signal from Figure 2., b) Residual between simulated and measured sea level signal

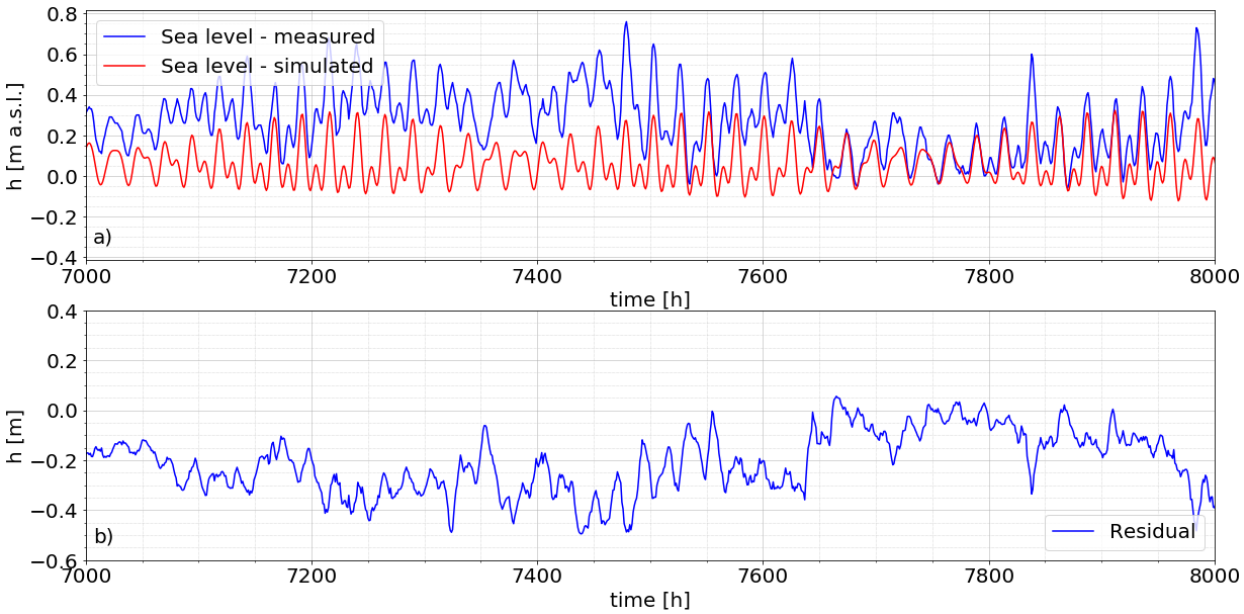

Figure 7. a) Measured and simulated sea level with 7fr between 7000 and 8000 hours of observed sea level signal from Figure 2., b) Residual between simulated and measured sea level signal

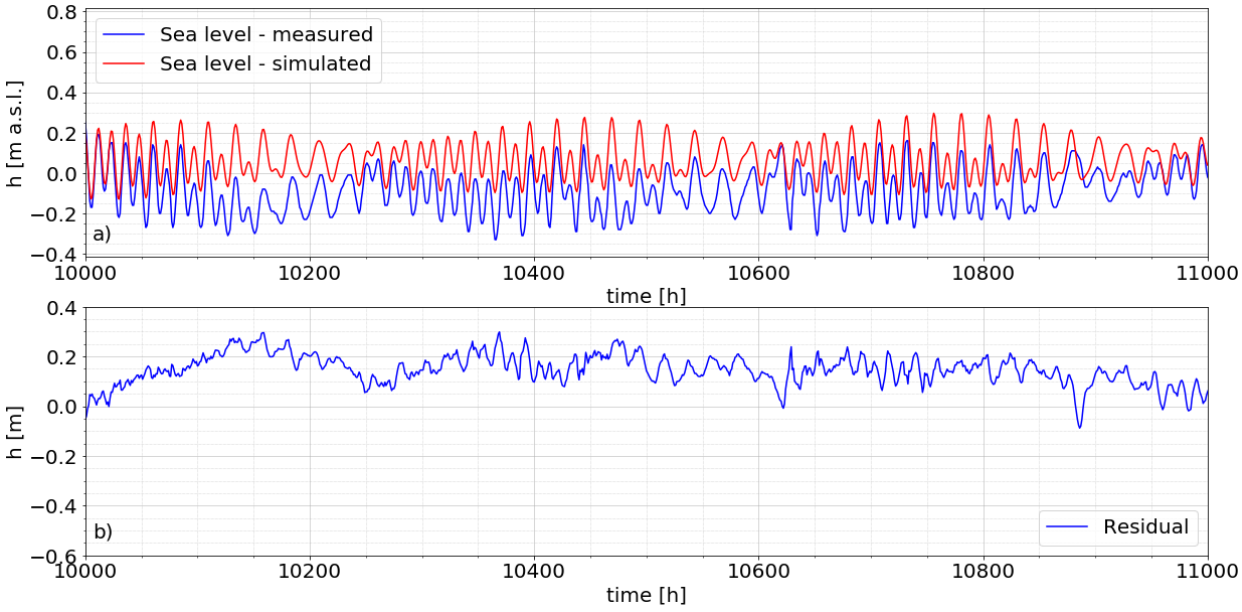

Figure 8. a) Measured and simulated sea level with 7fr between 10000 and 11000 hours of observed sea level signal from Figure 2., b) Residual between simulated and measured sea level signal

Root Mean Square Error (RMSE) and Pearson correlation coefficient have been used as error model estimation between observed and predicted sea level signal. RMSE is calculated as follows:

$$RMSE = \sqrt{\frac{1}{N}\sum_{i=1}^{N}\left(h_i - h_{sea\_i}\right)^2} \qquad (8)$$

where N is total number of samples, h_i stands for measured sea level signal and h_{sea_i} for simulated sea level signal. RMSE represents average residual between observed signals and has same unit as observing signals.

Pearson correlation coefficient can be calculated as

$$P_{h.h_{more}} = \frac{E\left[(h-\mu_h)\left(h_{more}-\mu_{h_{more}}\right)\right]}{\sigma_h \sigma_{h_{more}}} \qquad (9)$$

where *P* stands for Pearson correlation coefficient, *h* and h_{sea} are measured and observed sea level, E is expectation, σ_h and σ_{hsea} represent standard deviation of h and h_{sea}, and μ_h and μ_{hsea} are mean value of h

and h_{sea}. Pearson correlation coefficient is a measure of linear correlation between two variables. The result of Pearson correlation coefficient always has a value between -1 and 1, where 1 stands for total correlation, 0 for no correlation and -1 for total negative correlation between observed series.

For the entire observed and simulated set of 12444 data, the RMSE value is 0.136 [m], while Pearson's correlation coefficient is 0.578 [-]. The high value of RMSE and low value of correlation coefficient indicate that sea level fluctuations are not only subjected to tidal variations but also to other factors.

5 Kaštela bay barometric pressure features

Barometric pressure data are obtained from two meteorological stations, the meteorological station Split-Airport and the meteorological station Split-Marjan. The meteorological station Split-Airport is located at 21 m a.s.l. and the barometric pressure values are recorded three times a day at 7 am, 2 pm and 9 pm. The meteorological station Split-Marjan is located at 122 m a.s.l. and has an hourly measurement frequency including barometric pressure values. Logs of barometric pressure were obtained from both meteorological stations for the period 01.01.2010. to 31.12.2014..

Due to the location of Kaštela Bay, the meteorological station Marjan-Airport has been considered as relevant, but due its low measurement frequency, the data from Split-Marjan are used for further analysis. First, the data from Split-Marjan are compared with the data from Split- Airport and a mean difference of 12.67 hPa with a standard deviation of 0.67 hPa is found. All data from Split-Marjan are corrected for the values of 12.67 hPa.

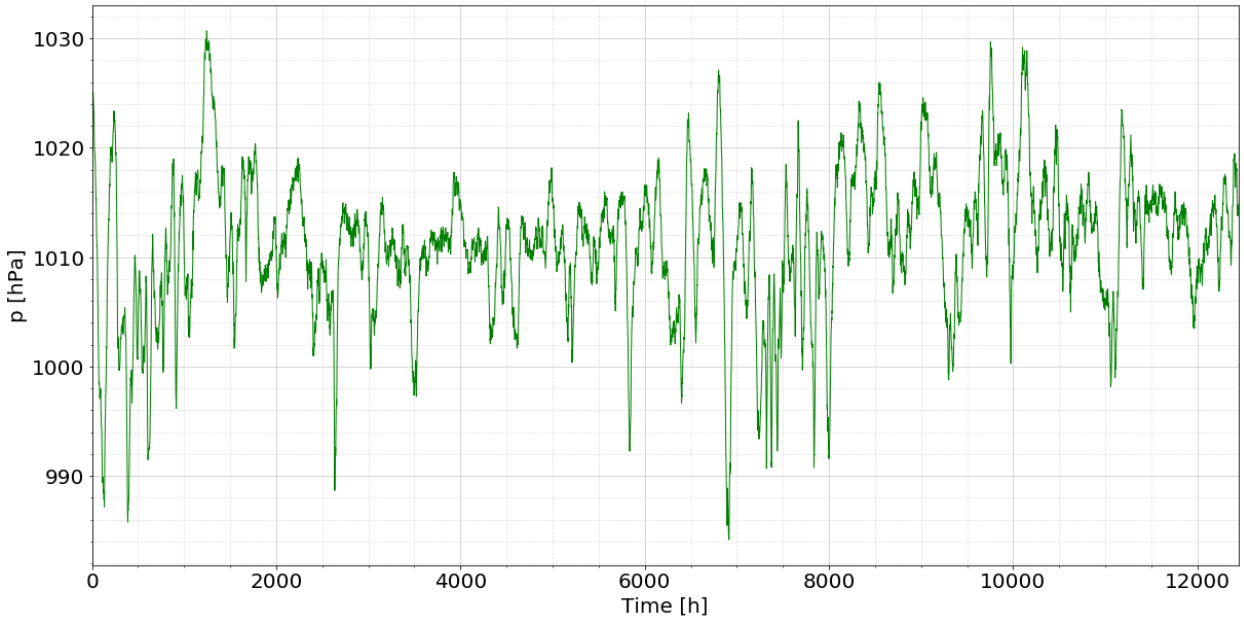

Figure 9. Observed values of barometric pressure from meteorological station Split-Marjan corrected for value of 12.67 hPa for the period of 25.01.2010. at 12:00h to 27.06.2011. at 23:00h

The available data from the Split-Marjan station has a continuous record with no missing data for the entire 5 year period. However, since the sea level signal does not have the same continuity as the barometric pressure, the same period of barometric pressure is included in the further analysis as sea level.

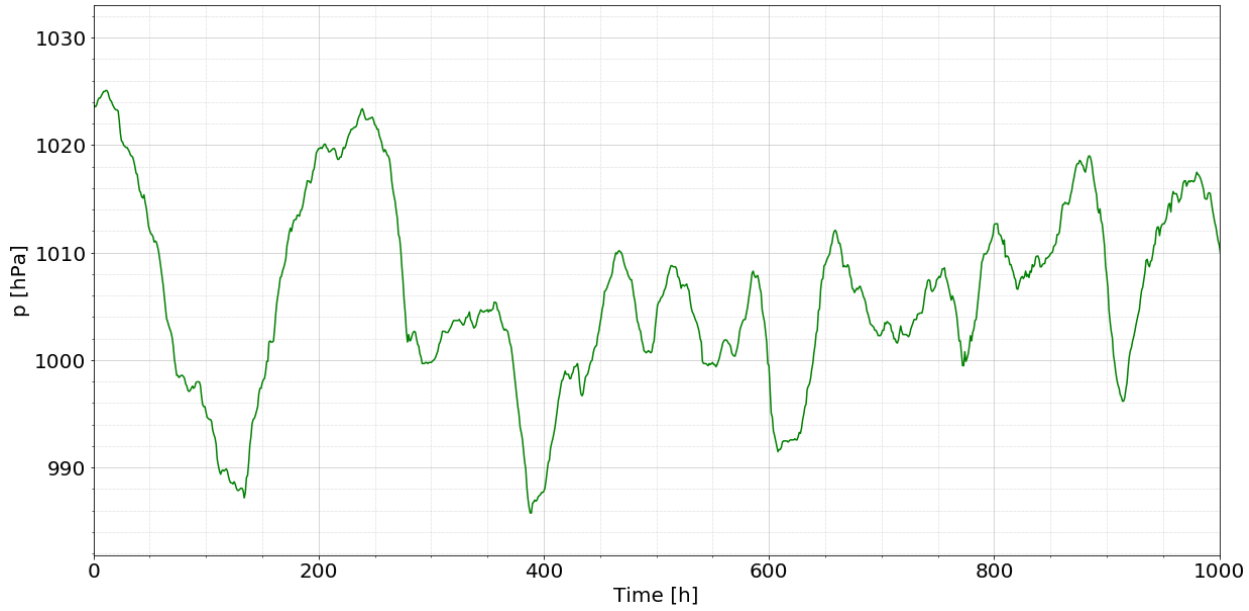

Figure 10. First 1000 data of barometric pressure from Figure 9.

6 Barometric pressure contribution to sea level oscillations

Increasing the barometric pressure by 1 [cm] of the saltwater column lowers the sea level approximately by 1 [cm], and vice versa, decreasing the barometric pressure by 1 [cm] raises the sea level by 1 [cm] [Ponte 1993]. This effect is called the Invert Barometric effect (IB). The sea level rise caused by the change of the barometric pressure can be calculated as follows.

$$h_{at} = \frac{-p_a}{\rho g} \qquad (1)$$

h_{at} is sea level as a consequence from change in barometric pressure, p_a is barometric pressure [Pa], ρ is density of fluid [kg/m^3] and g is gravitational acceleration [m/s^2]. Therefore, simulated sea level is updated for the values of h_{at}.

$$h_{sea} = h_t + h_{at} + \bar{h} \qquad (2)$$

where third right hand term represents mean sea level values as calculated from the observed signal, h_t represents tidally induced sea level oscillations and h_{at} holds for barometric induced mean sea level change.

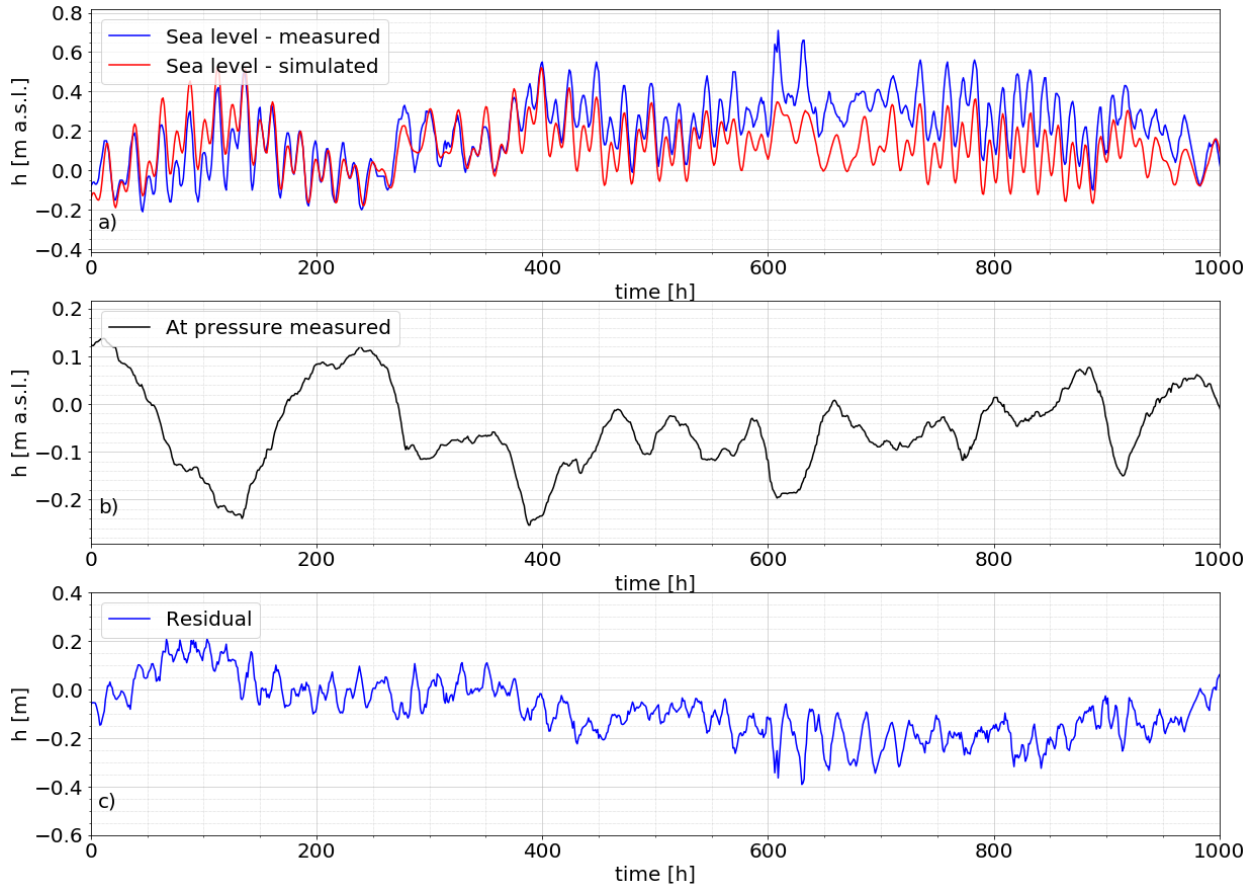

Figure 11. Observed and simulated sea level by Eq. (2) for the first 1000 hours of observed sea level signal., b) Observed barometric pressure, c) Residual between simulated and observed sea level signal

Figures 9-11 show the effect of barometric pressure on the simulated signal with 7 frequencies. The simulated signal has a similar trend to the observed sea level signal with a residual remaining between the simulated and observed signal. When the sea level signal is simulated using the tidal components and the inverted barometric effect, the RMSE decreases to 0.1057 [m] and the Pearson correlation coefficient increases to 0.77 [-], further highlighting the effect of barometric pressure and its contribution to observed sea level definition.

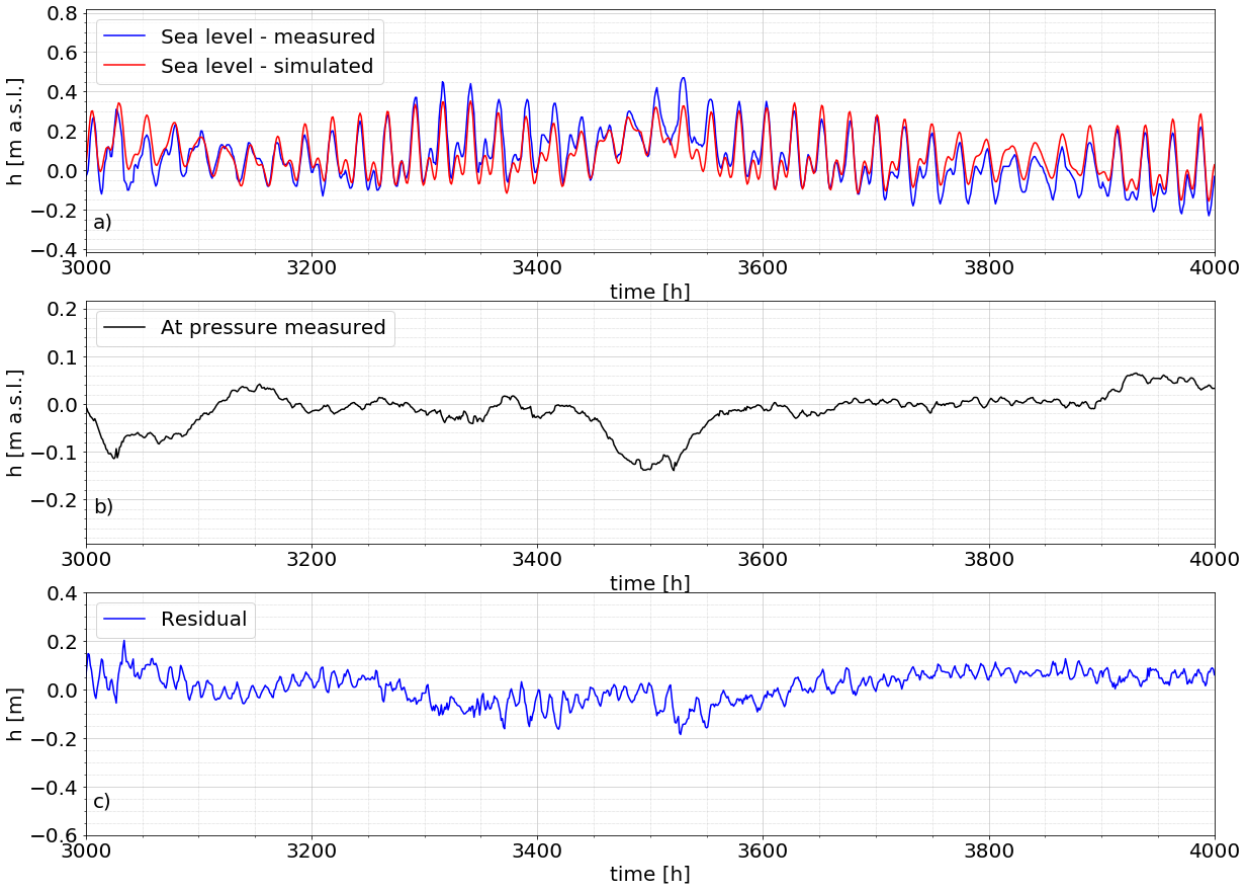

Figure 12. Observed and simulated sea level by Eq. (2) between 3000 and 4000 hours of observed sea level signal, b) Observed barometric pressure, c) Residual between simulated and observed sea level signal

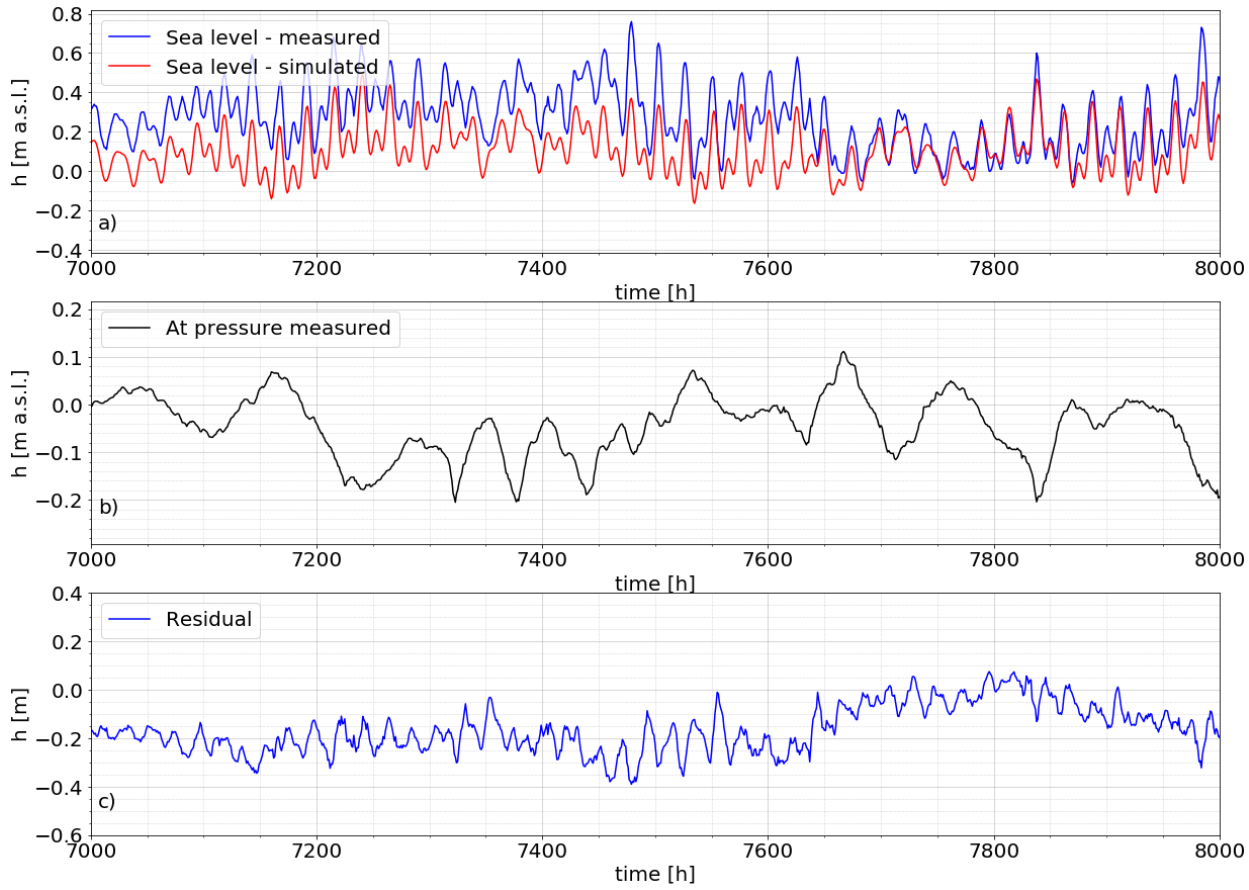

Figure 13. Observed and simulated sea level by Eq. (2) between 7000 and 8000 hours of observed sea level signal, b) Observed barometric pressure, c) Residual between simulated and observed sea level signal

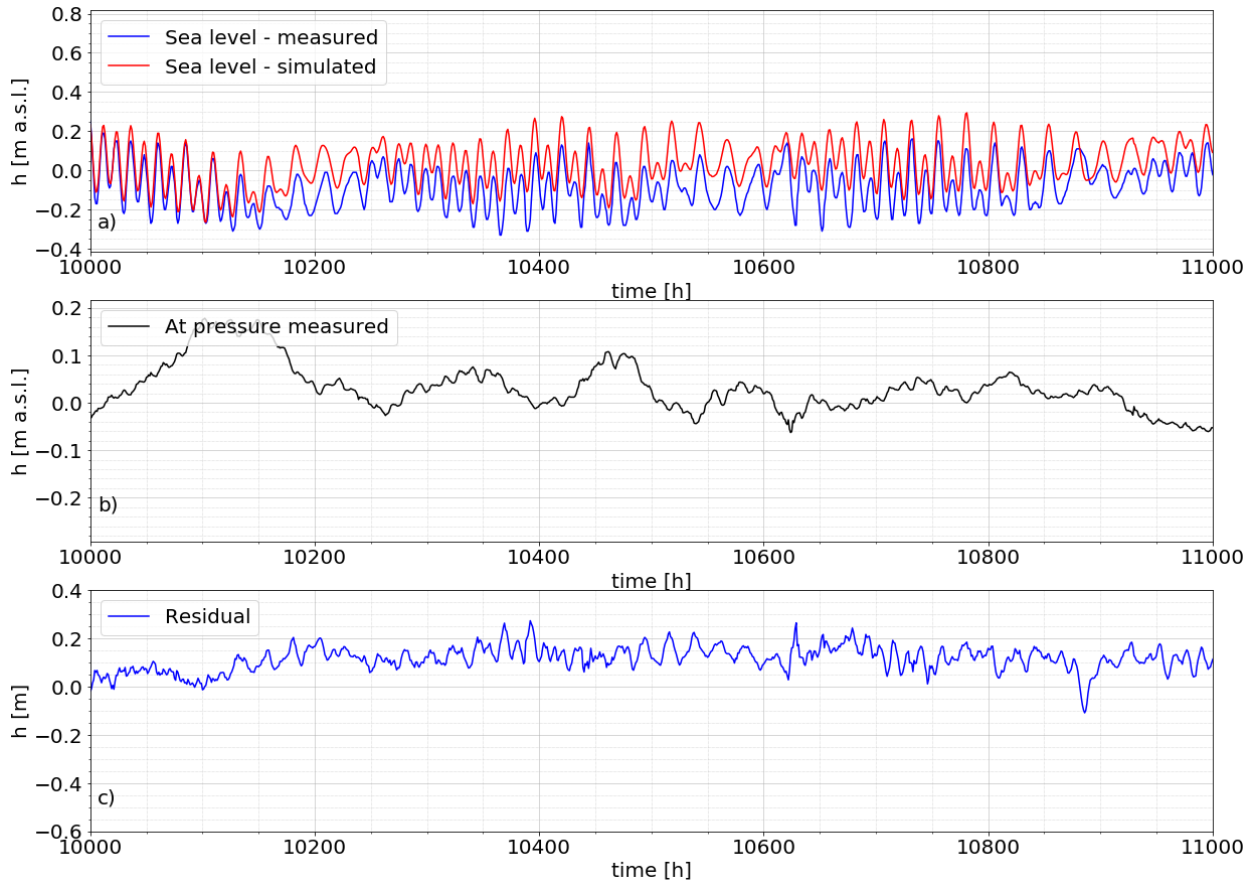

Figure 14. Observed and simulated sea level by Eq. (2) between 10000 and 11000 hours of observed sea level signal, b) Observed barometric pressure, c) Residual between simulated and observed sea level signal

For the purpose of extended understanding the residual shown in in Figures 11-14 both signals, the observed sea level and the observed barometric pressure, have been transferred from time domain to the frequency domain (Figure 15).

Figure 15 shows ASD of both sea level and barometric pressure have similar amplitudes found along frequencies between $5x10^{-7}$ [Hz] and $3x10^{-6}$ [Hz], indicating the influence of barometric pressure on sea level. Amplitudes in components having frequencies lower than $5x10^{-7}$ [Hz] are higher in the sea level signal, indicating that besides tidal variations and barometric pressure variations, the influence of other

factors is also present, such as long periodic movement of sea caused by wind effect and seasonal oscillations [Wunsch and Stammer 1997, Le Traon and Gauzelin 1997, Ponte 1993]. Effects of these factors exceeds the scope of this report.

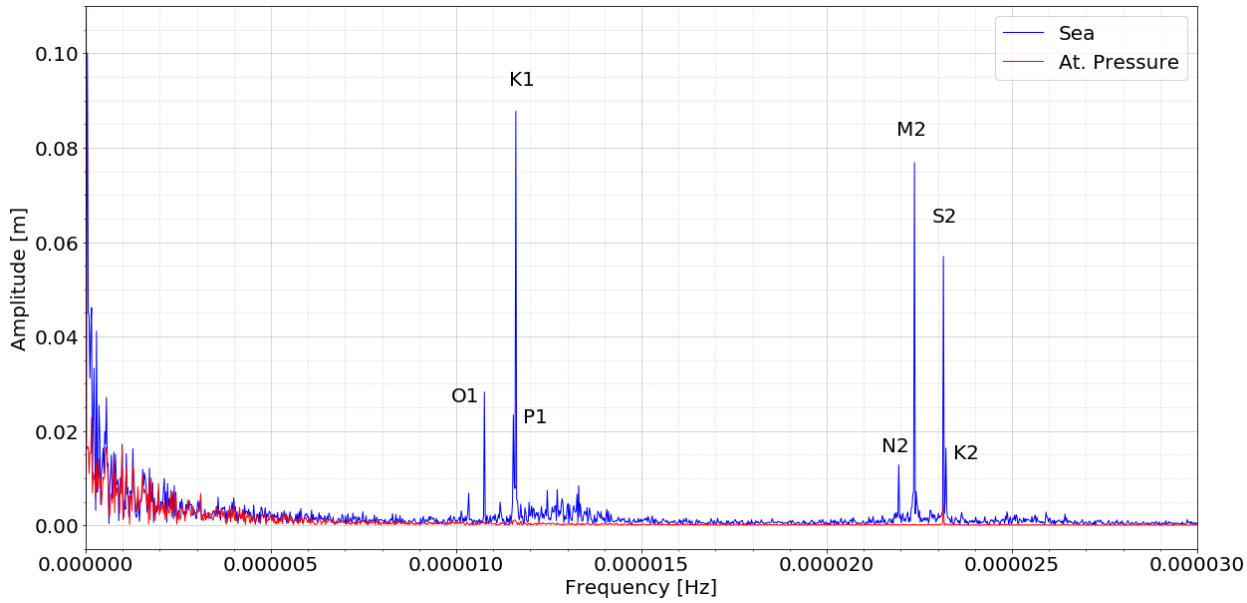

Figure 15. ASD of measured sea level and barometric pressure signal in meters of saltwater column

7 Validation of forecasting model from tidal oscillations and barometric pressure effect

To further minimise RMSE an effect of barometric pressure is added. Sea level signal is simulated using Eq. (2). Observed barometric pressure is obtained for the same validation period, both from meteorological station Split-Airport and Split-Marjan. Barometric pressure from meteorological station Split-Marjan is corrected for the difference between measured values from meteorological station Split-Airport and Split-Marjan. Simulated signal has been is corrected with 2.29 h phase shift prior the plot in Figures 16-19.

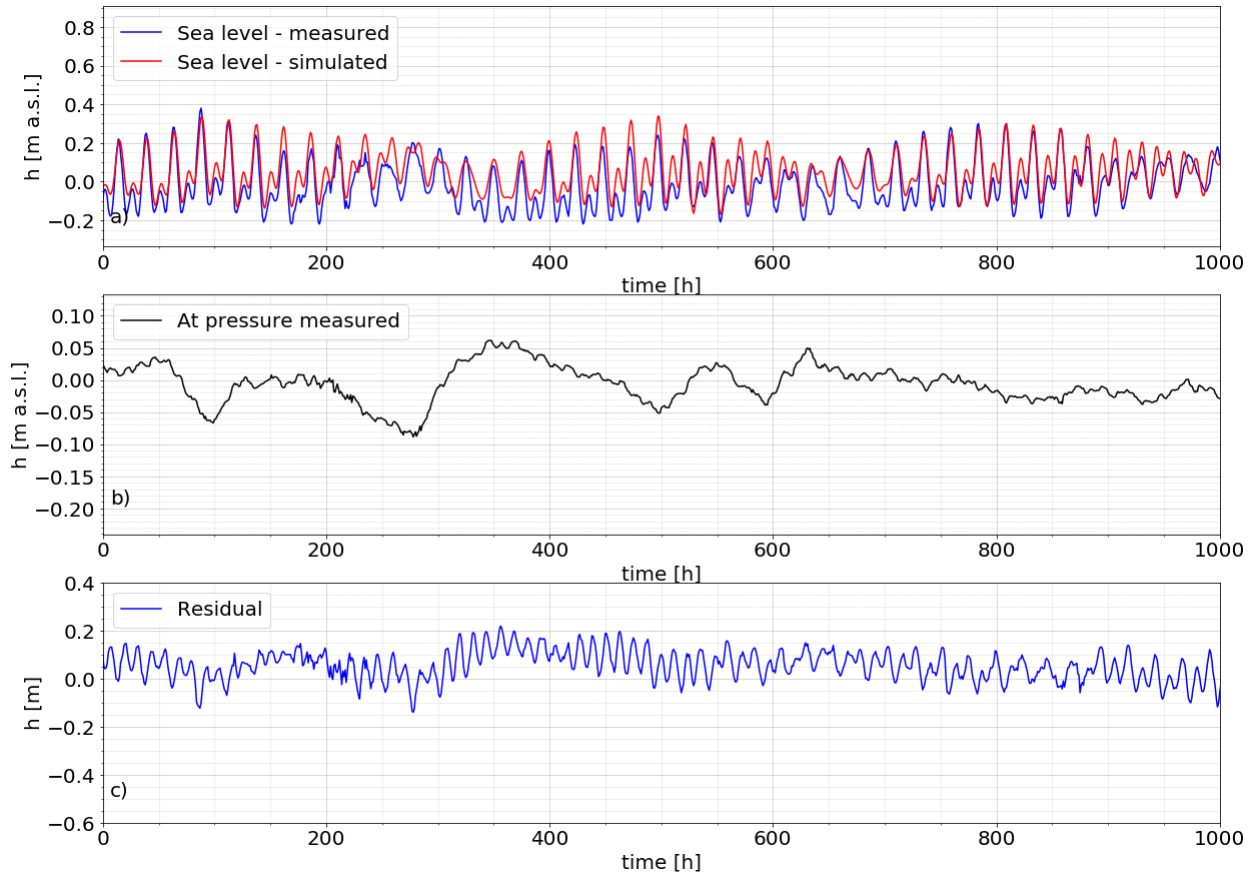

Figure 16. a) Observed and simulated sea level with Eq.(2) for first 1000 hours of observed sea level signal, b) Observed barometric pressure, c) Residual between simulated and observed sea level signal

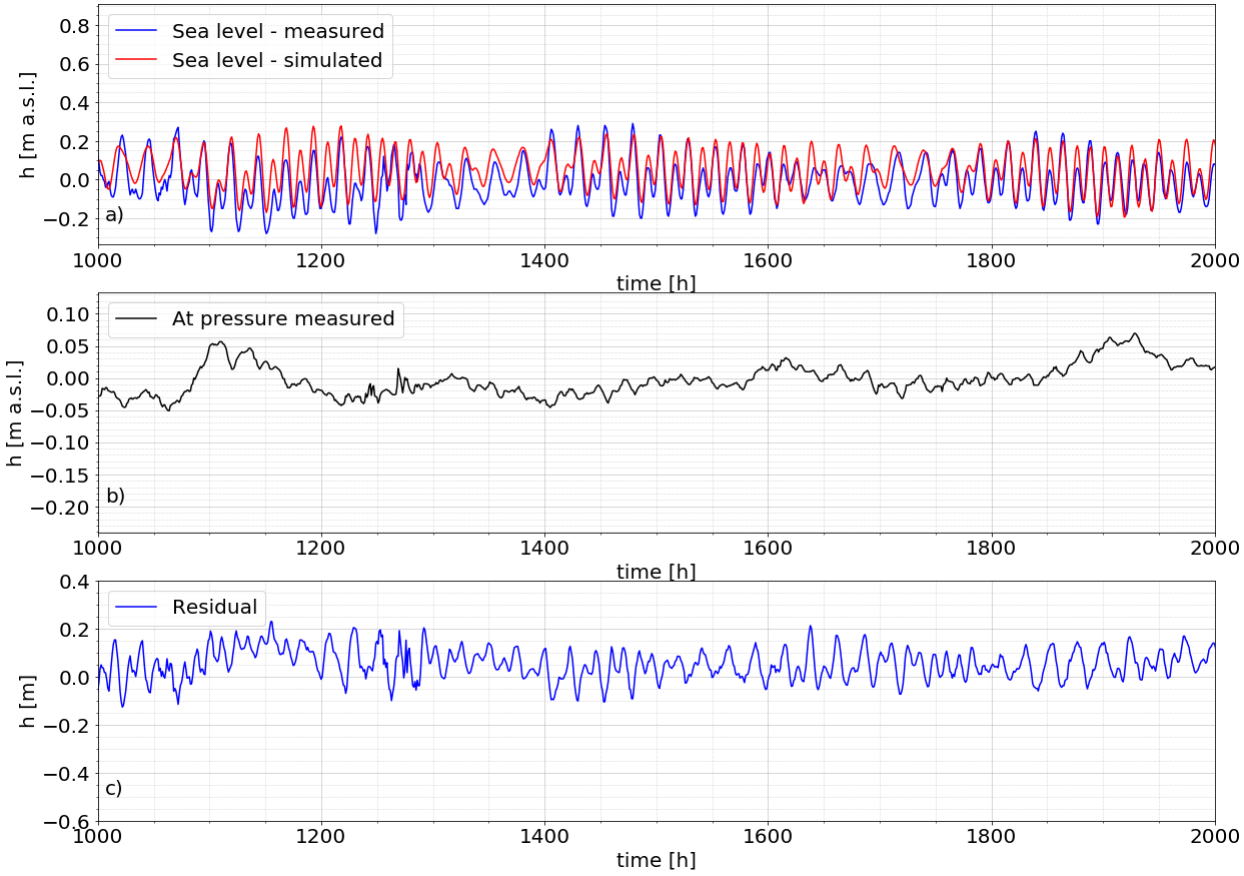

Figure 17. a) Observed and simulated sea level with Eq.(2) between 1000 and 2000 hours of observed sea level signal, b) Observed barometric pressure, c) Residual between simulated and observed sea level signal

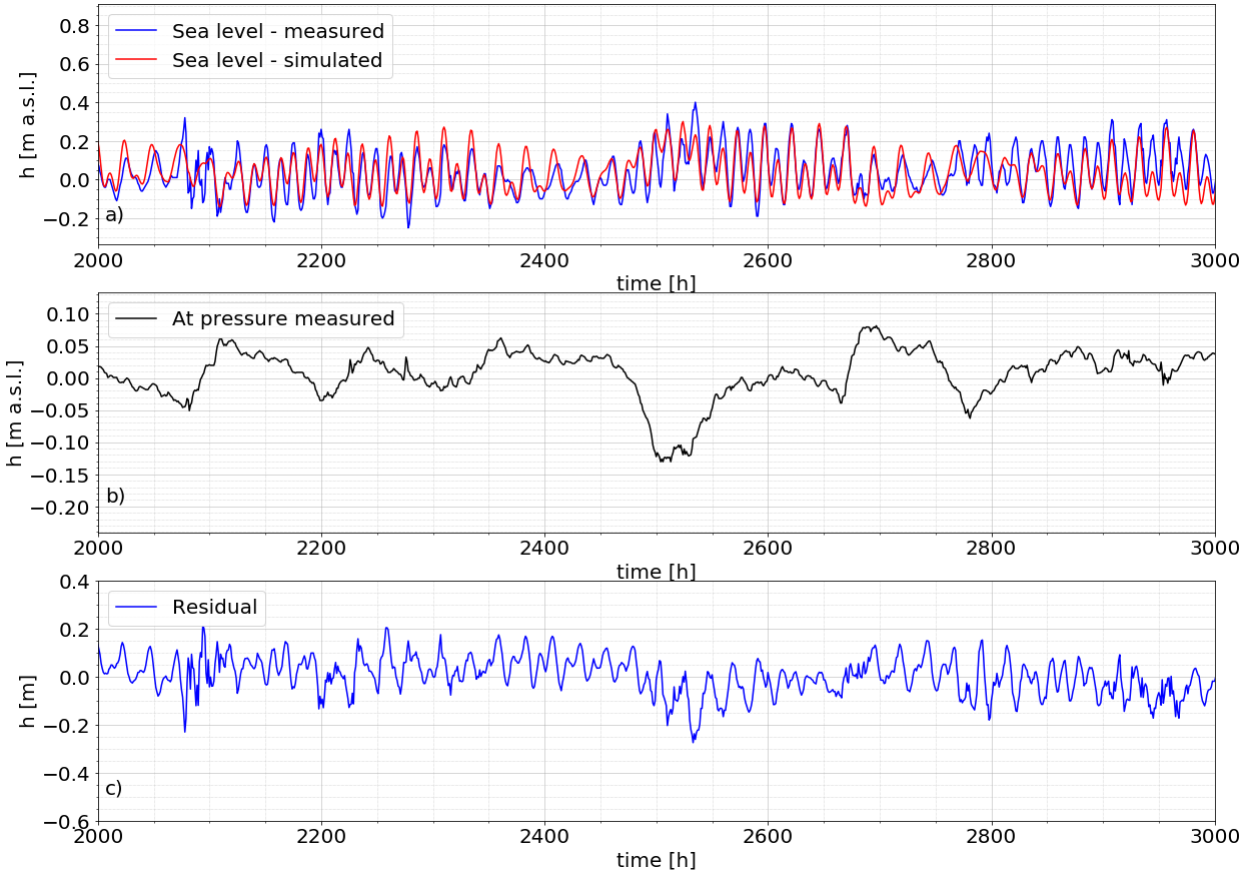

Figure 18. a) Observed and simulated sea level with Eq.(2) between 2000 and 3000 hours of observed sea level signal, b) Observed barometric pressure, c) Residual between simulated and observed sea level signal

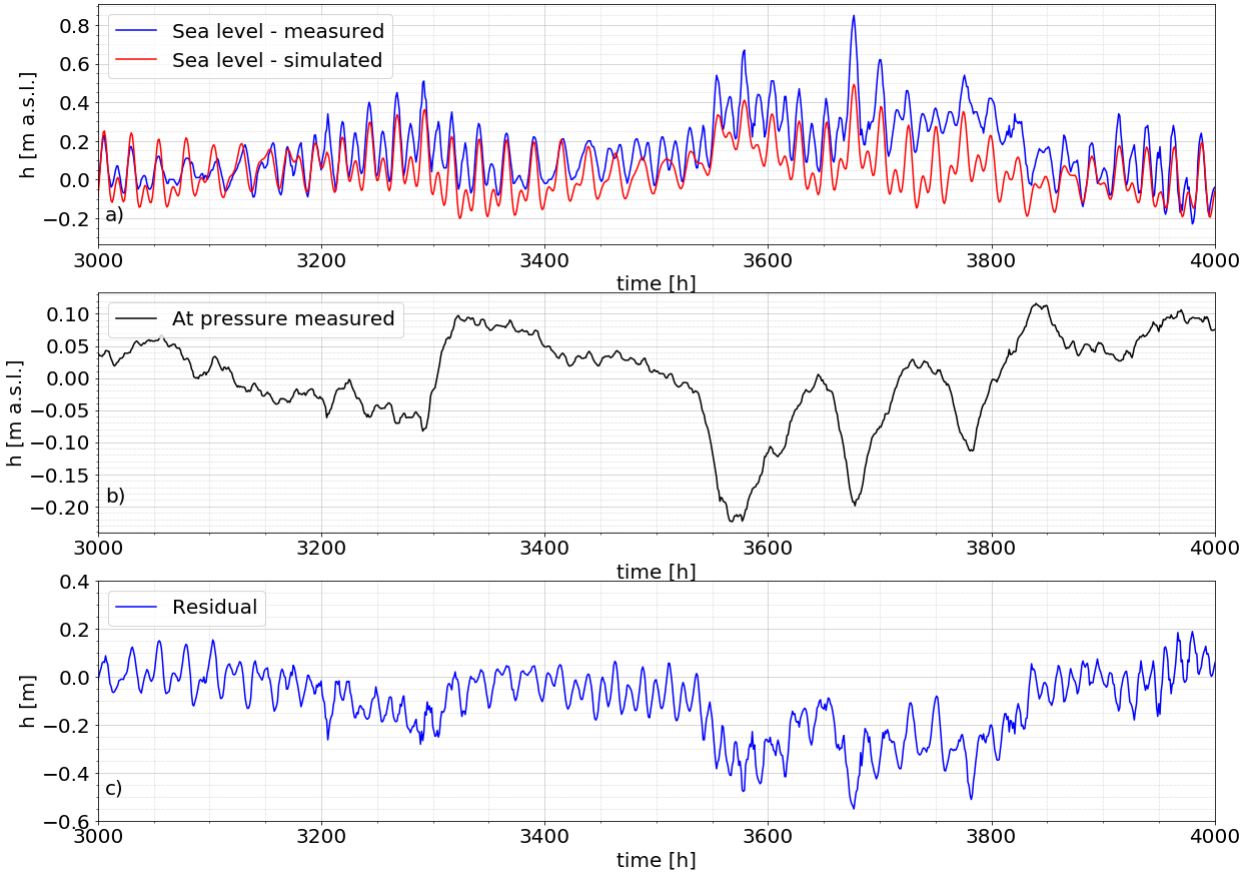

Figure 19. a) Observed and simulated sea level with Eq.(2) between 3000 and 4000 hours of observed sea level signal, b) Observed barometric pressure, c) Residual between simulated and observed sea level signal

For the total 4392 data of observed and simulated sea level series used for validation, the RMSE value is 0.098 [m], while Pearson's correlation coefficient is 0.731 [-].

Further improvement of the prediction model of sea level elevations is possible if the long and short term effects of wind and seasonal variations are taken into account. Long-term wind effects as well as seasonal oscillations need to be analysed together with sea currents over a large sea area, which is beyond the scope of this report. Waves are considered as short-term effects of winds and are analysed in other chapters of the report.

8 Determination of wave heights in front of the coastline

Based on the previously conducted analyses in this survey, below is an overview of wave heights determination and records, as well as their distribution along the coastline in the broader area of interest.

- For the relevant incident wave directions the lengths of effective fetch are determined;
- The intensity (speed) and duration of continuous wind occurrence is determined from the wind data;
- Based on the above defined, parameters of deep-water wave can be determined;
- With execution of model analysis, considering depth features, reflection properties of the coastline and the properties of the wave at the distance of 4 meters from the coastline, a significant wave height is defined which is compatible with hundred years return period;
- By comparing wave heights of realized wave at the distance of 4 meters and wave height of the deep-water wave, shoaling coefficient along coastline K_S is determined

Spatial properties on the behaviour of shoaling coefficient K_S [-] are described below and are shown in Figure 20. Numerical values are shown in the form of tables below and in the attachment of this chapter.

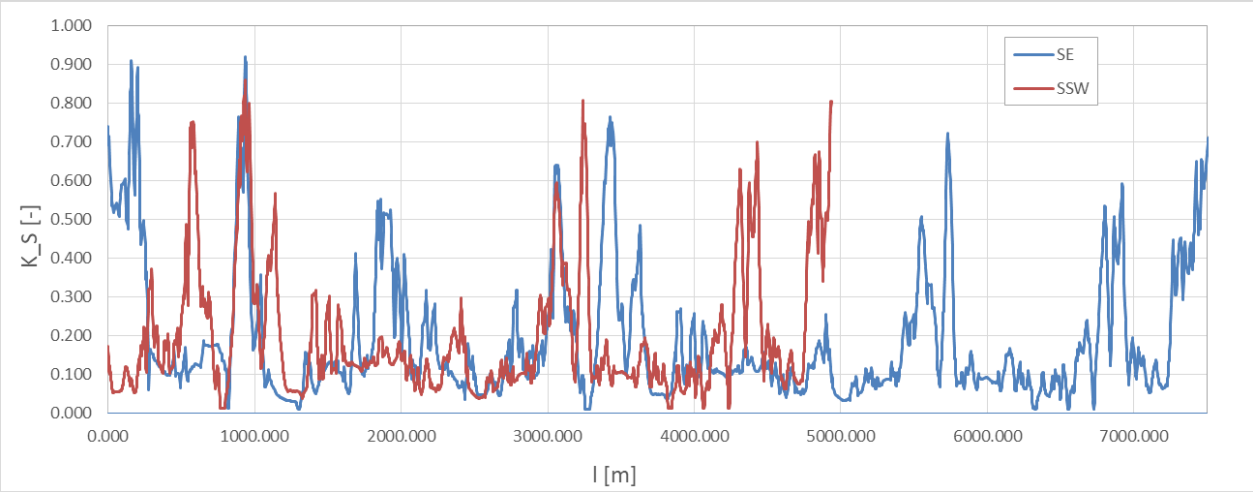

Figure 20. Graphical display of the shoaling coefficient for observed incident directions along the coastline

9 Kaštela bay characteristics

Kaštela bay is biggest bay of mid Dalmatia region, with length of 14.8 km, width of 6.6 km and maximum depth of app. 50 m. In its origin, Kaštela bay is a depression bounded by Peninsula Marjan, island Čiovo and mainland. From the north and north east it is bounded by mainland, from the south it is bounded by Marjan peninsula while form west and south west one finds Trogir area and Čiovo island.

River Jadro enters the bay in Solin, while stream Pantan mouth is located near the Trogir. Along the bay area several smaller islands are located: Školjić, Galera, Barbarinac and Šilo.

10 Baseline for the bathymetric features of Kaštela bay

Taking into consideration the lack of in situ geodetic survey conductance, the baseline for the bathymetric information used for purpose of this study, has been taken by web service Navionics (Figure 21). The user should be aware of the reliability of this source, such as the accuracy of expressed depth values as well as the relevant vertical datum.

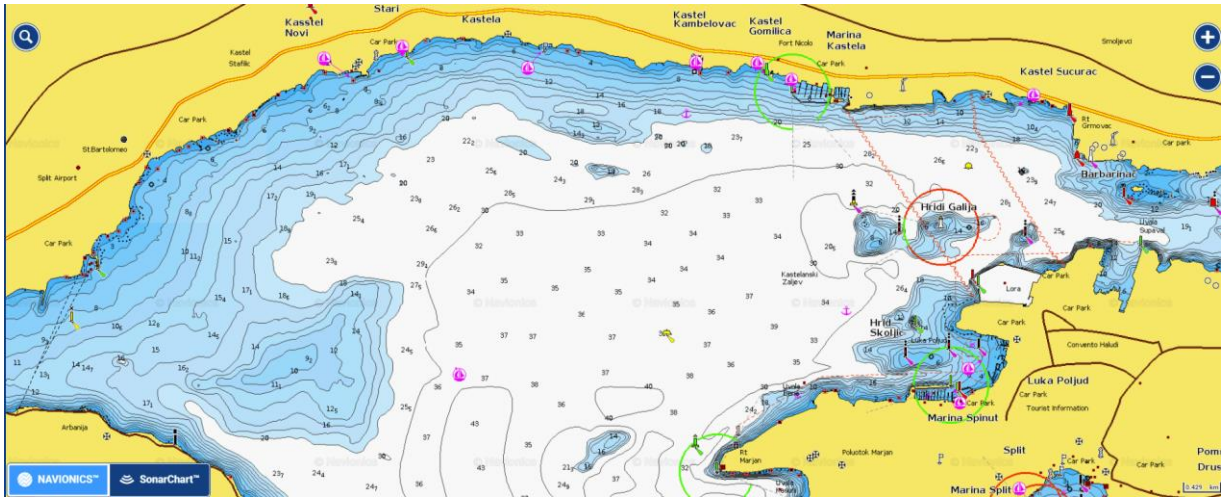

Figure 21. Kaštela bay batimetric features

11 Case study bathymetric features

Bathymetric features of Kaštela bay area have been shown in Figures 21 and 22. By the inspection of those sources, one can easily separate four sub areas:

- Coastal region along the Kaštela agglomeration – area nr. 1.;
- Western basin bounded by Čiovo, Trogir and Kaštel Novi - area nr. 2.;
- Eastern basin located close to the river Jadro mouth, harbor area and Vranjic - area nr. 3.;
- Mid bay - area nr. 4.;.

Area nr. 1. is characterised by dominantly regular bathymetry, with iso lines being parallel to coastline. Average sea bed slope equals to 2 to 5 %.

Area no. 2. is pretty shallow area compared to rest of the bay area and especially close to Pantan and Trogir area. Čiovo coastal area shows also shallow basins presence. At the very eastern part of this area one finds the existence of submerged reefs with tops located at around 9 m below the sea level.

Area nr. 3. is dominantly influenced and defined by the river Jadro and its contribution to bathymetric features being very shallow. Area with depth greater than 15 m is present strictly to the west from Barbarinac cliff.

Mid area represents the highest volumetric percentage of the sea water as found within the whole Kaštela bay. This implies the highest depth values, reaching up to 50 m beneath sea level.

From general point of view, Kaštela bay is categorised as deep one, relative to the Adriatic sea depth features. Following the wind generated wave period of 6.50 s, corresponding to 100 yrs return period, deep water zone border should be reached at around 30-32 m depth.

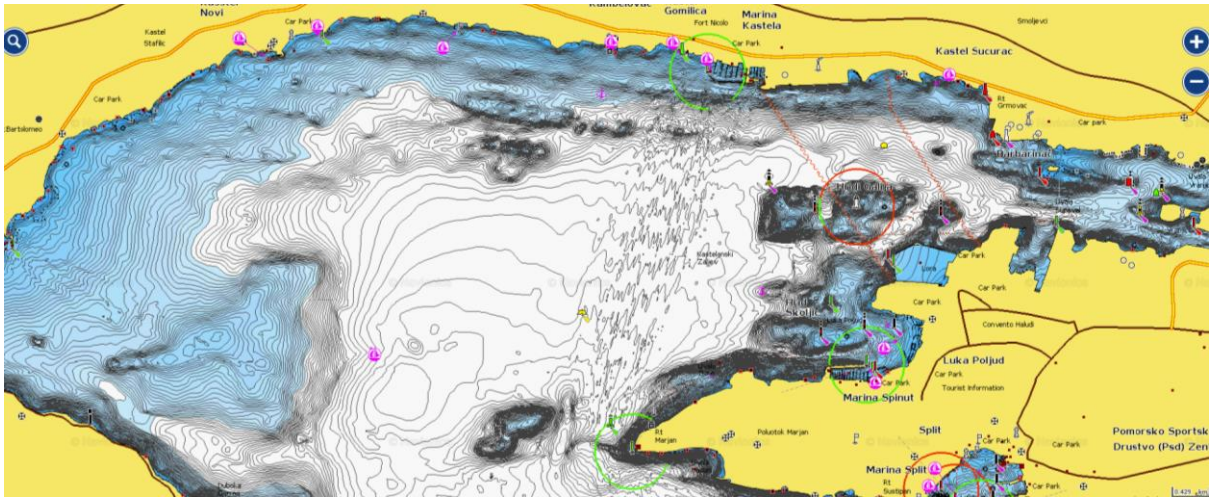

Figure 22. Batimetric features of Kaštela bay – dense grid

By the inspection of Figure 23, location with depth higher than 30 m has been detected at app. 1.35 km away from the coastline, to the south.

The bathymetric features of the pilot area (Figure 24) implies pretty regular bathymetry lines up to 15 -16 m depth with dominant direction west –east. Average sea bed slope equals to 3 % with only locally identified deviations.

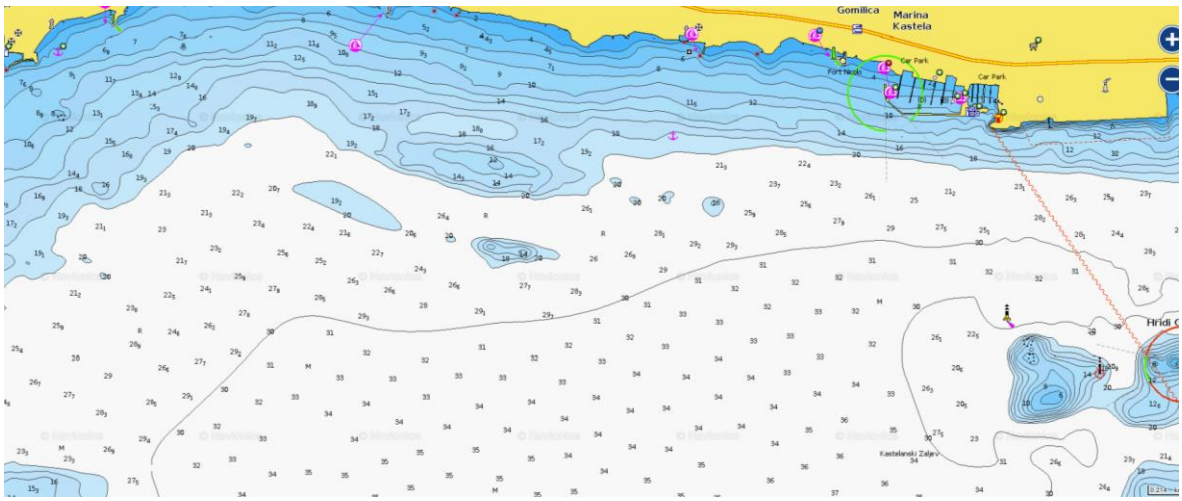

Figure 23. Depth view along the pilot area up to deep water

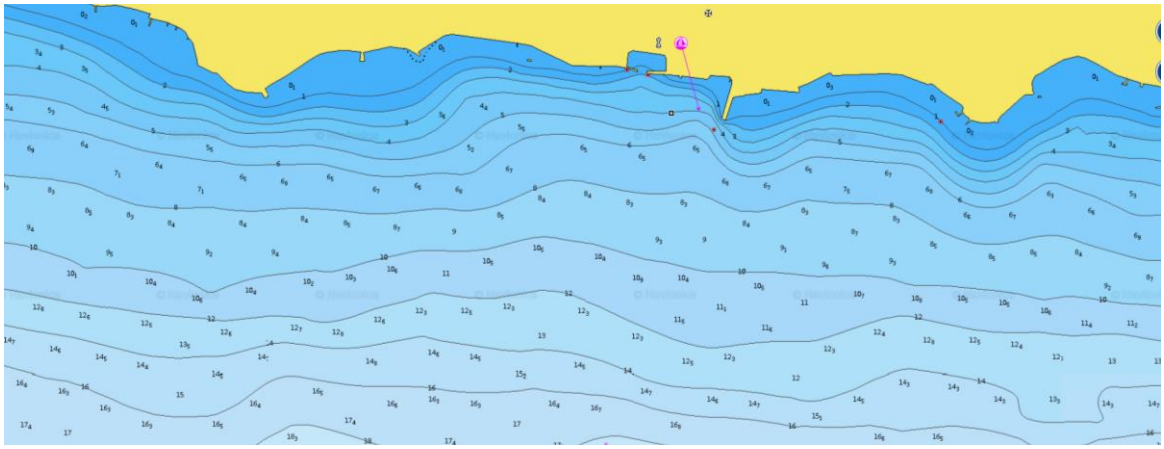

Figure 24. Bathymetry of the pilot area near field

12 Automatic meteorological station Split

Meteorological stations are organizational units of meteorological service at which meteorological observations (measurements and observations) are made according to the unified international regulations.

- According to the purpose and volume of work, as well as the equipment and qualification of the employees meteorological stations of the basic network are divided into:
- observatories,
- main or synoptic stations,
- regular or climatological stations,
- precipitation gauge stations i
- automatic stations.

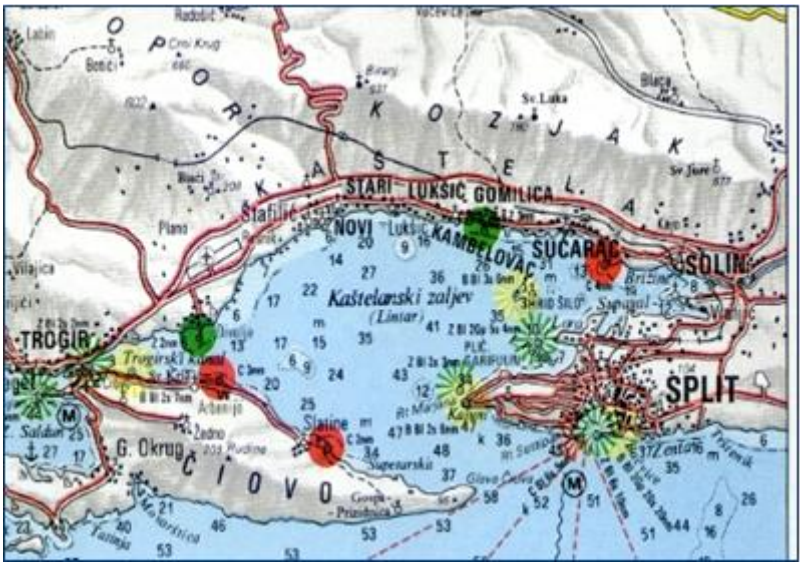

Figure 25. Position of the meteorological station Split Marjan

Figure 26. The position of the anemometer on the roof of meteorological station Split Marjan

Meteorological station Split with geographical coordinates: φ = 43 ° 31’ N, λ =16 ° 26' E, is located northwest of the city on the Marjan hill, at the atitude of h = 122 m (Figure 25). The terrain is a slope towards the sea on the SW-W-NW-N side. On the north is the bay of Kaštela and on the east city of Split. On the air distance of 7 km toward north is mountain Kozjak with the highest point at the atitude of 779 m.

Measuring system Fuess is located on the 5 m high terrace column on the building roof (12 m above ground). (Figure 26) Along its side, on August 20, 2003. on the same height, a sensor type 1, with measuring system microM was installed (Figure 25).

The only obstacles near meteorological building are on the west and northwest side (trees and terrain elevation overgrown with trees more than 10 m of height). Roughness class of the terrain is 2.5 (z_0 = 0.2).

Table 2. Main characteristics of electric anemograph Fuess

Unit	Fuess	mikroM
WIND SPEED		
sampling		1 s
measuring interval	0.8-1.3 do (40) 60 m/s	0.2 do 75 m/s
resolution	0.5 m/s	0.1 m/s
accuracy	0.5 m/s	0.1 m/s
averageing	hour	10-min
WIND DIRECTION		
Type	vjetrulja	vjetrulja 6-bitna
Interval	0°–360°	0°–360°
resolution	5°–10°	6°
accuracy	5°–10°	3°

As there are two different types of wind speed and wind direction, the archived data depend on the measurement method:

- Wind speed and direction data gained by the classic Feuss measuring are consisted of average hourly wind speed with corresponding wind direction and maximum current wind speeds (1-3 seconds) in corresponding hour or day. The average hourly wind speed is determined from the distance made in an hour. From all available hourly wind speeds it's possible to extract dana about maximum wind speed for a specific month or a year which is then called maximum average hourly wind speed for observed month or year. In the same way it's possible to determine maximum current wind speed for a specific month or a year which is then called maximum wind gust in a given month or year.
- Direction and wind speed data measured with digital measuring system microM (Tritonel type, marked mmSP and mmDR) are consisted of: average 10-minutes wind speed and dominant direction in those 10 minutes, maximum current wind speed (maximum wind gust – secondary value) and related direction, as well as the time when the maximum current wind speed was measured. From all available 10-minutes wind speeds it's possible to observe the

maximum wind speeds per month or year which are then called maximum average 10-minuted wind speeds. Calculation od average hourly wind speeds and related direction in given hour are based on the 10-minutes wind speeds and directions. Maximum monthly and annual values are determined by analog way, same as the data with classic measuring system.

In order to complement the image of the wind regime, data from climatological stations are used, where there is no anemograph yet the wind direction and strength are observed. Wind strength is assessed visually according to the effects of the wind on objects in nature in three climatological terms (7, 14 and 21 h) and is expressed in degrees of the Beaufort scale. This scale contains 0–12 degrees, which are associated with corresponding average wind speeds.

Beaufort scale (Table 3 i 4) was introduced for maritime purpose in the sailing boat time, so the intensity of the wind was estimated by the number of sails which standard sailing boat could have stretched in the given time.

Later was the scale updated according to the phenomenon, which are caused by the wind on the mainland:

- if leaves don't move and the smoke rises vertically, than it's silence,
- light breeze which men don't feel yet, but the smoke doesn't rise vertically,
- men just feel breeze on the face and the anemometer starts to turn,
- light wind constantly sways the leaves
- and moderate swings and smaller branches,
- moderately strong wind becomes uncomfortable for men, sways smaller branches and small trees,
- strong wind sways bigger branches and it's hard to carry an open umbrella,
- during very strong wind is hard to walk, wind sways bigger broadleaf trees, generating waves on the lake or the sea,
- stormy wind prevents any walking against the wind, stems are swaying and branches are being broken,
- storm throws tiles and causing smaller damages on the building,

- while a strong storm is pulling trees and making damages on buildings,
- the hurricane wind has a devastating effect on a larger area,
- and a hurricane devastates the whole area.

The direction of the wind is also determined visual with anemometer, which has only four directions. The observer is obliged to evaluate the wind direction to 16 directions and mark it with the direction from which the wind occurs.

Table 3. Beaufort scale

Beaufort (Bf)	Velocity		
	m/s	knot	km/h
0	0-0.2	< 1	<1
1	0.3-1.5	1-3	1-5
2	1.6-3.3	4-6	6-11
3	3.4-5.4	7-10	12-19
4	5.5-7.9	11-16	20-28
5	8.0-10.7	17-21	29-38
6	10.8-13.8	22-27	39-49
7	13.9-17.1	28-33	50-61
8	17.2-20.7	34-40	62-74
9	20.8-24.4	41-47	75-88
10	24.5-28.4	48-55	89-102
11	28.5-32.6	56-63	103-117
12	32.7 >	64 >	118 >

Table 4. Douglas scale

Intensity	Wave height (m)
0	0
1	0 - 0,1
2	0,1 - 0,5
3	0,5 - 1,25
4	1,25 - 2,5
5	2,5 - 4
6	4 - 6
7	6 - 9
8	9 - 14
9	preko 14

13 Distribution of scalar and vector components of wind speed

Wind, as the vector component, is determined by speed and direction, which is marked with the direction from which the wind occurs. Together with other meteorological elements, the wind characterizes processes in the atmosphere, which cause different weather conditions.

Wind speed measured on meteorological stations is determined with various factors (weather conditions of synoptic scale, surrounding topography, relation between mainland and sea, time of the day and year etc.). Strictly speaking, direct use of measured wind speeds on the station would only apply on the evaluation of the current regime, characteristic for that specific station.

Wind conditions in the Adriatic are strictly determined by geographical position, distribution of baric system of general circulation, sea and mainland influence, part of the day, year, etc. Certainly, some of the localities are under the influence of other various factors, which are exposure, concavity, convexity, slope, altitude, type of vegetation, existence of urban obstacles, etc . Thus, the wind is extremely spatially and weatherly variable meteorological parameter because it depends on orographic and other local conditions in the area. Due to developed orography of the coastal area and the influence of distribution of baric systems in synoptic and meso scales, it is obvious that there is complex local and circulatory flow regime in coastal area.

Measured wind dana (speed and direction) in meteorological service are gathered in relatively rare network of dots. Existing network of measuring dots is chosen in the way that provides gaining general characteristics of larger scale on the height of 10 m above ground in order to reduce friction impact due to the roughness of the substrate. However, the representativeness of the values at some point for a wider area depends on the terrain configuration, the roughness of the terrain and the proximity of shelters (obstacles) around the measuring point, the proximity of the sea etc.

To show the flow regime in Split area annual and seasonal tables of contingency are analyzed, that is relative and absolute frequencies (probabilities) of occurrence of individual speeds with the corresponding wind direction from the main meteorological station Split (2000 to 2009) were analyzed.

Results of the analysis are given in Tables 5-6.

Most common win directions in Split area are: NE (20.9 %), NNE (11.4 %), SE (10.0 %), cases of total number of data during a year. Those are familiar winds- bura and jugo (Figure 27).

Bura is a dry, cold and gust northeast wind that is in correlation with cold north air breach from colder areas. It occasionally occurs, especially in colder part of the year, in the north part of the east coast of Adriatic, but also in some other regions on Earth. It is a significant natural phenomenon, because it has an influence on life, organisms and vegetation evolution. Bura comes from the lan dan occurs, crossing the slopes of a mountains, mostly in the direction of the sea. It occurs usually with great, sometimes hurricane force, especially where the mountains stretch near the sea shore.

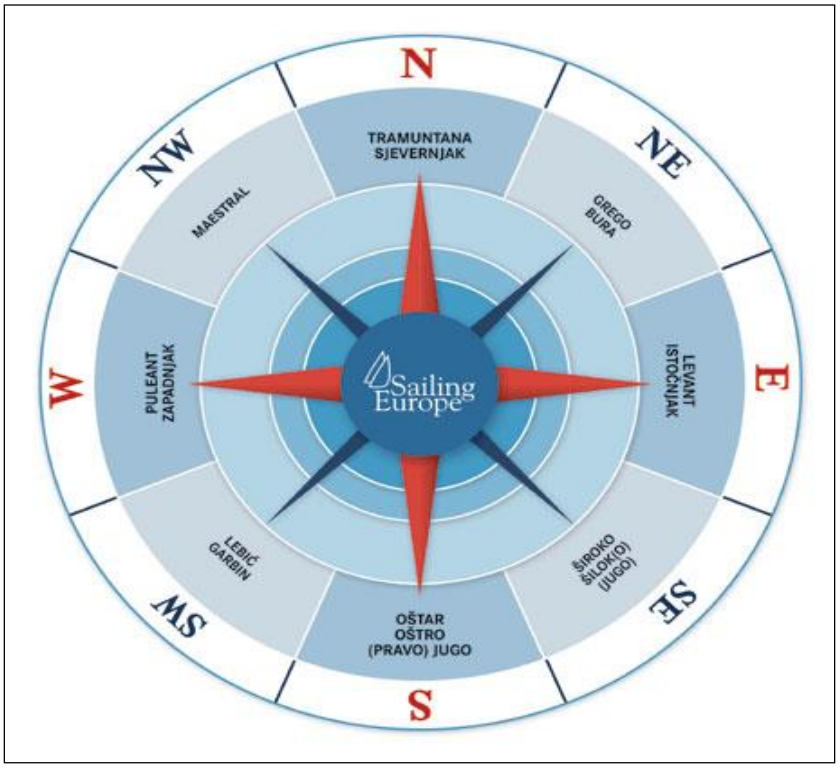

Figure 27. A wind rose with the nomenclature of the wind of a particular direction

Unlike the bura, jugo occurs at an uniform speed and creates large waves. Jugo or Široko is a wind blowing from the southeast in the Adriatic, and is usually associated with an oncoming cyclone from the western

Mediterranean. Jugo or Južina is also the name for the time brought by that wind and which is characterized by extremely bad biometeorological conditions. In the southern current, warm air flows from North Africa, which embraces maritime characteristics along the way.

SW wind which occurs in Split area in 9.5 % on annual scale should also be mentioned. That is lebić which occurs when a cyclone front goes threw Western Europe towards Bay of Genova. It creates big waves and blurs the sea. It is particularly strong in winter and autumn time.

Maestral (which occurs in Split area in 3.1 % of the time) is a refreshing northwest wind which in warmer days occurs from the sea towards mainland. It mainly occurs during the summer and only by the shore, rarely going further than 20 M (miles) towards mainland and it's strictly surface wind (up to 300 m of height). It starts around 10 A.M.. Around 2 P.M. it achieves its maximum and it's always finished before sunset (usually around 6 P.M.) Maestral goes with good weather and at the same time significantly alleviates summer heat. It normally occurs like a light wind (up to 4 Bf). In the Gulf of Trieste it is the weakest, towards the south it is getting stronger, and in the Gate of Otranto it reaches a strength of 6-7 Bf, with quite heavy sea. On our coast maestral occurs mainly from NW, turns to the WNW, and along the Albanian coast to the SW. During the day maestral changes its course to the right, towards the sun. Iti s often followed by nice weather cumulus.

NE and NNE winds are the most common winds in this area. Throughout all seasons, they are the most common, so their frequency ranges from 27.7% in winter to 15.0% in summer. In winter and spring, SE wind occurs with a frequency of about 10.0%, while in summer is at its lowest (6.2%). NW wind (maestral) is slightly more emphasized in summer (3.8%) than in other parts of the year, which is understandable, considering that the maestral occurs in the warmer part of the year. Its frequency is lowest in spring and autumn (2.8%).

Silences, that is windless situations, in the Split area are most common in summer (3.4%) and in spring (4.0%), and rarest in winter (7.7%). At the annual level, the percentage of silence is around 5.1%.

Moderate wind (5.5 to 10.7 m / s, that is 4 and 5 Bf) occurs in the Split area in 22.6% of cases per year. Moderate wind most often occurs in winter (27.7%), autumn (24.6%), spring 23.6%, while in summer

it is slightly more rare and occurs in 13.4%. NE, NNE, SE and ESE winds mainly occur in moderate strength. Strong wind (> 10.7 m / s, ie 6 Bf and 7 Bf) occurs in the annual average in 4.6% of cases). In winter, however, its frequency is 7.4%, in autumn 5.2%, in spring 4.8%, and in summer it is insignificant and it's 1.0%. The strong wind on an annual basis mostly occurs from the SE direction. Stormy wind (> 17.1 m / s and ≥ 8 Bf) in the observed 10-year period was recorded in the Split area in 0.1% of cases per year, mainly in winter (0.3%), in spring and autumn (0.1%), and at least in summer (0.2%), mainly from the SE direction. Note that this statistic refers to average hourly speeds rather than current wind speeds.

Table 5. Relative contingency table for Split period 2000.–2009.

Scale(Bf)	0	1	2	3	4	5	6	7	8	9	10	11	12	Sum
Velocity. (m/s)	0.0-0.2	0.3-1.5	1.6-3.3	3.4-5.4	5.5-7.9	8.0-10.7	10.8-13.8	13.9-17.1	17.2-20.7	20.8-24.4	24.5-28.4	28.5-32.6	32.7-36.9	
N		14.8	16.6	4.9	2.0	0.6	0.2	0.01						39.0
NNE		11.7	27.5	21.9	25.5	19.2	6.5	1.2	0.2	0.1				113.9
NE		17.4	60.1	50.1	42.4	28.5	7.9	2.0	0.6	0.06	0.02			209.0
ENE		13.8	38.1	17.9	4.5	1.4	0.2	0.03						76.0
E		9.1	13.7	8.3	2.4	0.2	0.01	0.02						33.8
ESE		10.5	14.9	15.9	22.1	14.5	5.7	1.1	0.01					84.7
SE		10.6	11.9	14.3	22.3	24.2	13.3	3.4	0.3					100.4
SSE		11.0	13.1	3.2	2.6	2.6	1.8	0.5	0.06					34.9
S		11.3	10.2	1.6	1.3	1.2	0.8	0.5	0.01					27.0
SSW		11.1	27.5	6.1	1.8	1.3	0.7	0.2	0.02					48.7
SW		21.0	49.2	21.8	2.5	0.3	0.1	0.01						94.9
WSW		14.0	20.2	12.7	1.7	0.02								48.7
W		4.0	6.3	1.9	0.2	0.01								12.4
WNW		5.3	9.5	1.7	0.05	0.01								16.6
NW		9.5	16.6	4.2	0.4	0.03	0.02							30.8
NNW		10.8	10.2	2.7	0.5	0.09								24.3
C	5.1													5.1
Sum	5.1	186.0	345.7	189.3	132.3	94.0	37.2	9.0	1.2	0.2	0.02			1000.0

Table 6. Absolute contingency table for Split period 2000.–2009.

Scale (Bf) / Velocity (m/s)	0 0.0-0.2	1 0.3-1.5	2 1.6-3.3	3 3.4-5.4	4 5.5-7.9	5 8.0-10.7	6 10.8-13.8	7 13.9-17.1	8 17.2-20.7	9 20.8-24.4	10 24.5-28.4	11 28.5-32.6	12 32.7-36.9	Sum
N		1274	1427	419	170	54	13	1						3358
NNE		1010	2368	1881	2193	1648	563	104	19	10				9796
NE		1494	5175	4307	3645	2453	678	172	49	5	2			17980
ENE		1186	3281	1544	391	118	15	3						6538
E		786	1181	714	210	15	1	2						2909
ESE		901	1281	1369	1902	1248	490	94	1					7286
SE		910	1025	1233	1919	2084	1142	294	29					8636
SSE		949	1125	277	227	220	158	42	5					3003
S		976	878	134	115	101	72	43	1					2320
SSW		959	2366	525	151	110	56	20	2					4189
SW		1807	4234	1873	219	25	10	1						8169
WSW		1204	1742	1096	143	2								4187
W		346	538	166	16	1								1067
WNW		455	817	150	4	1								1427
NW		819	1431	365	31	3	2							2651
NNW		929	876	231	45	8								2089
C	438													438
Sum	438	16005	29745	16284	11381	8091	3200	776	106	15	2			86043

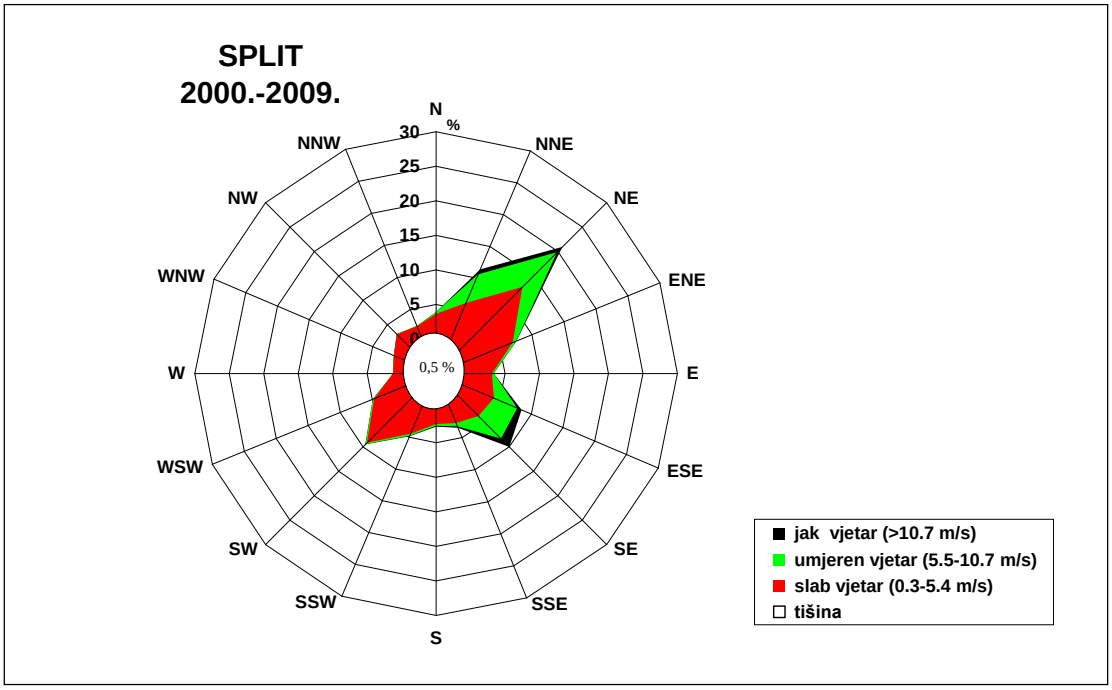

Figure 28. Annual wind rose for City of Split 2000.-2009.

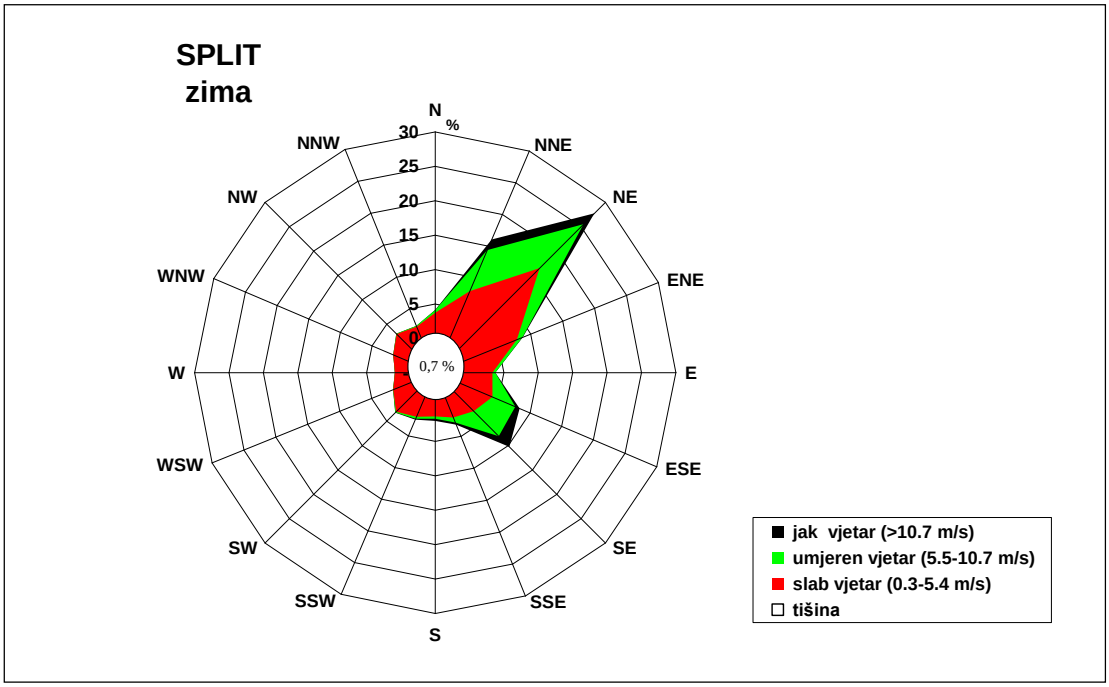

Figure 29. Seasonal wind rose for City of Split 2000.-2009. (winter)

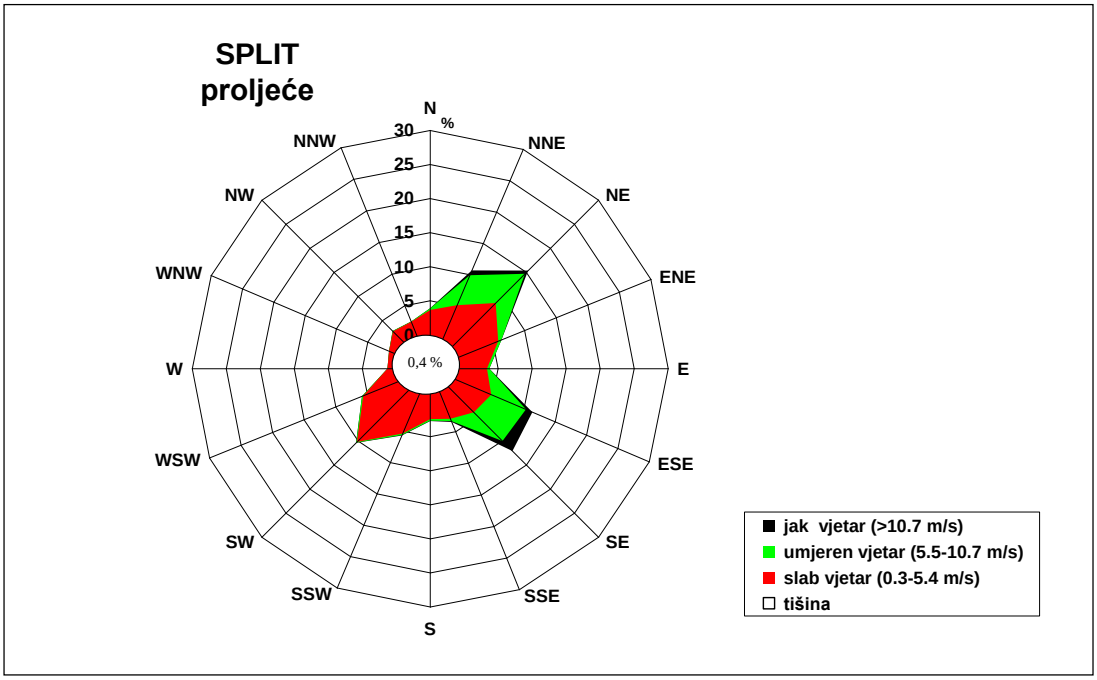

Figure 30. Seasonal wind rose for City of Split 2000.-2009. (spring)

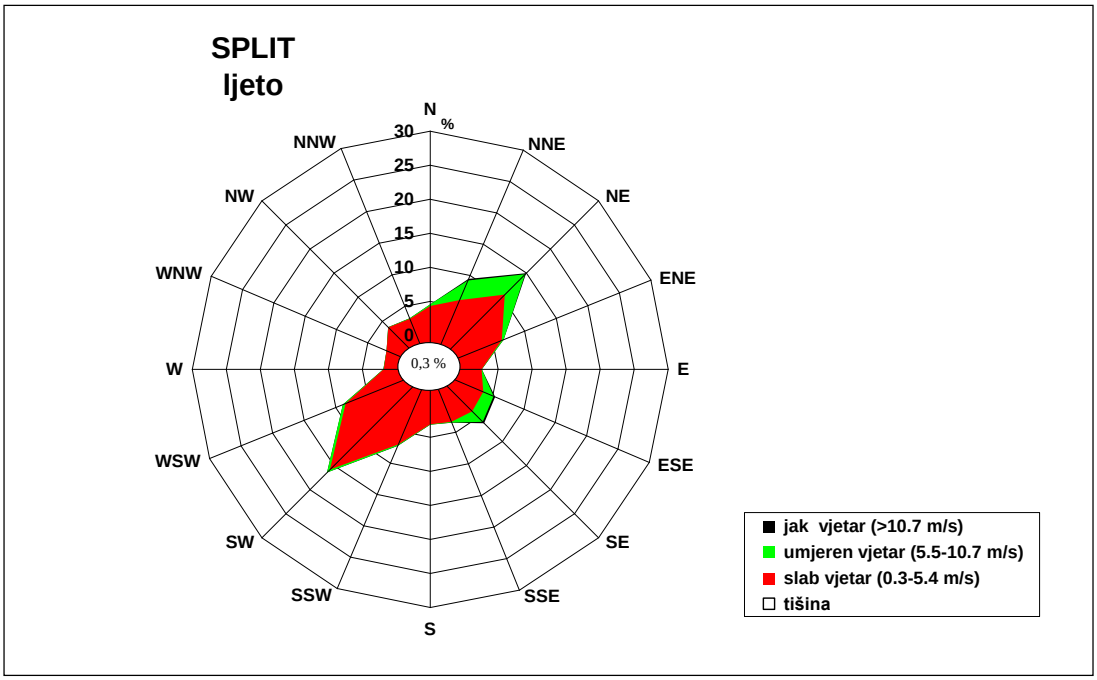

Figure 31. Seasonal wind rose for City of Split 2000.-2009. (summer)

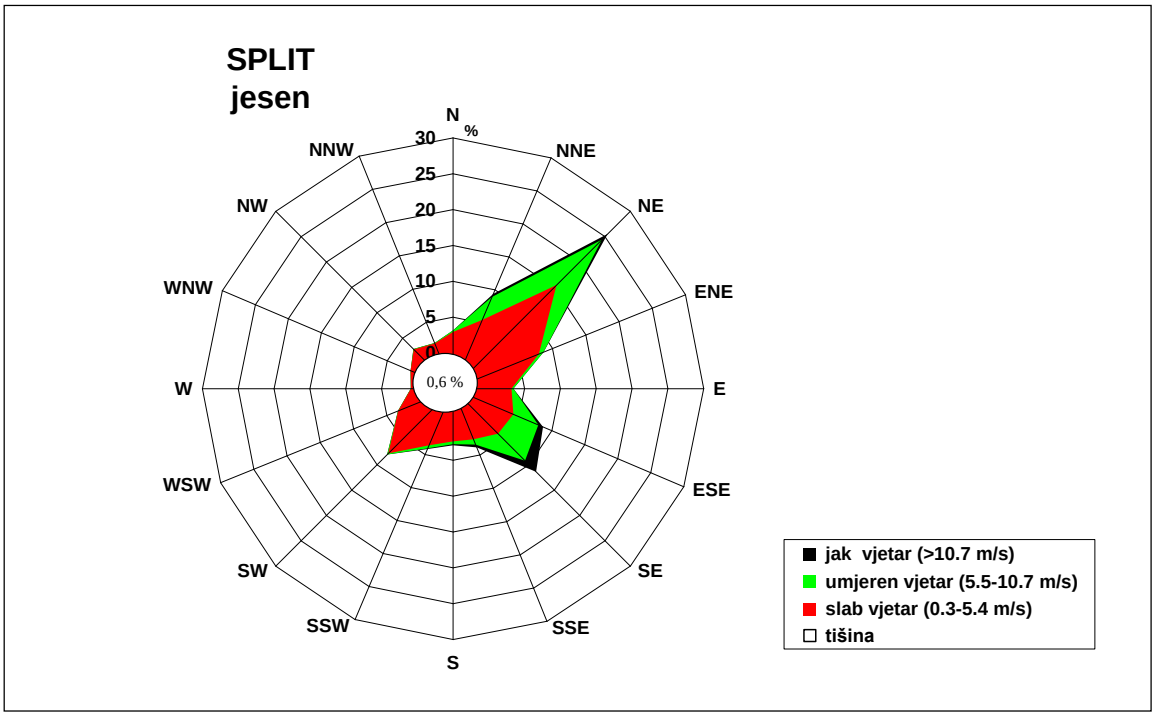

Figure 32. Seasonal wind rose for City of Split 2000.-2009. (autumn)

14 Characteristics of strong and stormy wind

Present analysis of wind speed in Split area has been made according to the hourly values of wind strength and direction from the meteorological station Split. However, the wind is not a discrete value, but continuous and it can show as strong or stormy wind outside the observation period. That is the reason why the observes records the time of the beginning and ending of the wind stronger that 6 Bf and 8 Bf. In this case, days with strong and stormy winds are determined from the maximum hourly speeds. A day with a strong / stormy wind is a day in which a wind over 6 Bf or over 8 Bf has been recorded at least once. In order to gain a complete image of the wind regime with strong and stormy winds in the required area from such a record, an analysis of the average monthly and annual number of days with strong and stormy wind for Split was made (2000 to 2009).

According to the analyzed 10 year period, strong wind (more than 6 Bf) in the area of Split occurs in average of 87 days per year. The highest number of days with strong wind (more than 6 Bf) was recorded in 2009, when there were 103, and the lowest in 2000, when there were 69. Analyzing the monthly data in a 10 year period, it can be seen that the frequency of strong wind was the highest in November (124 days, average 12.4 days) and December (119 days, average 11.9 days), and lowest in July (30 days, average 3.0 days) and August (31 days, average 3.1 days). .

Stormy wind (more than 8 Bf) in the area of Split in the observed 10 year period was recorded 117 times, which is an average of 11.7 days per year. The highest frequency of stormy wind was recorded during the winter months, that is through December (20 days) and March (20 days). The lowest frequency of this phenomenon was recorded in August (2 days) and July and September (2 days). The highest number of days with stormy wind was recorded in 2006 (24 days), and the lowest in 2002 (5 days).

Since the wind is a very variable meteorological element, the number of days with strong and stormy winds in the winter months in the Split area varies from year to year, as shown by the relatively large values of the standard deviation.

15 Characteristics of wind duration of strong and stormy wind

The effect of the wind on objects is not only a condition of speed but also of duration. That means that a strong wind gust can be less of a burden for an object or wave formation then longer lasting wind of smaller speed. For building design it's often necessary to know duration of the wind in certain direction for different speeds. he formation of waves at sea is caused by a stronger wind, so the average hourly wind speeds ≥ 5.5 m / s (from moderate wind to higher) were observed. Therefore, the duration of wind occurring in the area of Split (2000-2009) was analyzed on the basis of data on average hourly wind speeds and directions.

Since the analysis is made from average hourly wind speeds, then the speed classes are defined as follows:

- First class – 4 Bf corresponds to a speed class from 5.5 m/s to 7.9 m/s (moderate breeze)
- Second class – 5 Bf corresponds to a speed class from 8.0 m/s to 10.7 m/s (moderately strong wind)
- Third class – 6 Bf corresponds to a speed class from 10.8 m/s to 13.8 m/s (strong wind)
- Fourth class – 7 Bf corresponds to a speed class from 13.9 m/s to 17.1 m/s (very strong wind)
- Fifth class – 8 Bf corresponds to a speed class from 17.2 m/s to 20.7 m/s (stormy wind)
- Sixth class – 9 Bf corresponds to a speed class from 20.8 m/s to 24.4 m/s (strong stormy wind)
- Seventh class – 10 Bf corresponds to a speed class from 24.5 m/s to 28.4 m/s (hurricane wind)
- Eighth class – 11 Bf corresponds to a speed class from 28.5 m/s to 32.6 m/s (strong hurricane wind)
- Ninth class – 12 Bf corresponds to a speed class from above 32.6 m/s (hurricane)

Of the total number of observed data of average hourly wind speeds at the meteorological station Split (86043 hourly values, Table 6 - absolute frequencies), 27.4% (23571 data) refer to speeds higher than 5.5 m / s. As the speed class increases, the number of data also decreases, so in the first class there are

11381 data (13.2%), in the second 8091 (9.4%), in the third 3200 (3.7%), in the fourth 776 (0.9%), in the fifth 106 (0.1 %), in the sixth 15 (0.02%), in the seventh 2 data, while in the eighth and ninth grade there is no data. The other 72.6% of the data refer to wind speeds from 0.0 to 5.4 m / s.

Moderate breeze (first class – 4 Bf corresponds to a speed class from 5.5 m/s to 7.9 m/s) occurs the longest from NE, NNE, SE and SSE and their duration exceeds 16 hours.

Moderately strong wind (second class - 5 Bf corresponds to a speed class from 8.0 m/s to 10.7 m/s) occurs the longest also from NE, SE i ESE, so its duration can be over 16 hours continuously. In 27.2 % of cases moderately strong wind occurs from NE direction, and from the SE direction i 23.9 of cases. The most common is occurring from all directions for up to 1 hour (59.1 %). As the duration of occurrence increases, the percentage of representation decreases, which suggests that these are not common cases.

Strong wind (third class – 6 Bf corresponds to a speed class from 10.8 m/s to 13.8 m/s) has the most pronounced occurrence from NE (more than 16 hours) and SE (up to 15 hours), taking into consideration that in this class winds from WSW, W,WNW i NNW are not registered in 10-year period. Wind from the SE occurs in 31.5 % of the cases, and from the NE in 21.3 % of the cases.

Very strong wind (fourth class – 7 Bf corresponds to a speed class from 13.9 m/s to 17.1 m/s) occurs the longest from NE direction and it can take up to 12 hours, with frequency of 20.4 %. The SE wind is recorded more in this class and its duration can be up to 11 hours with frequency of 34.9 %.

Stormy wind (fifth class – 8 Bf corresponds to a speed class from 17.2 m/s to 20.7 m/s) occurs intensively from NE with frequency of 37.9 % and duration up to 7 hours. In this class wind from SE also occurs, it can take up to 4 hours, with frequency of 27.6 %.

Strong stormy wind (sixth class – 9 Bf corresponds to a speed class from 20.8 m/s to 24.4 m/s) occurs strictly from NE and NN, from 2 - 7 hours, with frequency of 50.0 %.

Hurricane wind (seventh class – 10 Bf corresponds to a speed class from 24.5 m/s to 28.4 m/s) occurs, as well as in the sixth class, from the NNE an NE (blowing up to 5 hours) and from SW (blowing up to 2 hours).

Winds with an average hourly speed over 11Bf (corresponds to a speed class of 28.5 m / s to 32.6 m / s - strong hurricane - eighth class) and 12 Bf (corresponds to a speed class of over 32.6 m / s - ninth class) were not recorded in 10 year period in the area of Split.

From the above analysis of the data from Table 7, a conclusion can be made, that increasing the wind speed reduces the possibility of wind occurring from different directions. At lower wind strengths (4 and 5 Bf), winds NE, SE and NNE dominate in the Split area. At intensities of 6 Bf, the NE (27.2%), SE (23.9%) and NNE directions (20.4%) are also present, and even at higher intensities these directions take over. By increasing the strength of the wind, its duration of occurring decreases. Only at 9 Bf NE and NNE winds occur.

Table 7. Relative occurrence frequencies of mean hourly value wind speed for Split, period 2000.–2009.

Velocity 5.5 m/s to 7.9 m/s																	
Duration (h)	**1**	**2**	**3**	**4**	**5**	**6**	**7**	**8**	**9**	**10**	**11**	**12**	**13**	**14**	**15**	**≥16**	**Sum**
N	12.9	3.7	0.8	1.0	0.2	0.2											18.8
NNE	111.5	39.8	17.4	8.6	4.1	3.0	1.4	1.5	0.2	0.8		0.3	0.2	0.3		0.3	189.6
NE	149.3	63.5	31.7	15.2	10.5	5.8	3.0	2.4	2.2	1.2	0.5	0.2	0.5	0.2		0.5	286.6
ENE	39.3	9.5	1.7	0.7													51.1
E	19.1	4.4	0.7	0.5	0.2		0.2	0.2									25.2
ESE	83.3	27.9	16.9	9.1	5.8	3.9	1.0	0.3	1.2	0.3	1.2					0.3	151.3
SE	93.8	36.1	15.9	6.8	3.9	2.5	1.4	1.0	0.7	0.8	0.7	0.2	0.2			0.3	164.2
SSE	22.0	5.1	0.5	0.7	0.2	0.2											28.6
S	11.8	3.2	0.2	0.2													15.4
SSW	13.7	3.4	1.2	0.2	0.2												18.6
SW	14.2	5.1	2.0	1.4	0.2												22.9
WSW	9.5	2.0	2.4	0.5	0.2												14.6
W	1.5	0.5															2.0
WNW	0.7																0.7
NW	4.4	0.2	0.2														4.7
NNW	4.4	1.0	0.2	0.2													5.8
n/p																	
Sum	591.4	205.3	91.7	45.0	25.2	15.6	6.9	5.4	4.2	3.2	2.4	0.7	0.8	0.5	0.0	1.5	1000.0
Velocity 8.0 m/s to 10.7 m/s																	

Duration (h)	1	2	3	4	5	6	7	8	9	10	11	12	13	14	15	≥16	Sum
N	6.4	1.9	0.3	0.3	0.6												9.4
NNE	100.7	48.5	22.7	10.3	6.9	6.1	1.9	3.1	0.8	0.8	0.6	0.6	0.6	0.3			203.8
NE	129.2	58.5	28.3	18.3	9.7	8.9	6.7	2.5	3.6	2.2	1.9	0.6	0.6		0.6	0.6	272.0
ENE	20.2	5.3	0.3	0.3													26.1
E	3.1	0.6															3.6
ESE	83.7	33.8	16.6	6.9	6.4	3.1	1.1	1.7	1.9	0.8	0.6	0.3			0.3	0.3	157.5
SE	109.8	57.1	27.2	18.3	10.5	4.7	3.9	2.2	1.7	0.8	0.8	0.8		0.3	0.0	1.1	239.3
SSE	26.6	6.7	1.9	2.2	0.3	0.8											38.5
S	16.1	3.9			0.8												20.8
SSW	13.6	5.5	1.1	0.3	0.3												20.8
SW	2.5	1.9	0.3														4.7
WSW	0.6																0.6
W	0.3																0.3
WNW	0.6																0.6
NW	0.8																0.8
NNW	0.8				0.3												1.1
n/p																	
Sum	515.0	223.8	98.7	56.8	35.8	23.6	13.6	9.4	8.0	4.7	3.9	2.2	1.1	0.6	0.8	1.9	1000.0

Velocity 10.8 m/s to 13.8 m/s

duration (h)	1	2	3	4	5	6	7	8	9	10	11	12	13	14	15	≥16	Sum
N	5.4	0.7	0.7														6.7
NNE	104.3	41.7	22.2	11.4	4.7	3.4	2.7	2.0									192.5
NE	113.7	45.1	21.5	10.8	8.1	6.1	4.7	0.7	2.0							0.7	213.3
ENE	2.0	1.3	0.0	1.3													4.7
E	0.7																0.7
ESE	69.3	34.3	13.5	8.7	6.7	4.7	2.7	0.7	0.7	0.7	1.3						143.3
SE	145.4	61.9	47.8	23.6	8.7	8.1	6.7	2.7	3.4	3.4	0.7	2.0			0.7		314.9
SSE	32.3	12.1	6.1	2.7	0.7	1.3	1.3										56.5
S	23.6	8.1	2.0	0.7													34.3
SSW	16.2	6.1	1.3	1.3													24.9
SW	6.7																6.7
WSW																	0.0
W																	0.0
WNW																	0.0
NW	1.3																1.3
NNW																	

n/p																	
Sum	520.9	211.3	115.1	60.6	28.9	23.6	18.2	6.1	6.1	4.0	2.0	2.0			0.7	0.7	1000.0
Velocity 13.9 m/s to 17.1 m/s																	
duration (h)	**1**	**2**	**3**	**4**	**5**	**6**	**7**	**8**	**9**	**10**	**11**	**12**	**13**	**14**	**15**	**≥16**	**Sum**
N	2.5																2.5
NNE	100.5	27.6	15.1	7.5		5.0											155.8
NE	118.1	37.7	15.1	10.1	10.1		7.5	2.5				2.5					203.5
ENE	7.5																7.5
E		2.5															2.5
ESE	85.4	17.6	12.6	5.0	5.0		5.0										130.7
SE	180.9	85.4	40.2	12.6	7.5	5.0	5.0	5.0	2.5	2.5	2.5						349.2
SSE	37.7	12.6	7.5	5.0													62.8
S	27.6	7.5	2.5	7.5	2.5	2.5											50.3
SSW	17.6	12.6	2.5														32.7
SW	2.5																2.5
WSW																	
W																	
WNW																	
NW																	
NNW																	
n/p																	
Sum	580.4	203.5	95.5	47.7	25.1	12.6	17.6	7.5	2.5	2.5	2.5	2.5					1000.0
Velocity 17.2 m/s to 20.7 m/s																	
duration (h)	**1**	**2**	**3**	**4**	**5**	**6**	**7**	**8**	**9**	**10**	**11**	**12**	**13**	**14**	**15**	**≥16**	**sum**
N																	
NNE	120.7	51.7	34.5														206.9
NE	155.2	120.7	51.7		34.5		17.2										379.3
ENE																	
E																	
ESE	17.2																17.2
SE	155.2	51.7	34.5	34.5													275.9
SSE	51.7	17.2															69.0
S	17.2																17.2
SSW	34.5																34.5
SW																	

WSW																	
W																	
WNW																	
NW																	
NNW																	
n/p																	
Sum	551.7	241.4	120.7	34.5	34.5		17.2										1000.0
Velocity 20.8 m/s to 24.4 m/s																	
Duration (h)	**1**	**2**	**3**	**4**	**5**	**6**	**7**	**8**	**9**	**10**	**11**	**12**	**13**	**14**	**15**	**≥16**	**Sum**
N																	
NNE	375.0						125.0										500.0
NE	375.0	125.0															500.0
ENE																	
E																	
ESE																	
SE																	
SSE																	
S																	
SSW																	
SW																	
WSW																	
W																	
WNW																	
NW																	
NNW																	
n/p																	
Sum	750.0	125.0					125.0										1000.0
Velocity 24.5 m/s to 28.4 m/s																	
duration (h)	**1**	**2**	**3**	**4**	**5**	**6**	**7**	**8**	**9**	**10**	**11**	**12**	**13**	**14**	**15**	**≥16**	**Sum**
N																	
NNE																	
NE	1000.0																1000.0
ENE																	
E																	
ESE																	

SE																	
SSE																	
S																	
SSW																	
SW																	
WSW																	
W																	
WNW																	
NW																	
NNW																	
n/p																	
sum	1000.0																1000.0

16 Fetch definition

There is a wide spectra of methods and computational models intended to resolve the problems of defining fetch length. One of the methods used for computation of effective fetches was developed by Saville (year of 1954.). He assumed that the wind transmits the energy on a water surface in the direction of the wind blowing. He believes that the wind transmits energy not only in that, but also in directions that deviate from the main direction by +/- 42 °.

The procedure in determining the effective wave follows these steps according to:

The main ray is being situated in the direction of the blowing wind, then is rotated by 6° clockwise (up to -42°) and counterclockwise (up to +42°) and the directions threw the same starting point are set. The length of each ray from the starting point to the first obstacle point are determined and the sum of their projections on the central ray is calculated. That sum is devided by the sum of the cosines of the angles of the central ray and other rotated rays, by which the value of the length of effective fetch is gained.

$$F_{EFF} = \frac{\sum_{i=1}^{15} f_i \cdot \cos^2 \theta_i}{\sum_{i=1}^{15} \cos \theta_i}$$

F_{EFF} = effective fetch [km]

Θ_i = line angle [°]

f_i = line length [km]

Another method that is used is called simple fetches method, where the fetches are determined threw arithmetic center fetches in steps of 3° (overall range 24°). This method is more conservative from the one above, but easier for implementation. Both methods assume that the wave direction is related to wind direction, and that the spectral energy form is independent of the fetch form.

The results of the calculation of the effective fetch length for wind directions that are critical in terms of the subject structure and intervention are defined based on the following criteria:

- Position of the intervention in relation to the position of the island and mainland in the environment
- Significant frequencies of higher wind speeds for individual directions
- Significant fetch lengths as the dominant factor in defining significant wave height

In terms of the development of the waves of significant heights, it can be immediately detected that the winds of the third and fourth quadrants are critical in terms of their effect on objects in the area. Given the direction of the coastline, the winds of the first and second quadrants are not relevant in this case.

In this way, seven relevant directions have been defined for which the length of the fetch will be defined (ESE, SE, SSE, S, SSW, SW, WSW).

The graphic display of the effective fetch calculation is shown graphically (Figure 33-39). It is important to emphasize that the results were obtained by the Saville method.

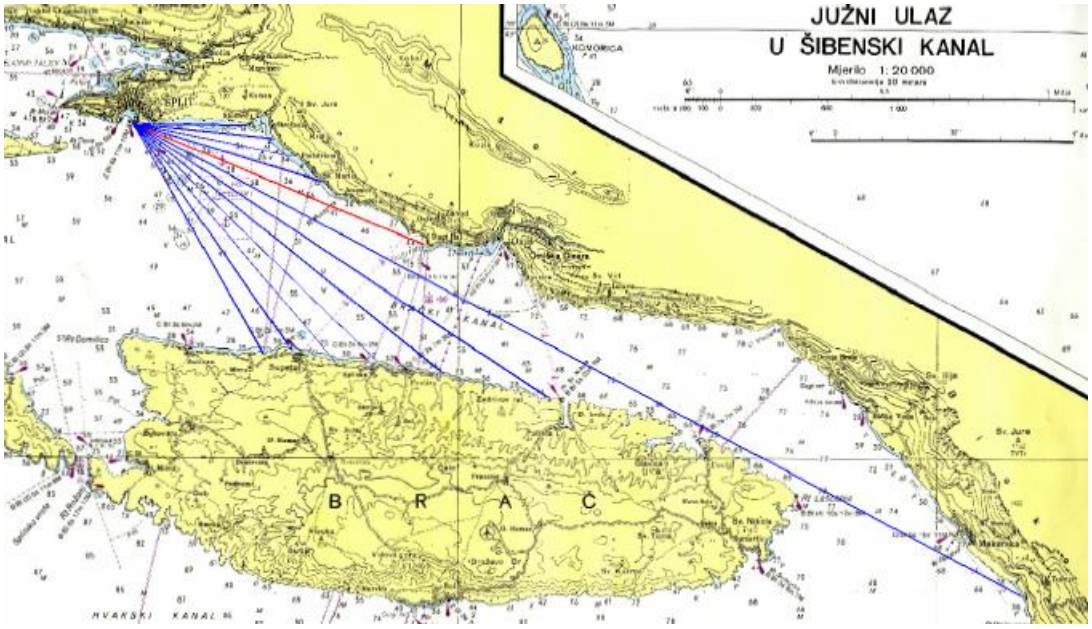

Figure 33. Fetch definition for incident direction ESE

Table 8. Fetch definition for incident direction ESE

Kut α (°)	cosα	cos²α	d (km)	Σd		d·cos²α
42	0,743	0,552	14,9			8,23
36	0,809	0,655	15,6			10,21
30	0,866	0,750	17,6			13,20
24	0,914	0,835	19,3			16,11
18	0,951	0,905	22,5			20,35
12	0,978	0,957	28,1			26,89
6	0,995	0,989	56,7	196,8	227,3	56,08
0	1,000	1,000	17,8			17,80
-6	0,995	0,989	11,2			11,08
-12	0,978	0,957	9,1			8,71
-18	0,951	0,905	8			7,24
-24	0,914	0,835	6,5			5,42
-30	0,866	0,750	0			0,00
-36	0,809	0,655	0			0,00
-42	0,743	0,552	0			0,00
Σ(30)	10,407					
Σ(42)	13,511					201,31
Lef.=	18,9	km				

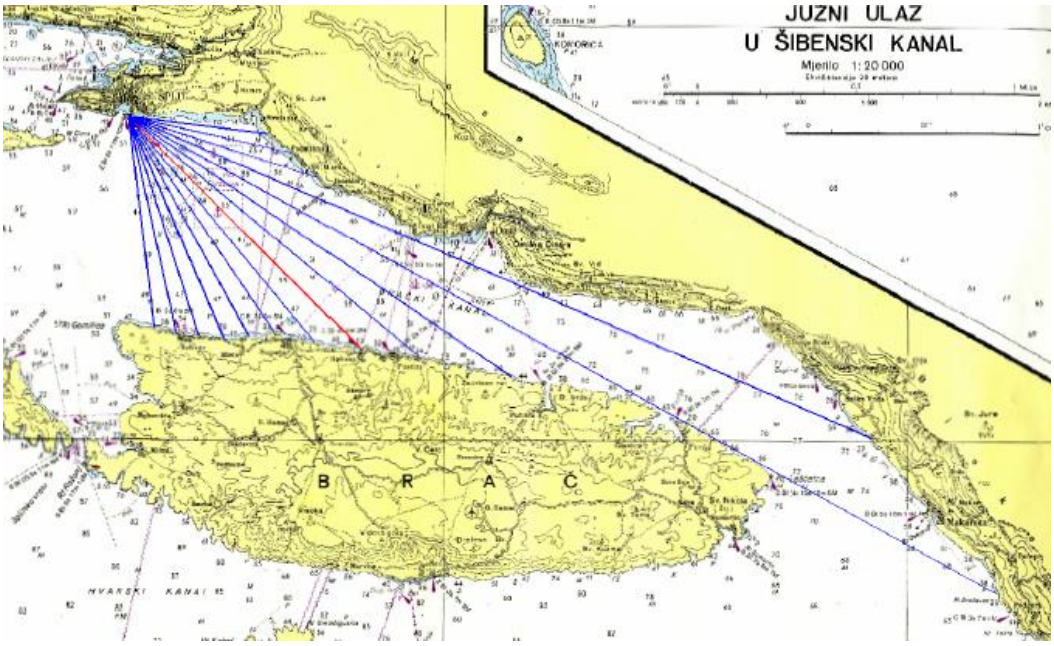

Figure 34. Fetch definition for incident direction SE

Table 9. Fetch definition for incident direction SE

Kut α (°)	cosα	cos²α	d (km)	Σd		d·cos²α
42	0,743	0,552	12,3		300,9	6,79
36	0,809	0,655	12,8			8,38
30	0,866	0,750	13,3	257,9		9,98
24	0,914	0,835	14			11,68
18	0,951	0,905	14,6			13,21
12	0,978	0,957	15,1			14,45
6	0,995	0,989	17			16,81
0	1,000	1,000	19			19,00
-6	0,995	0,989	21,8			21,56
-12	0,978	0,957	26,8			25,64
-18	0,951	0,905	57,7			52,19
-24	0,914	0,835	47,1			39,31
-30	0,866	0,750	11,5			8,63
-36	0,809	0,655	9,7			6,35
-42	0,743	0,552	8,2			4,53
Σ(30)	10,407					
Σ(42)	13,511					258,50
Lef.=	24,8	km				

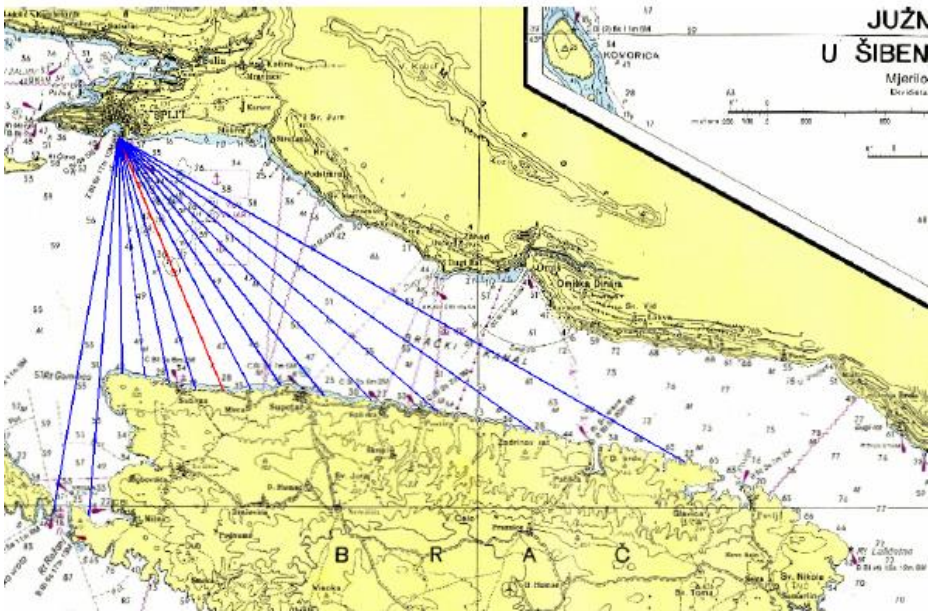

Figure 35. Fetch definition for incident direction SSE

Table 10. Fetch definition for incident direction SSE

Kut α (°)	cosα	cos²α	d (km)	Σd		d·cos²α
42	0,743	0,552	33,2			18,34
36	0,809	0,655	25,9			16,95
30	0,866	0,750	21,4			16,05
24	0,914	0,835	18,5			15,44
18	0,951	0,905	16,8			15,20
12	0,978	0,957	15			14,35
6	0,995	0,989	14,4			14,24
0	1,000	1,000	13,9	169,6	265,8	13,90
-6	0,995	0,989	13,3			13,15
-12	0,978	0,957	12,7			12,15
-18	0,951	0,905	12,3			11,13
-24	0,914	0,835	12			10,01
-30	0,866	0,750	19,3			14,48
-36	0,809	0,655	19,3			12,63
-42	0,743	0,552	17,8			9,83
Σ(30)	10,407					
Σ(42)	13,511					207,85
Lef.=	19,7	km				

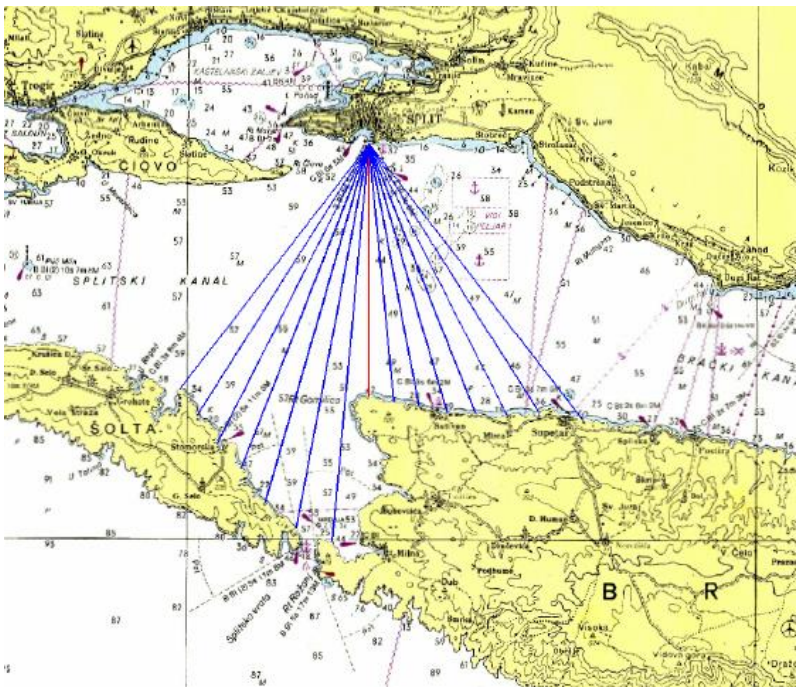

Figure 36. Fetch definition for incident direction S

Table 11. Fetch definition for incident direction S

Kut α (°)	cosα	cos²α	d (km)	Σd		d·cos²α
42	0,743	0,552	14,7		226,8	8,12
36	0,809	0,655	15,2			9,95
30	0,866	0,750	15,9	165,4		11,93
24	0,914	0,835	16,5			13,77
18	0,951	0,905	17,6			15,92
12	0,978	0,957	18,5			17,70
6	0,995	0,989	18,9			18,69
0	1,000	1,000	11,9			11,90
-6	0,995	0,989	12,2			12,07
-12	0,978	0,957	12,6			12,06
-18	0,951	0,905	13,2			11,94
-24	0,914	0,835	13,7			11,43
-30	0,866	0,750	14,4			10,80
-36	0,809	0,655	15			9,82
-42	0,743	0,552	16,5			9,11
Σ(30)	10,407					
Σ(42)	13,511					185,20
Lef.=	16,8	km				

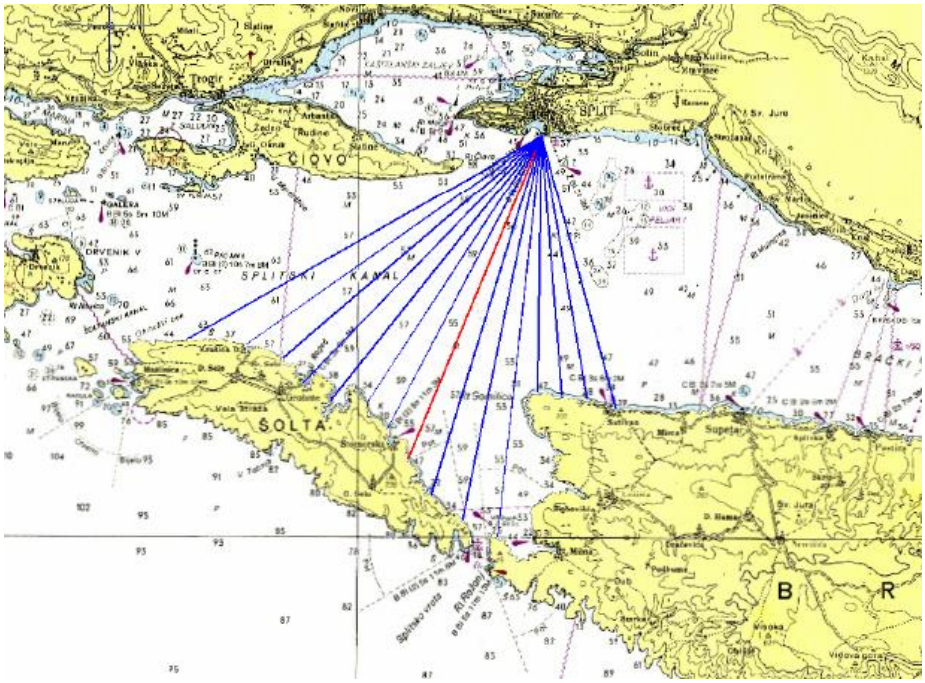

Figure 37. Fetch definition for incident direction SSW

Table 12. Fetch definition for incident direction SSW

Kut α (°)	cosα	cos²α	d (km)	Σd		d·cos²α
42	0,743	0,552	13,2			7,29
36	0,809	0,655	12,5			8,18
30	0,866	0,750	12,2			9,15
24	0,914	0,835	12			10,01
18	0,951	0,905	18,8			17,00
12	0,978	0,957	18,3			17,51
6	0,995	0,989	17,6			17,41
0	1,000	1,000	16,4	173,5	235,3	16,40
-6	0,995	0,989	15,4			15,23
-12	0,978	0,957	15			14,35
-18	0,951	0,905	15,8			14,29
-24	0,914	0,835	16			13,35
-30	0,866	0,750	16			12,00
-36	0,809	0,655	16,9			11,06
-42	0,743	0,552	19,2			10,60
Σ(30)	10,407					
Σ(42)	13,511					193,85
Lef.=	17,4	km				

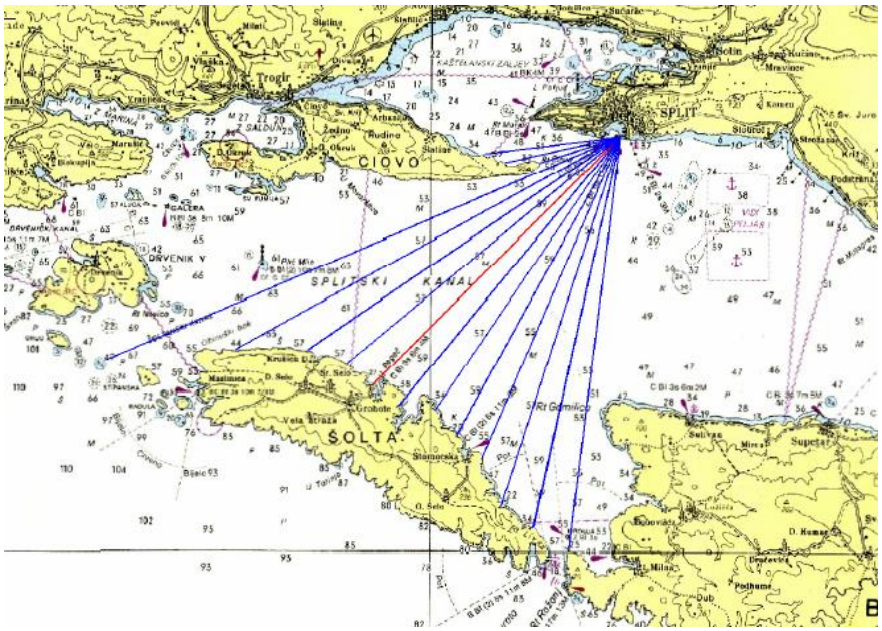

Figure 38. Fetch definition for incident direction SW

Table 13. Fetch definition for incident direction SW

Kut α (°)	cosα	cos²α	d (km)	Σd		d·cos²α
42	0,743	0,552	18,8			10,38
36	0,809	0,655	18,1			11,85
30	0,866	0,750	17,6			13,20
24	0,914	0,835	15,8			13,19
18	0,951	0,905	15,3			13,84
12	0,978	0,957	14,9			14,26
6	0,995	0,989	15,8			15,63
0	1,000	1,000	15,8	177,3	225,9	15,80
-6	0,995	0,989	16			15,83
-12	0,978	0,957	17,1			16,36
-18	0,951	0,905	19,8			17,91
-24	0,914	0,835	25,3			21,11
-30	0,866	0,750	3,9			2,93
-36	0,809	0,655	5,4			3,53
-42	0,743	0,552	6,3			3,48
Σ(30)	10,407					
Σ(42)	13,511					189,29
Lef.=	17,0	km				

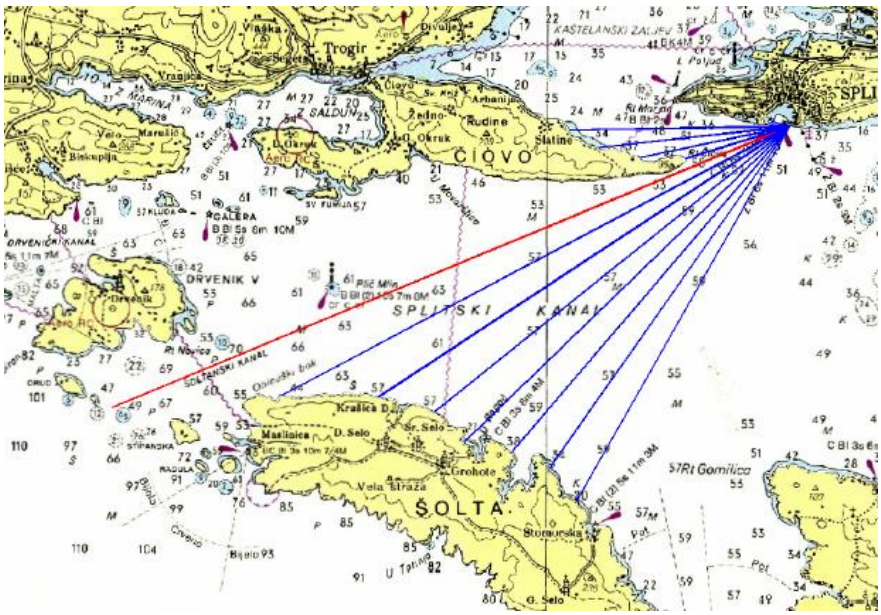

Figure 39. Fetch definition for incident direction WSW

Table 14. Fetch definition for incident direction WSW

Kut α (°)	cosα	$\cos^2\alpha$	d (km)	Σd		$d\cdot\cos^2\alpha$
42	0,743	0,552	15,2		166,9	8,39
36	0,809	0,655	14,8			9,69
30	0,866	0,750	15,1	135,5		11,33
24	0,914	0,835	16			13,35
18	0,951	0,905	16,1			14,56
12	0,978	0,957	17,4			16,65
6	0,995	0,989	20,3			20,08
0	1,000	1,000	25,9			25,90
-6	0,995	0,989	3,9			3,86
-12	0,978	0,957	5,4			5,17
-18	0,951	0,905	6,8			6,15
-24	0,914	0,835	7,8			6,51
-30	0,866	0,750	0,8			0,60
-36	0,809	0,655	0,7			0,46
-42	0,743	0,552	0,7			0,39
Σ(30)	10,407					
Σ(42)	13,511					143,08

Lef.= 13,0 km

17 Limitations of fully developed sea state

For the purpose of defining the relevant input dana, it's necessary to reach the minimum duration of the wind exceedance for the defined fetch length. To define it, one can use:

$$t_{\min} = 43 \cdot \frac{X^{0,73}}{U^{0,46} \cdot g^{0,27}}$$

t_{min} = minimum duration of the wind [s]

X = fetch length [m],

U = wind speed [m/s]

To solve the problem of defining the minimum fetch for a given wind and the corresponding averaging scale, the expression is reformulated:

$$X_{\min} = \sqrt[0,73]{\frac{t \cdot U^{0,46} \cdot g^{0,27}}{43}}$$

Alternative to solve te minimum wind duration can be found in:

$$t_{\min} = X^{0,73} \cdot U^{-0,46}$$

$$X_{\min} = t^{1,37} \cdot U^{0,63}$$

where:

t_{min} = minimum duration of the wind [h]

X = fetch length [km],

U = wind speed [m/s]

Solutions of Goda and Wilson differs only slightly so it is up to the user to select proper method without significant discrepancies in the solutions obtained. When the wind duration is greater than minimum necessary one for the fully developed sea state, one should use effective fetch length. Contrary, minimum fetch should be used.

18 Selection of relevant incident directions of wind and waves

The question of choosing the relevant incident directions of waves is brought down on the analysis of the facts, which are a product of specific attributes of micro location of the area. First of all, it is necessary to consider the combination of fetch length, the duration of wind in specific direction and the wind speed, and to isolate one or more relevant incident directions. Furthermore, the indebtedness of the coast and the direction of the coastline should be taken into account.

With the insight into the wind duration, it seems that the incident directions of the fourth quadrant have the longest duration of consecutive wind blowing, especially SE.

Table 15. Absoule contigency table of the mean hourly wind speed - Split meteorological station, 2000.–2009.

Velocity 5.5 m/s to 7.9 m/s																	
Duration (h)	**1**	**2**	**3**	**4**	**5**	**6**	**7**	**8**	**9**	**10**	**11**	**12**	**13**	**14**	**15**	**≥16**	**Sum**
N	12.9	3.7	0.8	1.0	0.2	0.2											18.8
NNE	111.5	39.8	17.4	8.6	4.1	3.0	1.4	1.5	0.2	0.8		0.3	0.2	0.3		0.3	189.6
NE	149.3	63.5	31.7	15.2	10.5	5.8	3.0	2.4	2.2	1.2	0.5	0.2	0.5	0.2		0.5	286.6
ENE	39.3	9.5	1.7	0.7													51.1
E	19.1	4.4	0.7	0.5	0.2		0.2	0.2									25.2
ESE	83.3	27.9	16.9	9.1	5.8	3.9	1.0	0.3	1.2	0.3	1.2					0.3	151.3
SE	93.8	36.1	15.9	6.8	3.9	2.5	1.4	1.0	0.7	0.8	0.7	0.2	0.2			0.3	164.2
SSE	22.0	5.1	0.5	0.7	0.2	0.2											28.6
S	11.8	3.2	0.2	0.2													15.4
SSW	13.7	3.4	1.2	0.2	0.2												18.6
SW	14.2	5.1	2.0	1.4	0.2												22.9
WSW	9.5	2.0	2.4	0.5	0.2												14.6
W	1.5	0.5															2.0
WNW	0.7																0.7
NW	4.4	0.2	0.2														4.7
NNW	4.4	1.0	0.2	0.2													5.8
n/p																	

Sum	591.4	205.3	91.7	45.0	25.2	15.6	6.9	5.4	4.2	3.2	2.4	0.7	0.8	0.5	0.0	1.5	1000.0
Velocity 8.0 m/s to 10.7 m/s																	
Duration (h)	**1**	**2**	**3**	**4**	**5**	**6**	**7**	**8**	**9**	**10**	**11**	**12**	**13**	**14**	**15**	**≥16**	**Sum**
N	6.4	1.9	0.3	0.3	0.6												9.4
NNE	100.7	48.5	22.7	10.3	6.9	6.1	1.9	3.1	0.8	0.8	0.6	0.6	0.6	0.3			203.8
NE	129.2	58.5	28.3	18.3	9.7	8.9	6.7	2.5	3.6	2.2	1.9	0.6	0.6		0.6	0.6	272.0
ENE	20.2	5.3	0.3	0.3													26.1
E	3.1	0.6															3.6
ESE	83.7	33.8	16.6	6.9	6.4	3.1	1.1	1.7	1.9	0.8	0.6	0.3			0.3	0.3	157.5
SE	109.8	57.1	27.2	18.3	10.5	4.7	3.9	2.2	1.7	0.8	0.8	0.8		0.3	0.0	1.1	239.3
SSE	26.6	6.7	1.9	2.2	0.3	0.8											38.5
S	16.1	3.9			0.8												20.8
SSW	13.6	5.5	1.1	0.3	0.3												20.8
SW	2.5	1.9	0.3														4.7
WSW	0.6																0.6
W	0.3																0.3
WNW	0.6																0.6
NW	0.8																0.8
NNW	0.8				0.3												1.1
n/p																	
Sum	515.0	223.8	98.7	56.8	35.8	23.6	13.6	9.4	8.0	4.7	3.9	2.2	1.1	0.6	0.8	1.9	1000.0
Velocity 10.8 m/s to 13.8 m/s																	
duration (h)	**1**	**2**	**3**	**4**	**5**	**6**	**7**	**8**	**9**	**10**	**11**	**12**	**13**	**14**	**15**	**≥16**	**Sum**
N	5.4	0.7	0.7														6.7
NNE	104.3	41.7	22.2	11.4	4.7	3.4	2.7	2.0									192.5
NE	113.7	45.1	21.5	10.8	8.1	6.1	4.7	0.7	2.0							0.7	213.3
ENE	2.0	1.3	0.0	1.3													4.7
E	0.7																0.7
ESE	69.3	34.3	13.5	8.7	6.7	4.7	2.7	0.7	0.7	0.7	1.3						143.3
SE	145.4	61.9	47.8	23.6	8.7	8.1	6.7	2.7	3.4	3.4	0.7	2.0			0.7		314.9
SSE	32.3	12.1	6.1	2.7	0.7	1.3	1.3										56.5
S	23.6	8.1	2.0	0.7													34.3
SSW	16.2	6.1	1.3	1.3													24.9
SW	6.7																6.7
WSW																	0.0

W																	0.0
WNW																	0.0
NW	1.3																1.3
NNW																	
n/p																	
Sum	520.9	211.3	115.1	60.6	28.9	23.6	18.2	6.1	6.1	4.0	2.0	2.0			0.7	0.7	1000.0
Velocity 13.9 m/s to 17.1 m/s																	
duration (h)	**1**	**2**	**3**	**4**	**5**	**6**	**7**	**8**	**9**	**10**	**11**	**12**	**13**	**14**	**15**	**≥16**	**Sum**
N	2.5																2.5
NNE	100.5	27.6	15.1	7.5		5.0											155.8
NE	118.1	37.7	15.1	10.1	10.1		7.5	2.5				2.5					203.5
ENE	7.5																7.5
E		2.5															2.5
ESE	85.4	17.6	12.6	5.0	5.0		5.0										130.7
SE	180.9	85.4	40.2	12.6	7.5	5.0	5.0	5.0	2.5	2.5	2.5						349.2
SSE	37.7	12.6	7.5	5.0													62.8
S	27.6	7.5	2.5	7.5	2.5	2.5											50.3
SSW	17.6	12.6	2.5														32.7
SW	2.5																2.5
WSW																	
W																	
WNW																	
NW																	
NNW																	
n/p																	
Sum	580.4	203.5	95.5	47.7	25.1	12.6	17.6	7.5	2.5	2.5	2.5	2.5					1000.0
Velocity 17.2 m/s to 20.7 m/s																	
duration (h)	**1**	**2**	**3**	**4**	**5**	**6**	**7**	**8**	**9**	**10**	**11**	**12**	**13**	**14**	**15**	**≥16**	**sum**
N																	
NNE	120.7	51.7	34.5														206.9
NE	155.2	120.7	51.7		34.5		17.2										379.3
ENE																	
E																	
ESE	17.2																17.2
SE	155.2	51.7	34.5	34.5													275.9

SSE	51.7	17.2															69.0
S	17.2																17.2
SSW	34.5																34.5
SW																	
WSW																	
W																	
WNW																	
NW																	
NNW																	
n/p																	
Sum	551.7	241.4	120.7	34.5	34.5		17.2										1000.0
Velocity 20.8 m/s to 24.4 m/s																	
Duration (h)	**1**	**2**	**3**	**4**	**5**	**6**	**7**	**8**	**9**	**10**	**11**	**12**	**13**	**14**	**15**	**≥16**	**Sum**
N																	
NNE	375.0						125.0										500.0
NE	375.0	125.0															500.0
ENE																	
E																	
ESE																	
SE																	
SSE																	
S																	
SSW																	
SW																	
WSW																	
W																	
WNW																	
NW																	
NNW																	
n/p																	
Sum	750.0	125.0					125.0										1000.0
Velocity 24.5 m/s to 28.4 m/s																	
duration (h)	**1**	**2**	**3**	**4**	**5**	**6**	**7**	**8**	**9**	**10**	**11**	**12**	**13**	**14**	**15**	**≥16**	**Sum**
N																	
NNE																	

NE	1000.0															1000.0
ENE																
E																
ESE																
SE																
SSE																
S																
SSW																
SW																
WSW																
W																
WNW																
NW																
NNW																
n/p																
sum	1000.0															1000.0

In terms of frequency of occurrence, looking at Table 16, it is unquestionable that in terms of frequency dominance of the largest wind speed classes of the third and fourth quadrants, the incident directions of SE (jugo) and SSW (garbin) stand out, which, in combination with duration attribute, has as a result of a fact about their relevance when it comes to location, the area of Kaštel Kambelovac.

Table 16. Relative occurrence frequencies of mean hourly value wind speed for Split, period 2000.–2009.

Scale (Bf)	**0**	**1**	**2**	**3**	**4**	**5**	**6**	**7**	**8**	**9**	**10**	**11**	**12**	**Sum**
velocity (m/s)	**0.0-0.2**	**0.3-1.5**	**1.6-3.3**	**3.4-5.4**	**5.5-7.9**	**8.0-10.7**	**10.8-13.8**	**13.9-17.1**	**17.2-20.7**	**20.8-24.4**	**24.5-28.4**	**28.5-32.6**	**32.7-36.9**	
N		1274	1427	419	170	54	13	1						3358
NNE		1010	2368	1881	2193	1648	563	104	19	10				9796
NE		1494	5175	4307	3645	2453	678	172	49	5	2			17980
ENE		1186	3281	1544	391	118	15	3						6538
E		786	1181	714	210	15	1	2						2909
ESE		901	1281	1369	1902	1248	490	94	1					7286
SE		910	1025	1233	1919	2084	1142	294	29					8636
SSE		949	1125	277	227	220	158	42	5					3003
S		976	878	134	115	101	72	43	1					2320
SSW		959	2366	525	151	110	56	20	2					4189

SW		1807	4234	1873	219	25	10	1						8169
WSW		1204	1742	1096	143	2								4187
W		346	538	166	16	1								1067
WNW		455	817	150	4	1								1427
NW		819	1431	365	31	3	2							2651
NNW		929	876	231	45	8								2089
C	438													438
sum	438	16005	29745	16284	11381	8091	3200	776	106	15	2			86043

Regarding the fetch length of the two mentioned directions, it was determined:

- Length of effective fetch for incident direction SE = 24.8 km;
- Length of effective fetch for incident direction SSW = 17.4 km,

therefore, the conclusion is that the SSW and SE are the relevant incident wave directions for the purpose of this study.

19 Definition of the parameter of the deep-water wave

For the values of average hourly speed, minimum required durations of wind blowing, to achieve the phase of fully developed sea, have been previously defined. In case the time of the blow is shorter that the needed minimum, the total wind energy can't be transferred to the sea surface in the length of the effective fetch, so for the relevant fetch length, until achieving the phase of fully developed sea, minimum required length is accepted. In the case when the blowing time is longer than the minimum required, the state of a fully developed sea is not achieved because the effective length of the fetch is less than the minimum. For the relevant fetch length, until the phase of a fully developed sea is reached, in this case the effective fetch length is accepted.

After defining the relevant winds, Goda defines terms and nomograms to define significant wave heights and associated periods::

$$\frac{gH_S}{U^2} = 0{,}3\left\{1-\left[1+0{,}004\left(\frac{gX}{U^2}\right)^{1/2}\right]^{-2}\right\}$$

$$\frac{gT_S}{2\pi U} = 1{,}37\left\{1-\left[1+0{,}008\left(\frac{gX}{U^2}\right)^{1/3}\right]^{-5}\right\}$$

where:

H_S = significant wave height [m]

X = fetch length [m],

U = wind speed [m/s]

Another way of defining the parameters of a deep-water wave is based on the Groen-Dorrestein nomogram, which was created on the basis of measurements in the Mediterranean. Wind speed, fetch length and wind duration on this nomogram mutually correlated.

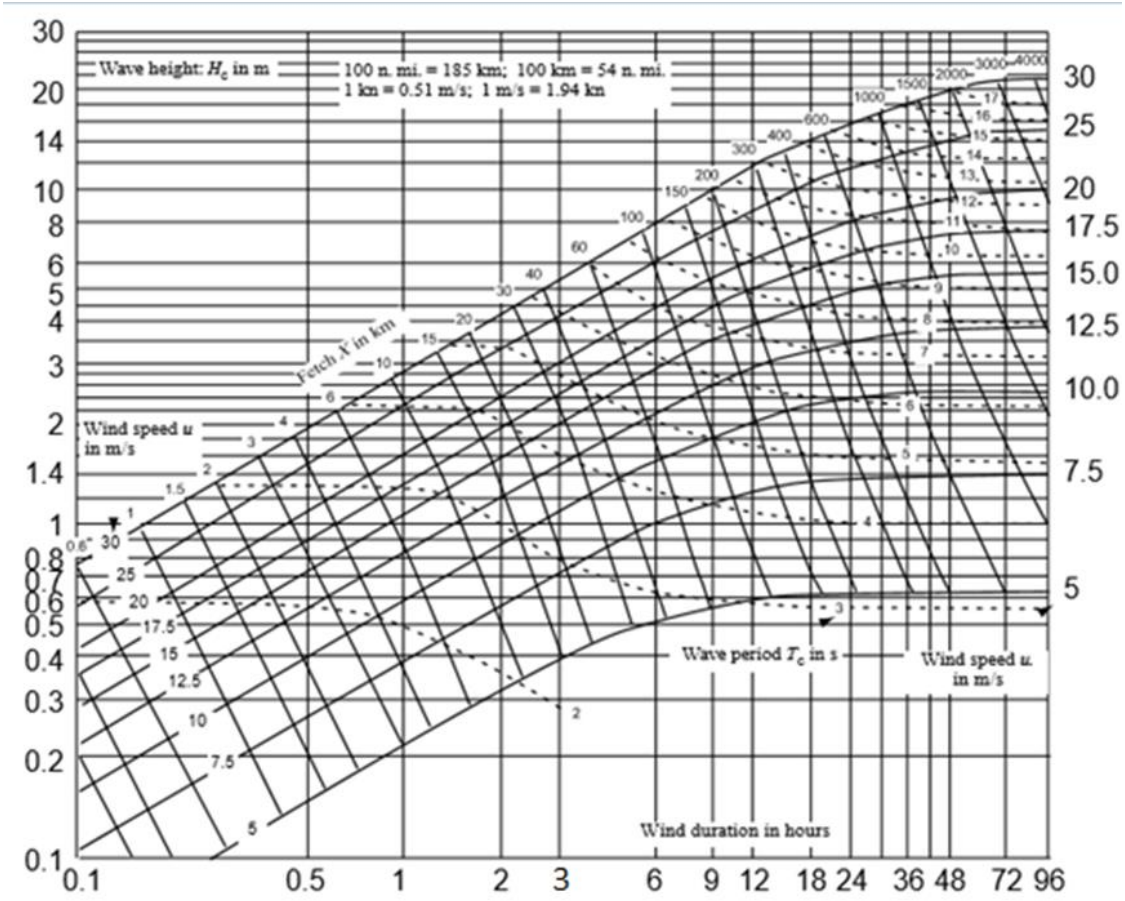

Figure 40. Groen - Dorrestein nomogram

Taking into consideration the data on fetches of the two relevant directions of the incident wave, wind duration for each of the two relevant directions and records of the existence of restrictions at the phase of fully developed sea, Tables 17 and 18. define and show deepwater wave parameters for those incident directions.

Table 17. Deepwater wave parameters – incident direction SE

V [m/s]	1.50	3.30	5.40	7.90	10.70	13.80	17.10	20.70
t [h]	13.00	13.00	13.00	13.00	17.00	15.00	11.00	4.00
F_{min} [km]	43.36	71.25	97.17	123.48	215.89	213.49	159.77	45.07
t_{min} [h]	8.65	6.02	4.80	4.03	3.50	3.12	2.82	2.59
F_{EFF} [km]	24.80	24.80	24.80	24.80	24.80	24.80	24.80	24.80
F_{MJ} [km]	24.80	24.80	24.80	24.80	24.80	24.80	24.80	24.80
H_S [m]			0.50	0.85	1.21	1.70	2.19	2.78
T_S [s]			2.60	3.15	3.65	4.00	4.35	4.76
L_0 [m]	0.00	0.00	10.55	15.49	20.80	24.98	29.54	35.38

Table 18. Deep/water wave parameters – incident direction SSW

V [m/s]	1.50	3.30	5.40	7.90	10.70	13.80	17.10	20.70
t [h]	5.00	5.00	5.00	5.00	5.00	4.00	3.00	1.00
F_{min} [km]	11.71	19.24	26.24	33.35	40.37	34.91	26.94	6.75
t_{min} [h]	6.68	4.65	3.70	3.11	2.70	2.41	2.18	2.00
F_{EFF} [km]	17.40	17.40	17.40	17.40	17.40	17.40	17.40	17.40
F_{MJ} [km]	11.71	17.40	17.40	17.40	17.40	17.40	17.40	6.75
H_S [m]			0.50	0.77	1.05	1.41	1.92	2.35
T_S [s]			2.50	2.95	3.15	3.60	3.98	4.15
L_0 [m]	0.00	0.00	9.76	13.59	15.49	20.23	24.73	26.89

20 Wave transformations

The following types of transformation are mainly related to wave phenomena occurring in the natural environment. When the waves approach the shoreline, they are affected by the seabed through processes such as refraction, shoaling, bottom friction and wave-breaking. However, wave-breaking also occurs in deep water when the waves are too steep. If the waves meet major structures or abrupt changes in the coastline, they will be transformed by diffraction. If waves meet a submerged reef or structure, they will overtop the reef. These phenomena will be further explained in the following. The following types of wave transformation occur mainly in connection with ports and the like. If the waves meet a steep structure, reflection will take place, and if the waves meet a permeable structure, partial transmission will take place.

Depth-refraction is the turning of the direction of wave propagation when the wave fronts travel at an angle with the depth contours at shallow water. The refraction is caused by the fact that the waves propagate more slowly in shallow water than in deep water. A consequence of this is that the wave fronts tend to become aligned with the depth contours. Currents can also result in refraction and this is termed current refraction.

Diffraction can be seen when there are sheltering structures such as breakwaters. Diffraction is the process by which the waves propagate into the lee zone behind the structures by energy transmittance laterally along the wave crests.

Shoaling is the deformation of the waves, which starts when the water depth becomes less than about half the wavelength. The shoaling causes a reduction in the wave propagation velocity as well as shortening and steeping of the waves.

Bottom friction causes energy dissipation and thereby wave height reduction as the water depth becomes more and more shallow. Friction is of special importance over large areas with shallow water

Depth-induced wave-breaking of individual waves starts when the wave height becomes greater than a certain fraction of the water depth. As a rule of thumb, the wave height of an individual wave at breaking

is often said to be around 80% of the water depth, but this is a very approximate figure. Breaking waves are generally divided into three main types, depending on the steepness of the waves and the slope of the shoreface:

Spilling takes place when steep waves propagate over flat shorefaces. Spilling breaking is a gradual breaking which takes place as a foam bore on the front topside of the wave over a distance of 6– 7 wavelengths.

Plunging is the form of breaking where the upper part of the wave breaks over its own lower part in one big splash whereby most of the energy is lost. This form of breaking takes place in cases of moderately steep waves on moderately sloping shorefaces.

Surging is when the lower part of the wave surges up on the foreshore in which case there is hardly any surf-zone. This form of breaking takes place when relatively long waves (swell) meet steep shorefaces.

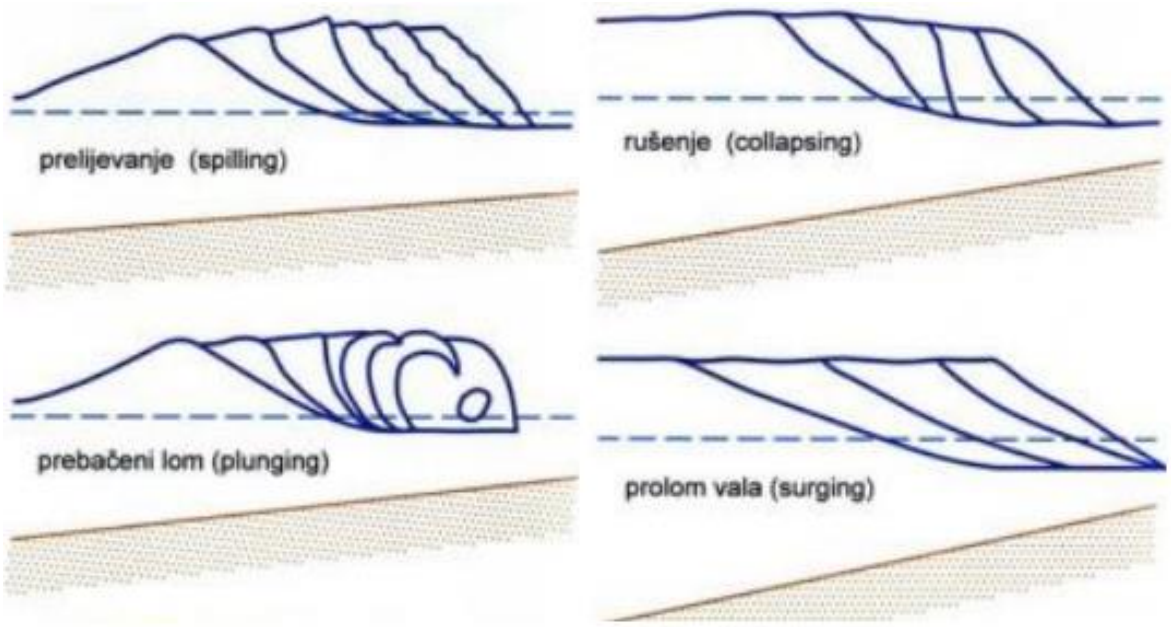

Figure 41. Wave break types

21 Wave field analysis

The model is based on extensions of the “combined refraction-diffraction” equation, which is applicable to both long and short waves and hence finds wide application in coastal engineering and harbour resonance studies. Being elliptic, the equation represents a boundary value problem, which can accommodate internal non-homogeneities (islands, structures, etc.) and boundaries. It hence forms a well-accepted basis for performing wave simulations in regions with arbitrarily-shaped (manmade or natural) boundaries and arbitrary depth variations without limitations on the angle of wave incidence or the degree and direction of wave reflection and scattering that can be modelled. In essence, it represents the complete two-dimensional wave-scattering problem for the non-homogeneous Helmholtz equation. Irregular wave conditions may be simulated by superposition of monochromatic simulations.

The wave phenomena that can be simulated with CGWAVE are: bathymetric refraction, diffraction by structures (e.g. breakwaters) and the bathymetry, reflection (from structures and natural boundaries (seawalls, coastlines, etc) as well as from bed slopes), friction, breaking, and floating (fixed) docks. The model uses a triangular finite-element formulation with grid sizes varying throughout the domain based on the local wavelength; the grids can be efficiently generated using the SMS graphical interface when a bathymetry file is provided. The model allows one to specify the desired reflection properties along the coastline and other internal boundaries. It is therefore particularly well-suited for simulating waves in harbours. While the basic equation is intended for monochromatic waves, irregular (i.e. spectral) wave conditions are simulated in CGWAVE through a linear superposition of monochromatic simulations (e.g. Panchang et al. 1990; Zhao et al. 2001.) Typically, simulations involving a domain containing hundreds of thousands of finite element nodes can be performed in a few minutes on a PC.

For harbour applications, the model also uses a semi-circle (as an open boundary) to separate the model domain from the outer sea. A typical CGWAVE model domain is shown in Figure 42. The input conditions are provided at the offshore ends of two one-dimensional cross-shore sections. (In practice, the input condition is known at the end of one of the transects. The condition at the offshore end of the other transect is obtained by appropriate phase translation.) A combination of the incident and reflected

waves is computed along these transects using a one-dimensional version of the governing equation; this partial solution is then mapped on to the semicircle to force the two-dimensional model. The remainder of the solution on the boundary consists of a scattered wave that emanates from within the domain; this component is allowed to radiate out through the use of an impedance boundary condition. In the model interior, a finite-element grid is used to represent the depth field, and the coastlines (denoted by B in Fig. 1) are assigned a reflection coefficient. For open ocean applications, all variations must be included inside a circle, outside which the depths are assumed constant.

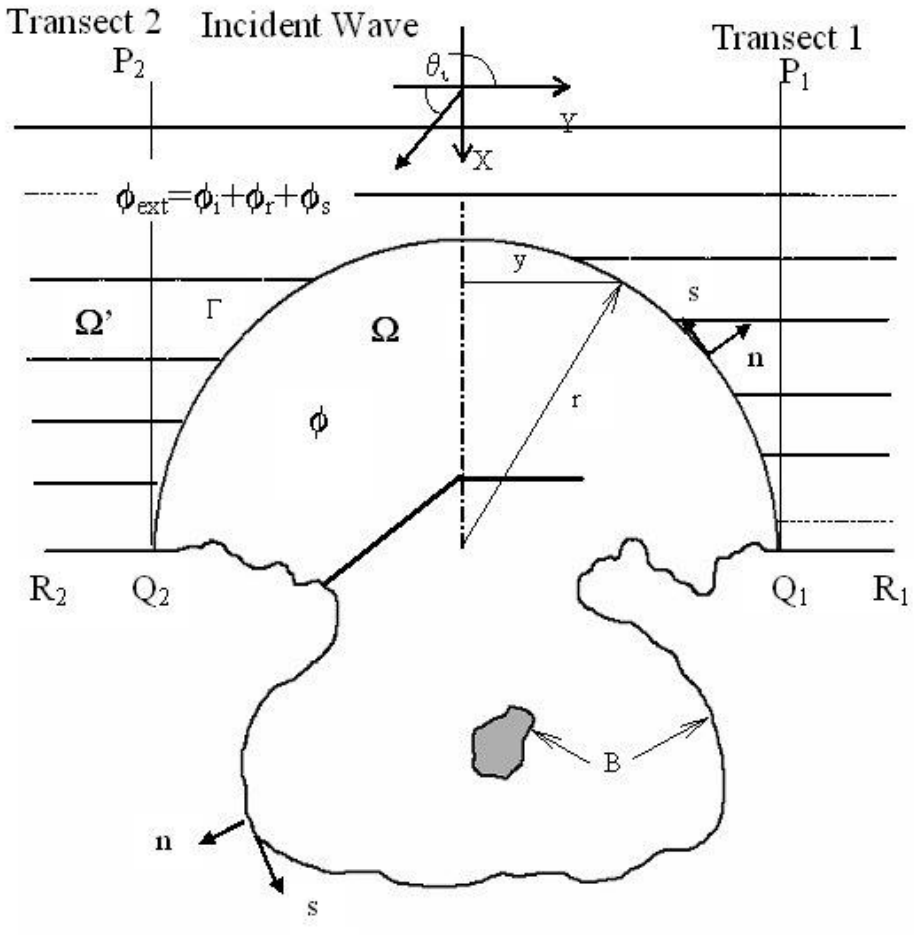

Figure 42. Typical domain of the wave transform model

For the study area, two relevant incident wave directions have been identified, respectively SE and SSW for whom detailed wave transform analysis is done and presented below. For the real wave definition JIONSWAP spectrum has been selected with parameter values as shown in Table 19.

Table 19. Spectral wave definitions

Incident direction	Hs (m)	T (s)	γ	nn
SE (165°)	3.05	6.40	3.3	4
SSW (160°)	2.60	5.90	3.3	4

Figures 43-48. offer the model setup, domain discretization, depth features and boundary conditions. By the inspection of depth values, it is obvious model domain covers eventually the deepwater area thus ensuring the insight to wave transform starting from the deepwater up to coastline.

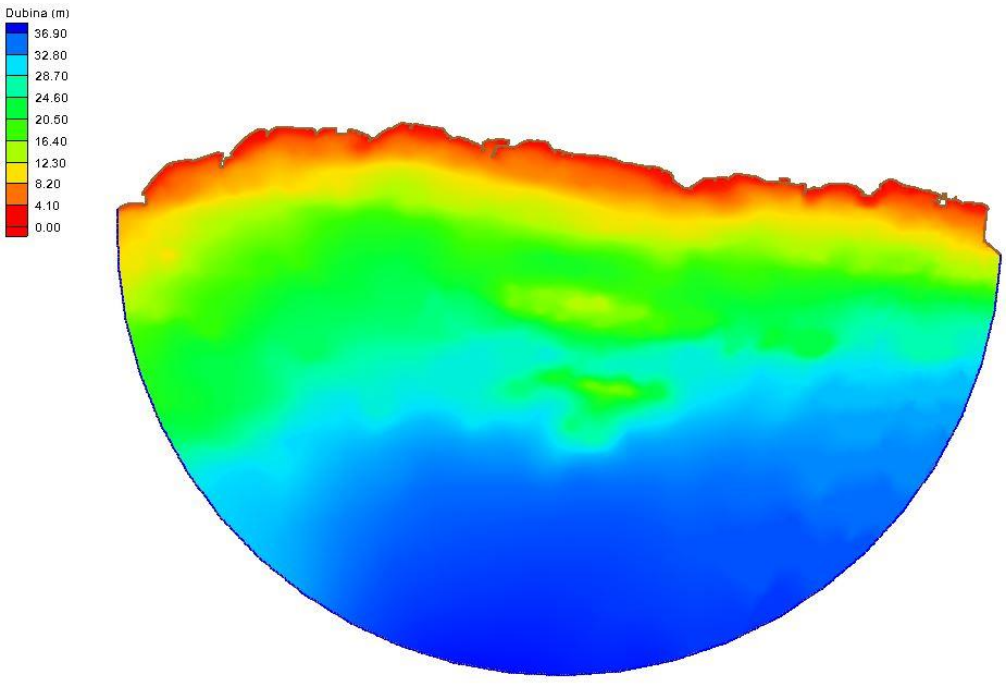

Figure 43. Bathymetry features along the study area

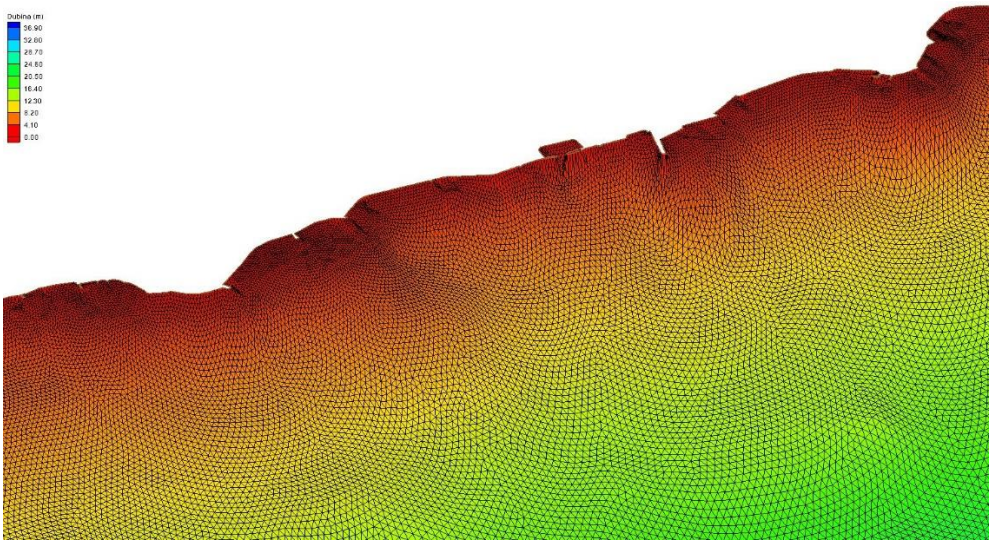

Figure 44. Bathymetry features – isometric view

Figure 45. Domain discretization

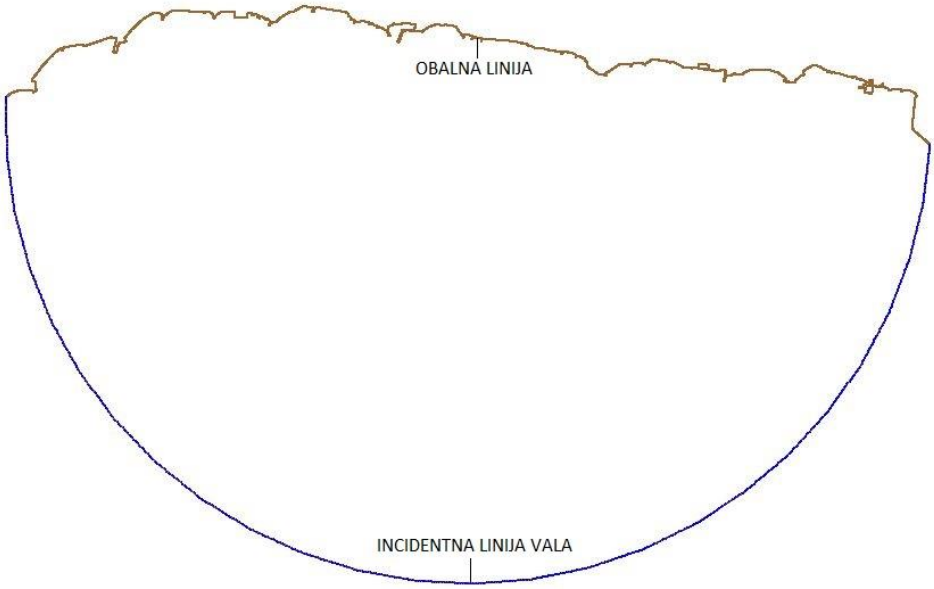

Figurea 46. Clasification of boundary conditions

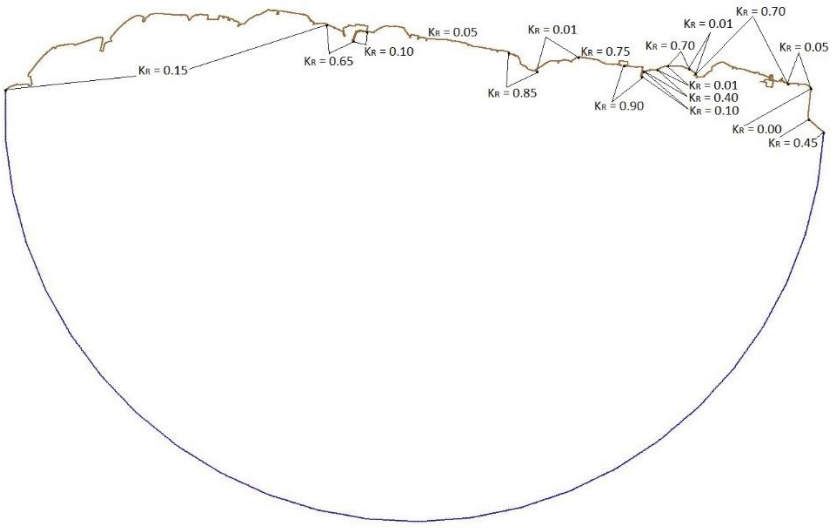

Figure 47. Reflectance features along the study area

Domain boundary is identified by either coastline or incident wave line. Discretization has been done by triangular elements whose size has been determined following the wave period values along the domain.

Identification of the reflection features has been done by in situ inspection of the project study area depending on the depth and costal structure type.

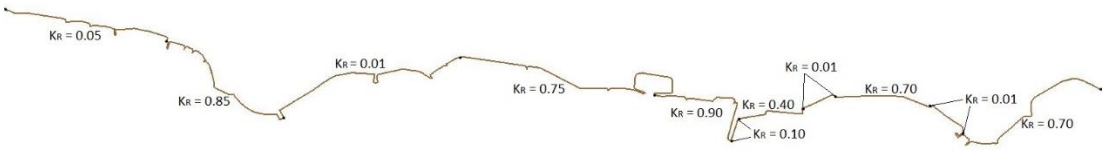

Figure 48. Reflectance features along the study area

22 Wave field properties – incident direction SE

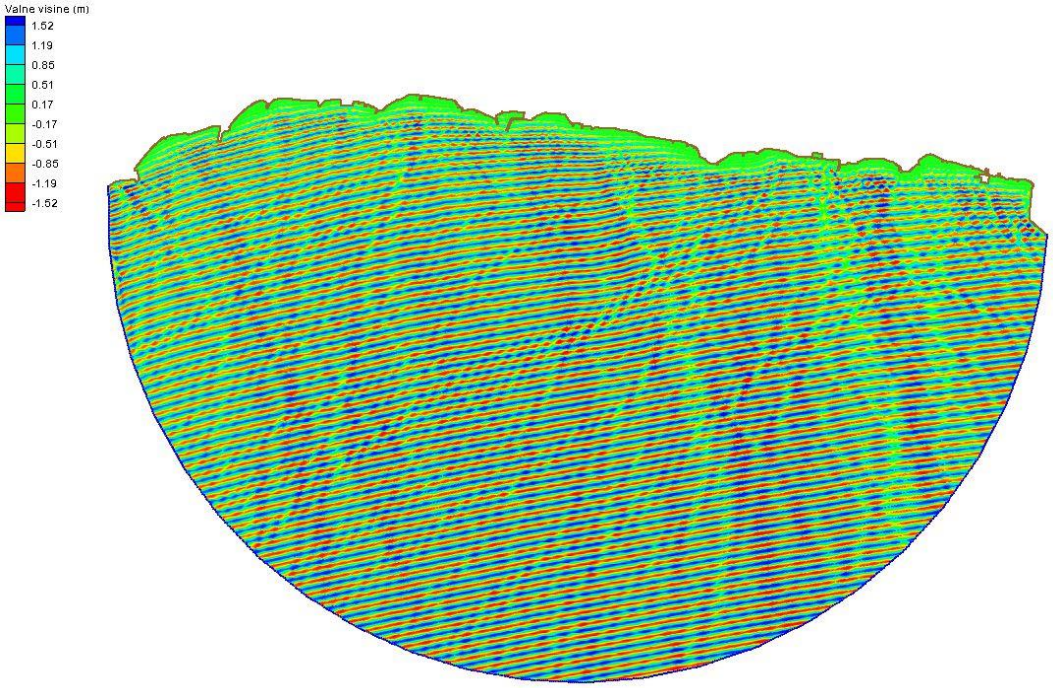

Figure 49. Wave field for SE incident direction – study area

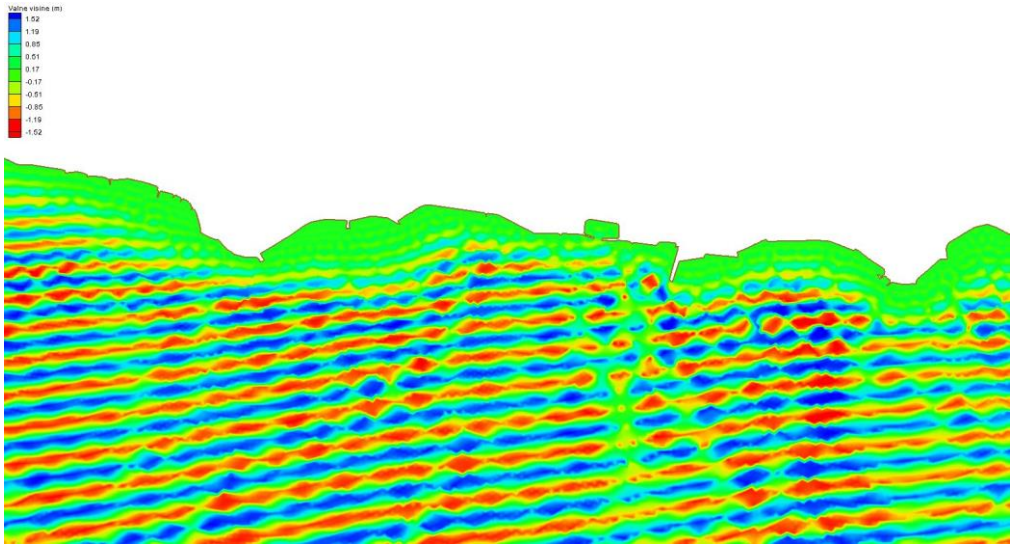

Figure 50. Wave field for SE incident direction – local study area

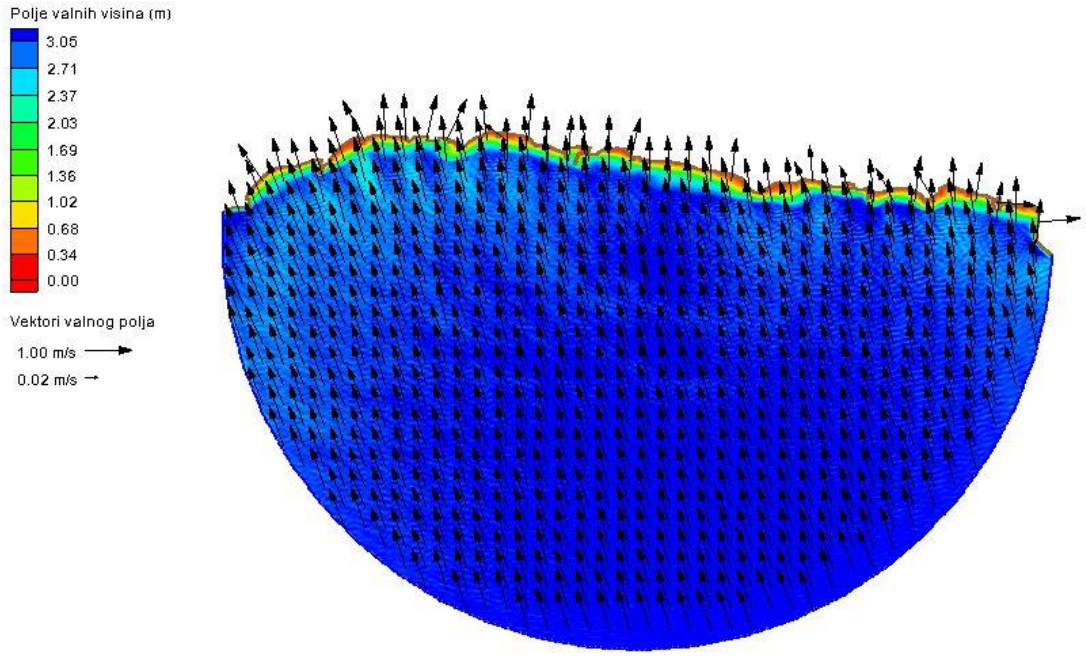

Figure 51. Wave heights and directions for SE incident direction – study area

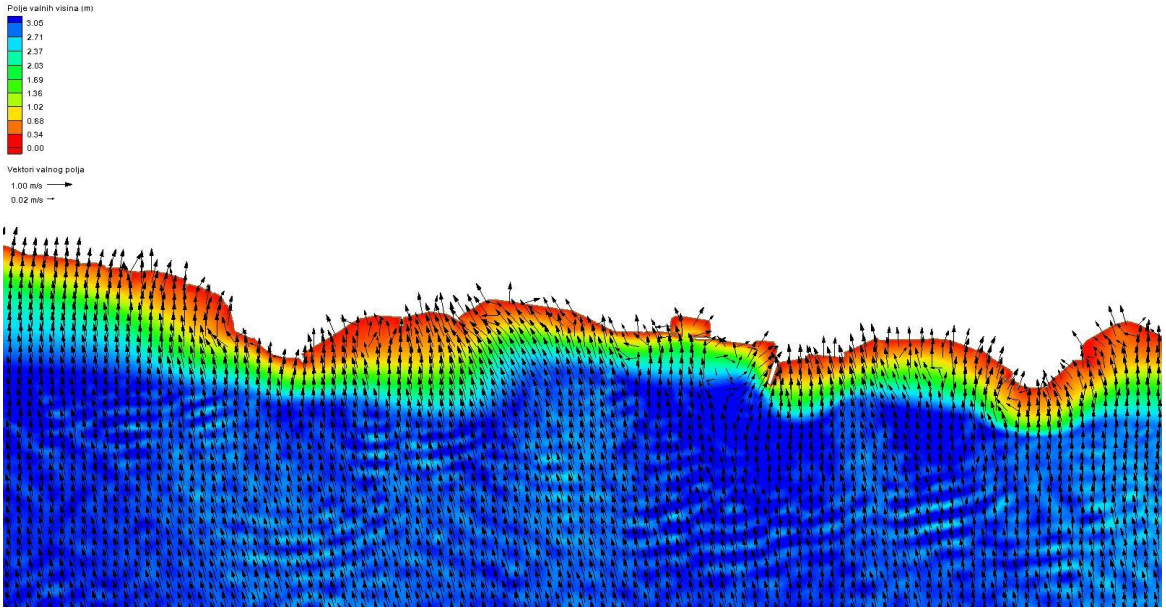

Figure 52. Wave heights and directions for SE incident direction – local study area

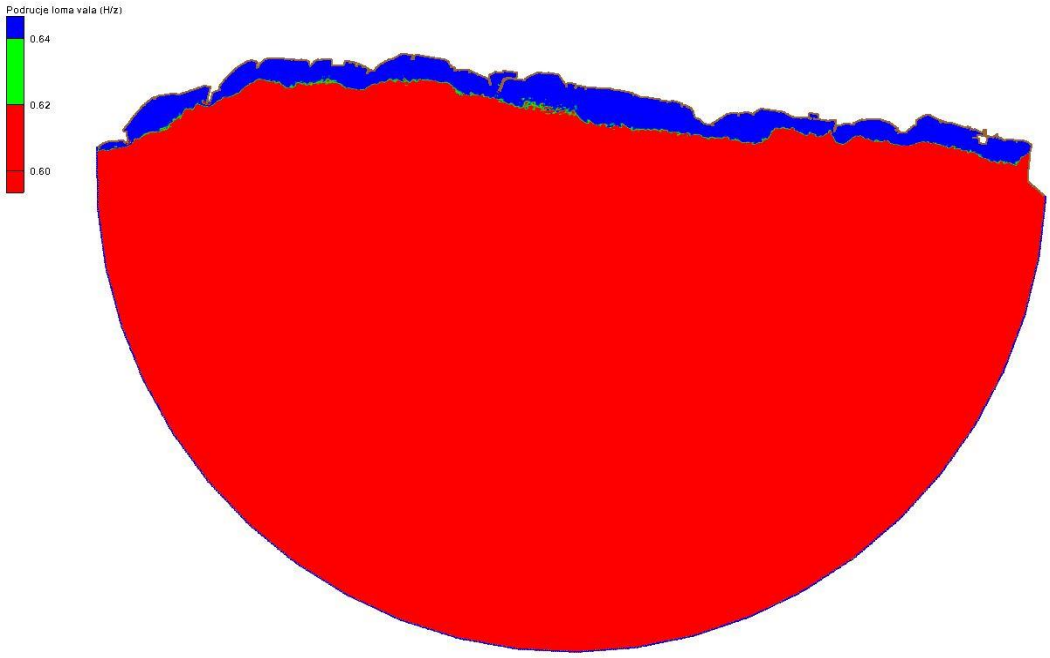

Figure 53. Wave break definition for SE incident direction – study area

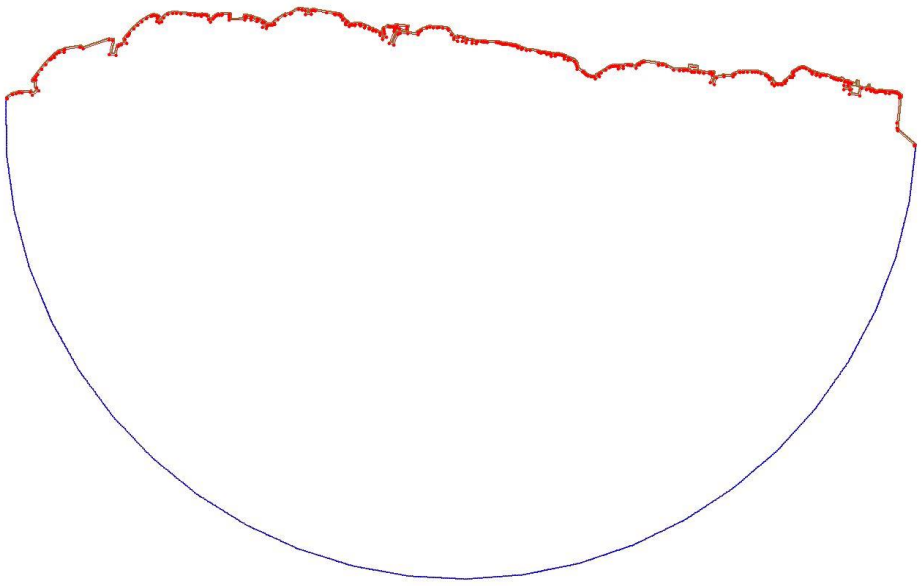

Figure 54. Control line output definition – incident direction SE

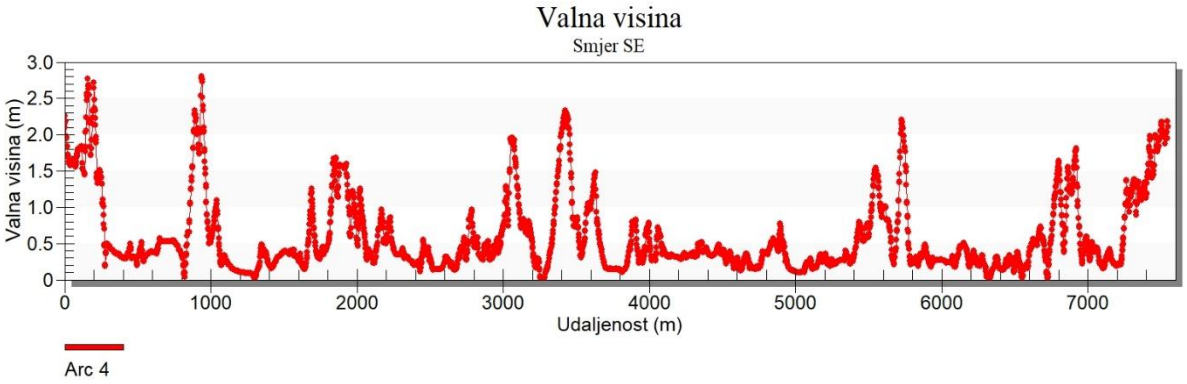

Figure 55. Modelled wave heights along the control line– incident direction SE

23 Wave field features – incident direction SSW

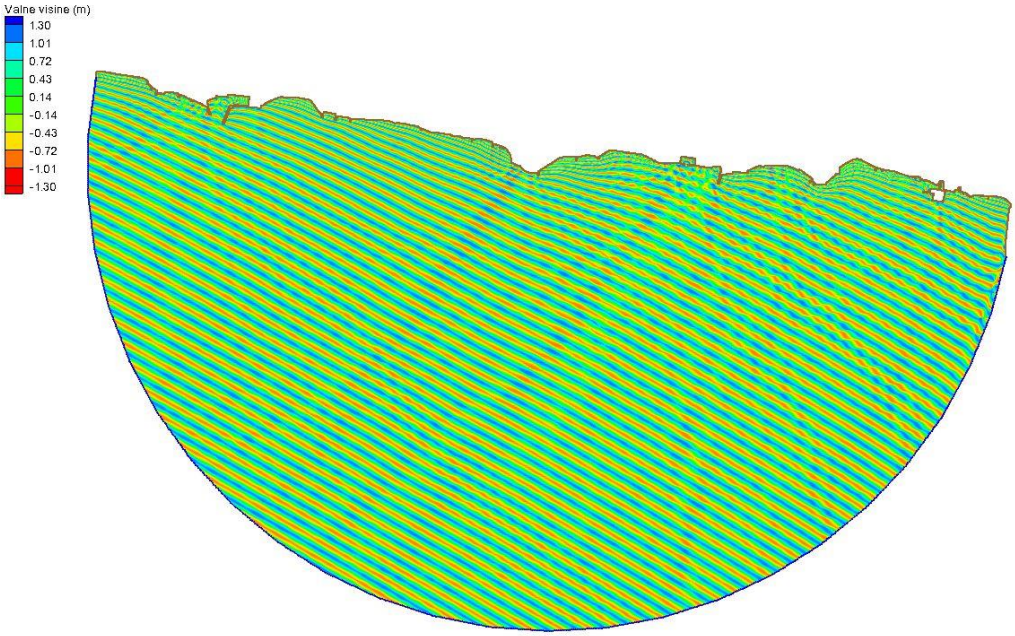

Figure 56. Wave field for SSW incident direction – study area

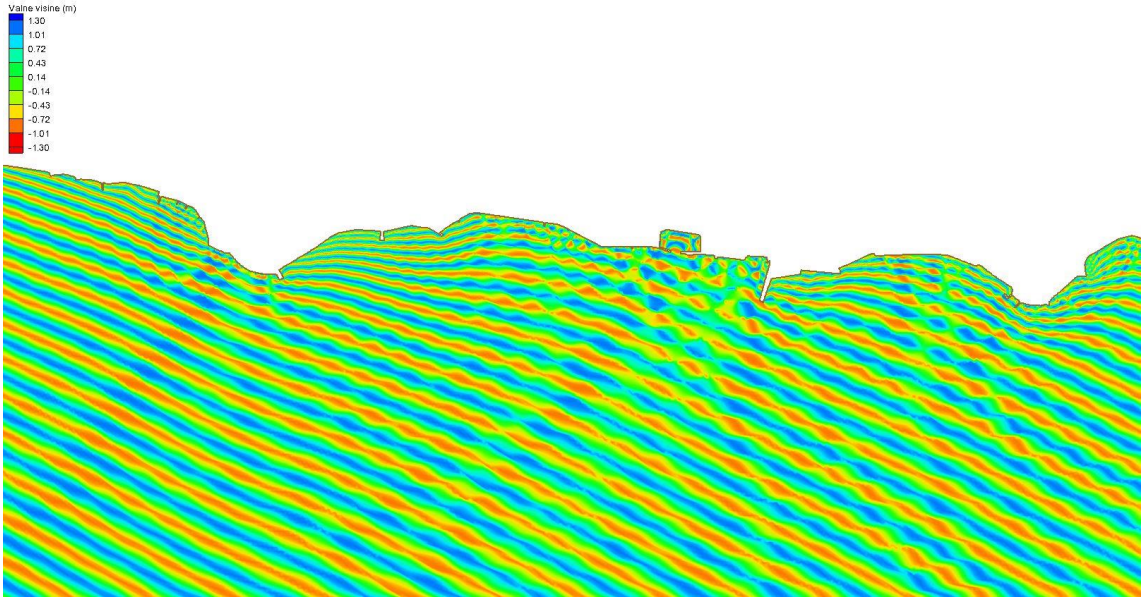

Figure 57. Wave field for SSW incident direction – local study area

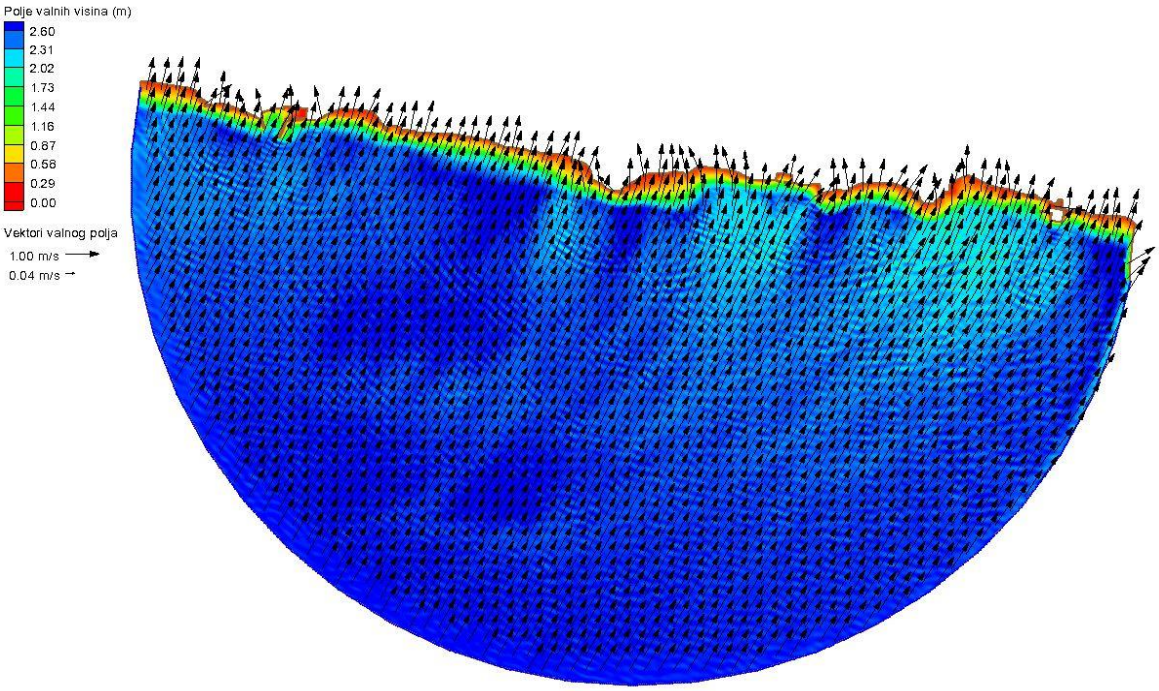

Figure 58. Wave heights and directions for SSW incident direction – study area

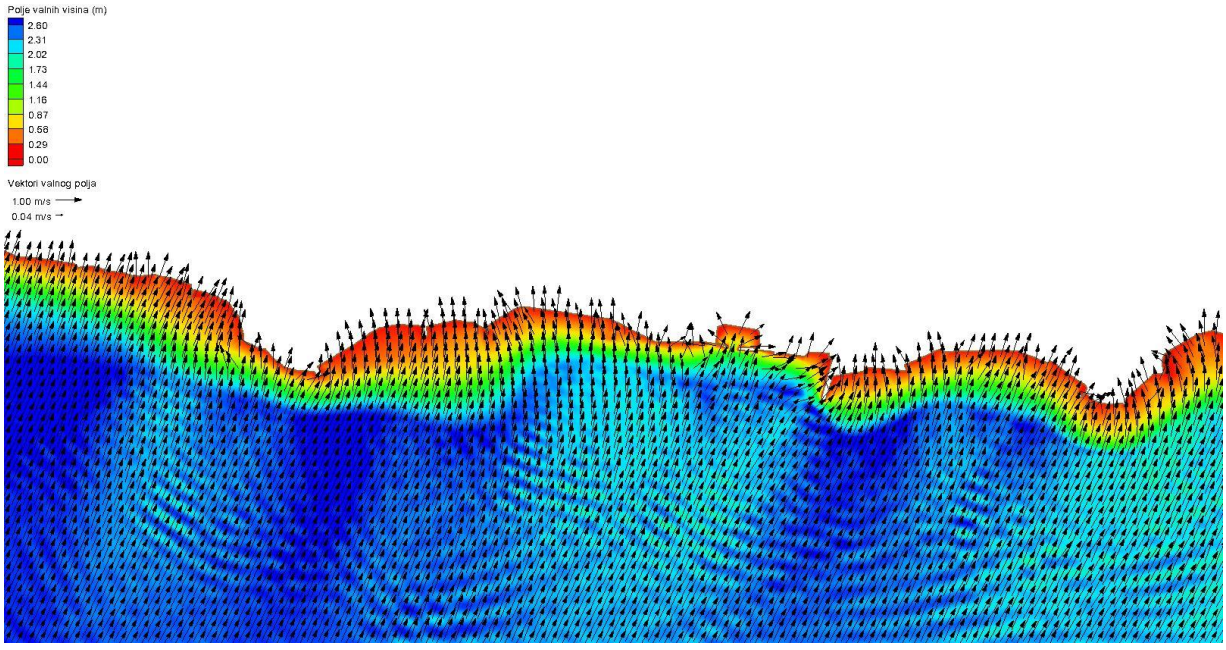

Figure 59. Wave heights and directions for SSW incident direction – local study area

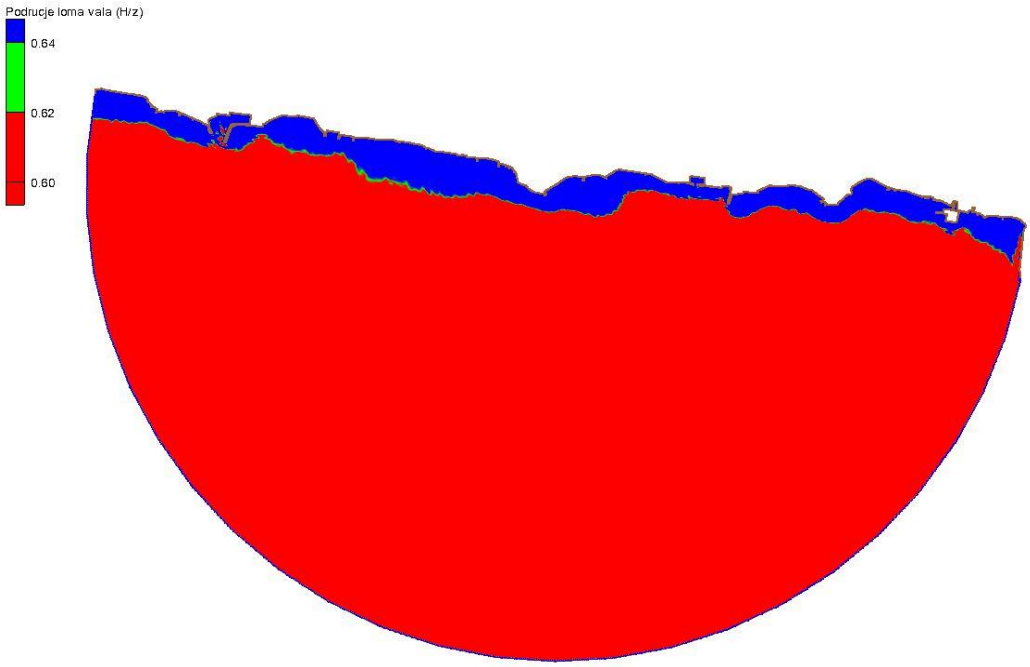

Figure 60. Wave break definition for SSW incident direction – study area

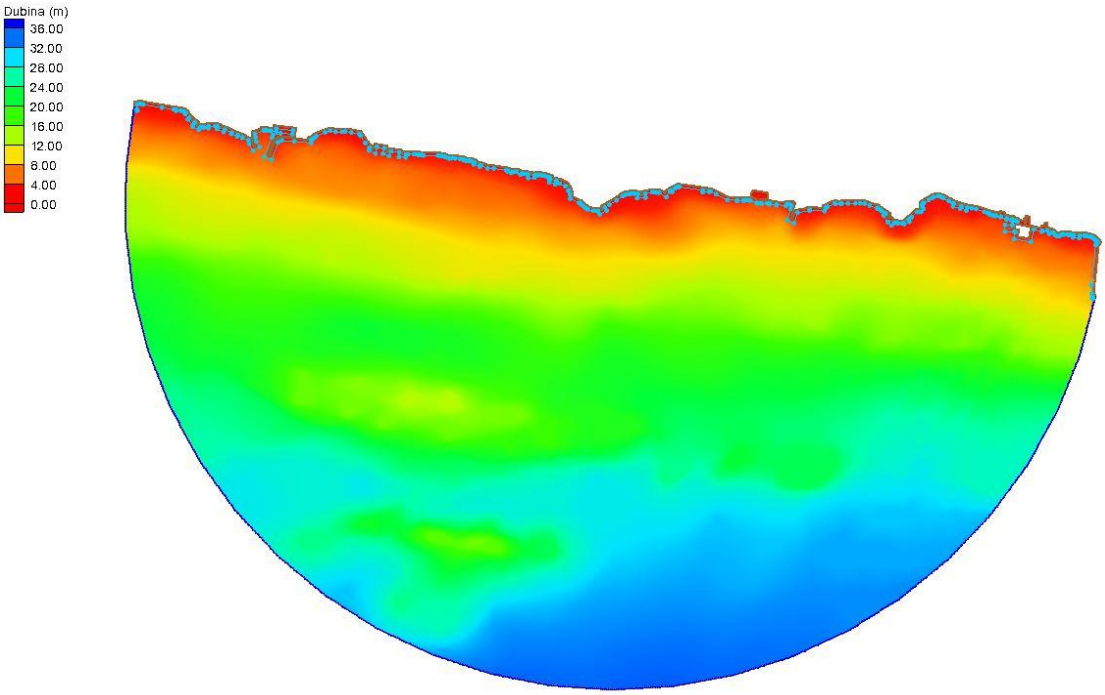

Figure 61. Control line output definition – incident direction SSW

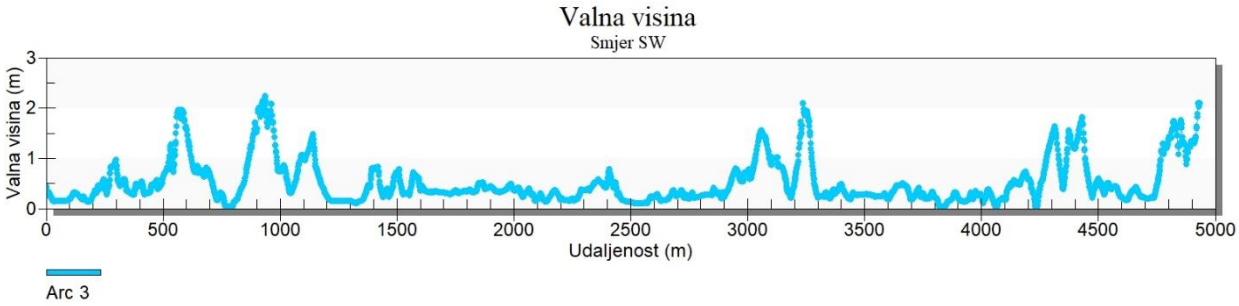

Figure 62. Modeled wave heights along the control line -– incident direction SSW

Finally, according to EU Floods Directive [3] flood exposure maps are based on scenarios associated with the probability of occurrence:

- floods with a low probability, or extreme event scenarios;
- floods with a medium probability (likely return period ≥ 100 years);
- floods with a high probability, where appropriate.

Probability of occurrence in this case is related to particular wind speed for the selected critical wind direction (SE). As a result, sea level for each part of Kaštel Kambelovac coastal area representing cumulative value of tidal, atmospheric pressure and wind impact is estimated (Table 20). Particular coastal zones are determined based on the coastal area elevation in relation to sea level (Figure 63).

Figure 63. Flooding zones in relation to particular coastal area elevation

Table 20. Relative sea level values (in meters above zero value) for each zone corresponding to probability of occurrence

Zone	Low probability	Moderate probability	High probability
1	0,383	0,371	0,349
2	0,383	0,371	0,349
3	0,577	0,559	0,526
4	0,461	0,446	0,420
5	0,268	0,260	0,244
6	0,704	0,682	0,642
7	1,639	1,588	1,494
8	1,359	1,317	1,239
9	0,361	0,350	0,329
10	0,344	0,333	0,314